Gravitropic Stimulation Modulates Glandular Trichome Formation and Essential Oil Composition in *Mentha* × *piperita* through Jasmonate-Dependent and -Independent Pathways

Zur Erlangung des akademischen Grades eines

Doktors der Naturwissenschaften

(Dr. rer. nat.)

von der KIT-Fakultät für Chemie und Biowissenschaften
des Karlsruher Instituts für Technologie (KIT)

genehmigte

DISSERTATION

von

M.Sc. Manuel Amann

1. Referent: Prof. Dr. Peter Nick
2. Referent: Prof. Dr. Holger Puchta

Tag der mündlichen Prüfung: 21. Juli 2026

Die vorliegende Dissertation wurde am Joseph Gottlieb Kölreuter Institut für Pflanzenwissenschaften (JKIP) des Karlsruher Instituts für Technologie (KIT), Lehrstuhl I für Molekulare Zellbiologie, im Zeitraum von Juni 2022 bis Juni 2026 in Zusammenarbeit mit der Vertical Farm Tech GmbH angefertigt. Ein Teil der Arbeiten erfolgte im Rahmen des Forschungsprojekts VFT4Pharma, das durch das Programm Invest BW des Ministeriums für Ernährung, Ländlichen Raum und Verbraucherschutz Baden-Württemberg gefördert wurde.

I. Statement

Hiermit erkläre ich, Manuel Amann, dass ich die vorliegende Dissertation, abgesehen von der Benutzung der angegebenen Hilfsmittel, selbstständig verfasst habe.

Alle Stellen, die gemäß Wortlaut oder Inhalt aus anderen Arbeiten entnommen sind, wurden durch Angabe der Quelle als Entlehnungen kenntlich gemacht.

Diese Dissertation liegt in gleicher oder ähnlicher Form keiner anderen Prüfungsbehörde vor.

Zudem erkläre ich, dass ich mich beim Anfertigen dieser Arbeit an die Regeln zur Sicherung guter wissenschaftlicher Praxis des KIT gehalten habe, einschließlich der Abgabe und Archivierung der Primärdaten, und dass die elektronische Version mit der schriftlichen übereinstimmt.

Karlsruhe, den 03. Juni 2026

_____

Manuel Amann

II. Acknowledgements

First and foremost, I thank my girlfriend, Wenjing, who supported me through all of it, at home just as much as with scientific questions. Without her backing I could not have carried this through the way I did.

I also thank my lab colleagues and friends, among them Nathalie, Sascha and Nitin, who made an otherwise often monotonous lab routine far more varied and were always ready to lend a hand. The same goes for the trainees Lena, Hanna, Daniel and Jolina, without whom the practical work would not have been possible at all. I am equally grateful to our ever-helpful technician Sabine, without whom the lab experience would not have been what it was. A special thanks goes to Vaidurya, my first mentor in the lab and the direct supervisor of my Bachelor's and Master's theses, for opening the door to scientific research for me.

This work took place in a special arrangement with Vertical Farm Tech GmbH, and without their initiative it would never have come about. My thanks go to all the colleagues and friends there, and to the many good after-work evenings and company celebrations I would not want to have missed.

I am grateful to my long-time friends at the Durlach fire brigade, and above all to my childhood friend Maurizio, who were always there when things were not going as they should and I needed to let off steam.

None of this would have been possible without my family, who supported me in the most varied ways and were there whenever I needed them.

Finally, I thank my doctoral supervisor, Peter Nick, who was always there with advice and practical help whenever unforeseen problems arose.

III. Abstract

Medicinal and aromatic plants are a key high-value crop class for controlled environment agriculture (CEA), but their economic value depends on reproducible modulation of phytochemical profiles. Chemical elicitors can raise residue and regulatory concerns, motivating the development of non-chemical alternatives. This work investigates gravitropic stimulation as a non-invasive elicitation strategy in *Mentha* × *piperita* under CEA conditions. Three questions were addressed: how peppermint perceives and responds to gravitropic stimulation, whether targeted tilting modulates biomass and secondary metabolite production, and whether jasmonic acid (JA) mediates these effects.

Plants were grown in custom-built aeroponic tilting modules. Three protocols were compared across increasing tilt intensities: daily tilting in light, daily tilting in darkness, and continuous tilting. The role of JA was tested through exogenous methyl jasmonate (MeJA) application and phenidone-mediated inhibition of JA biosynthesis.

Statolith-containing statocytes were present along the shoot axis, whereas gravitropic bending was largely restricted to young internodes. Gravity perception is therefore retained beyond the responsive zone, while curvature is constrained downstream by the developmental capacity for asymmetric elongation. Repeated tilting weakened the response in darkness but enhanced it in light. Gravitropic stimulation induced the JA marker JAZ1 together with the cell-wall marker Expansin in young internodes. At the whole-plant level, responses were strongly protocol- and dose-dependent. Daily tilting in light at mild intensity increased leaf biomass and essential oil yield. Trichome number increased either through leaf expansion at moderate intensity or through increased trichome density at severe intensity. Moderate and severe stimulation shifted oil composition toward menthofuran and away from menthol, while mild intensity shifted it toward menthone. The strongest yield gain and the undesirable menthofuran shift did not coincide.

MeJA reproduced the leaf-expansion-coupled trichome response and the mild-stress oil profile, but not the density-driven trichome initiation observed at higher gravitropic doses. Phenidone did not suppress the gravitropism-induced increase in trichome count, but consistently lowered menthofuran and largely reversed the shifts in pinene, eucalyptol and limonene. A JA-independent effect on menthol additionally emerged in older leaf pairs. JA is therefore a major, but not exclusive, mediator of the compositional response.

Overall, gravitropic stimulation emerges as a non-invasive, protocol- and dose-dependent elicitor of biomass, glandular trichome formation and essential oil composition in *Mentha* × *piperita*. The dose-and-protocol framework developed here suggests that gravitropic stimulation could become an additional controllable input variable in CEA-based medicinal plant production, alongside light, temperature and water.

Zusammenfassung

Arznei- und Aromapflanzen sind eine zentrale Hochwertkulturgruppe für Controlled Environment Agriculture (CEA). Ihr wirtschaftlicher Wert hängt jedoch von der reproduzierbaren Modulation phytochemischer Profile ab. Chemische Elizitoren können Rückstands- und Zulassungsfragen aufwerfen, was die Entwicklung nicht-chemischer Alternativen motiviert. Die vorliegende Arbeit untersucht die gravitropische Stimulation als nicht-invasive Elizitierungsstrategie an *Mentha* × *piperita* unter CEA-Bedingungen. Drei Fragen wurden adressiert: Wie nimmt Pfefferminze gravitropische Stimulation wahr und reagiert darauf? Lässt sich durch gezielte Kippung die Biomasse- und Sekundärstoffproduktion modulieren? Und vermittelt Jasmonsäure (JA) diese Effekte?

Die Pflanzen wurden in eigens entwickelten aeroponischen Kippmodulen kultiviert. Drei Protokolle wurden über zunehmende Kippintensitäten verglichen: tägliches Kippen im Licht, tägliches Kippen in Dunkelheit und kontinuierliches Kippen. Die Rolle der JA wurde durch exogene Methyljasmonat (MeJA)-Applikation und phenidonvermittelte Hemmung der JA-Biosynthese geprüft.

Statolithenhaltige Statozyten waren entlang der Sprossachse vorhanden, während die gravitropische Krümmung weitgehend auf die jungen Internodien beschränkt blieb. Die Gravitationswahrnehmung bleibt somit über die reaktionsfähige Zone hinaus erhalten, während die Krümmung stromabwärts durch die entwicklungsbedingte Kapazität zur asymmetrischen Elongation begrenzt wird. Wiederholtes Kippen schwächte die Reaktion in Dunkelheit, verstärkte sie jedoch im Licht. Die gravitropische Stimulation induzierte den JA-Marker JAZ1 zusammen mit dem Zellwandmarker Expansin in den jungen Internodien. Auf Ganzpflanzenebene waren die Reaktionen stark protokoll- und dosisabhängig. Tägliches Kippen im Licht bei milder Intensität steigerte die Blattbiomasse und die Ölausbeute. Die Drüsenhaarzahl nahm entweder durch Blattexpansion bei moderater Intensität oder durch erhöhte Drüsenhaardichte bei schwerer Intensität zu. Moderate und schwere Stimulation verschoben die Ölzusammensetzung hin zu Menthofuran und weg von Menthol, während milde Intensität sie hin zu Menthon verschob. Der stärkste Ausbeutegewinn und die unerwünschte Menthofuran-Verschiebung traten nicht gemeinsam auf.

MeJA reproduzierte die mit der Blattexpansion gekoppelte Drüsenhaarreaktion und das Ölprofil des milden Stresses, nicht jedoch die dichtegetriebene Trichominitiation der höheren gravitropischen Dosen. Phenidon unterdrückte den gravitropisch induzierten Anstieg der

Drüsenhaarzahl nicht, senkte jedoch konsistent den Menthofuran-Anteil und kehrte die Verschiebungen bei Pinen, Eucalyptol und Limonen weitgehend um. In den älteren Blattpaaren trat zusätzlich ein JA-unabhängiger Effekt auf Menthol hervor. JA ist demnach ein wesentlicher, jedoch nicht ausschließlicher Vermittler der Zusammensetzungsantwort.

Insgesamt erweist sich die gravitropische Stimulation als nicht-invasiver, protokoll- und dosisabhängiger Elizitor von Biomasse, Drüsenhaarbildung und Ölzusammensetzung in *Mentha* × *piperita*. Das hier entwickelte Dosis-und-Protokoll-Rahmenwerk legt nahe, dass die gravitropische Stimulation zu einer zusätzlichen steuerbaren Einflussgröße in der CEA-basierten Arzneipflanzenproduktion werden könnte – neben Licht, Temperatur und Wasser.

List of Contents

Abbreviations

ARF1	auxin response factor 1
CEA	controlled environment agriculture
COI1	coronatine insensitive 1
ctrl	control
GC-MS	gas chromatography–mass spectrometry
GPP	geranyl diphosphate
JA	jasmonic acid
JA-Ile	jasmonoyl-L-isoleucine
JAZ	jasmonate ZIM-domain protein family
JAZ1	jasmonate ZIM-domain protein 1
lp1-lp4	leaf pair 1 to leaf pair 4
MeJA	methyl jasmonate
MFS	menthofuran synthase
Ph	phenidone
PR	pulegone reductase
RT-PCR	reverse transcription PCR
RT-qPCR	quantitative reverse transcription PCR
SPME	solid-phase microextraction

1 Introduction

1.1 Scope and Motivation

Medicinal and aromatic plants are among the most attractive high-value crops for controlled environment agriculture. Their worth does not only lie in bulk biomass but in a defined phytochemical profile, and that profile must be reproducible from batch to batch. The central question for these crops is therefore not only how much a plant grows, but how reliably its secondary metabolism can be steered toward a target composition.

One established way to steer secondary metabolism is elicitation. A controlled stress or signaling stimulus is applied to push the plant toward the accumulation of pharmacologically relevant compounds (Naik and Al–Khayri, 2016; Shil and Dewanjee, 2022). Elicitor treatments are most often chemical. Applied substances, however, can leave residues and raise regulatory questions in a product intended for medicinal use, which motivates the search for non-chemical alternatives.

This thesis pursues one such alternative. Its central idea is that a purely mechanical input, the controlled reorientation of the plant against gravity, might itself serve as an elicitor. Instead of applying a compound, the approach would recruit the plant's own gravitropic signaling to influence its secondary metabolism. Whether such a stimulus can in fact modulate the phytochemistry of a medicinal plant, and through which internal signal, is the question this work sets out to answer.

Using gravitropism in this way means treating it not as a phenomenon to be observed but as a tool to be controlled. A tool can only be applied deliberately once its mechanism is understood. The following sections therefore turn first to gravitropism itself, to how plants perceive and respond to a change in orientation, before returning to the question of how this response could be harnessed as an elicitation strategy.

1.2 Gravitropism

Plants cannot relocate in response to environmental challenges and instead rely on directed growth to optimize their position in the environment. One of the most fundamental of these growth responses is gravitropism - the ability of plants to sense and respond to gravity. Research into this phenomenon spans over three centuries, from Knight's (1806) early recognition that gravity guides plant growth through to the landmark Cholodny-Went hypothesis (Went, 1926;

Cholodny, 1927), which established lateral auxin redistribution as the central driver of differential growth. Through gravitropism, roots grow downward into the soil to anchor the plant and acquire water and nutrients, while shoots grow upward to maximize exposure to light. Although the outcome appears simple, the underlying mechanism proceeds through three distinct phases: gravity perception by specialized cells, signal transduction via molecular cascades, and a differential growth response that produces the characteristic curvature.

1.2.1 Gravity Perception: Statoliths and Gravity-Sensing Cells

The first and most fundamental of these phases — gravity perception — relies on specialized cells called statocytes, found in the columella of the root cap and in the endodermal cell layer of shoots, which is also known as the starch sheath (Boonsirichai *et al.*, 2002; Morita, 2010). Statocytes contain dense, starch-filled plastids known as amyloplasts or statoliths. Upon changes in the gravitational vector, these statoliths sediment to the physiologically lower side of the cell (Morita, 2010). The starch-statolith hypothesis posits that this sedimentation constitutes the primary physical event in gravity sensing. This hypothesis continues to be strongly supported by experimental evidence across multiple plant systems (Boonsirichai *et al.*, 2002; Morita, 2010). The presence of statolith-containing amyloplasts in the starch sheath of *Mentha* × *piperita* shoots is shown in Figure 1.

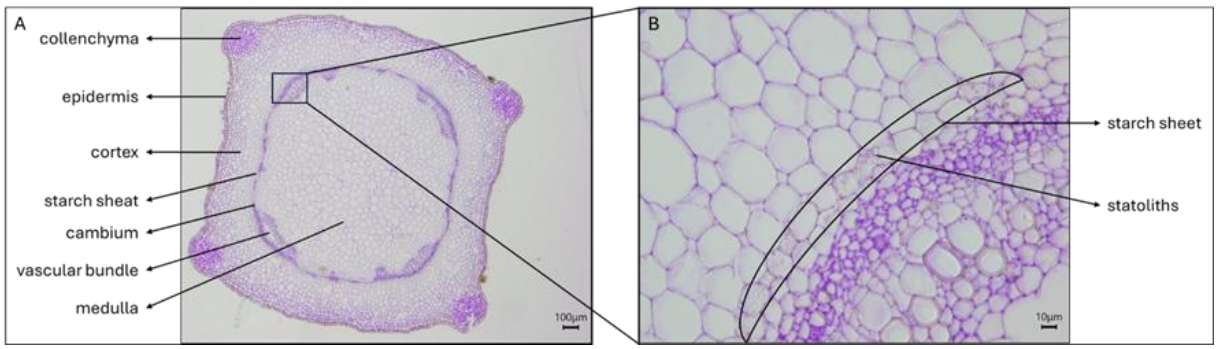

Figure 1 Anatomy of a *Mentha* × *piperita* internode cross-section. *(A) Overview of the internode cross-section showing the major tissue layers. These include collenchyma, epidermis, cortex, starch sheath, cambium, vascular tissue, and medulla. Scale bar = 100 µm. (B) Magnified view of the starch sheath region (boxed area in A). The curved line delineates the starch sheath containing statoliths (amyloplasts). These statoliths function as gravity-sensing organelles in the shoot endodermis. Scale bar = 10 µm.*

Statolith sedimentation is a dynamic process constrained by the actin cytoskeleton. The actin cytoskeleton governs sedimentation speed and directionality through cage-like confinement of amyloplasts (Zheng *et al.*, 2015). Beyond the actin-mediated confinement of amyloplasts, microtubules have been implicated as mechanical amplifiers in gravity sensing. Their rigid, elongate structure makes them suitable levers for transducing the small forces exerted by sedimenting statoliths into downstream signals. Reduction of microtubule dynamics, either

through microtubule-disrupting drugs or through the stabilizing agent taxol, impairs gravitropic responses. This indicates that dynamic microtubule turnover is required for gravity sensing (Nick, 2013). Upon reorientation, statoliths sediment toward the new lower side of the cell. There, physical interaction with membrane-associated signaling components is thought to initiate the gravitropic signaling cascade (Morita, 2010; Nishimura *et al.*, 2023). The role of starch in statolith function is important but not absolute. Starchless mutants retain residual gravitropic responses, and the degree of impairment correlates positively with the reduction in starch content. This indicates that statolith mass contributes quantitatively to sensing efficiency rather than being strictly required (Morita, 2010).

1.2.2 Signal Transduction: From Statolith Sedimentation to Cellular Polarity

How statolith sedimentation is converted into a polarized biochemical signal remains one of the least understood steps in gravitropism research (Morita, 2010; Baldwin *et al.*, 2013; Su *et al.*, 2017; Vandenbrink and Kiss, 2019). The boundary between perception and transduction is not sharply defined: sedimentation begins almost immediately after gravistimulation, and membrane depolarization and altered Ca^{2+} fluxes are detectable within seconds (Sievers *et al.*, 1984; Behrens *et al.*, 1985; Leitz *et al.*, 2009). Current models are framed as a contrast between force-sensing and position-sensing — whether perception depends on the mechanical force exerted by sedimenting statoliths or on their spatial position within the statocyte.

Force-sensing models propose that sedimenting statoliths mechanically stimulate intracellular membranes, the cytoskeleton, or mechanosensitive ion channels (Pickard and Ding, 1993; Blancaflor, 2013). Displaced statoliths locally deform the cortical ER (Leitz *et al.*, 2009), providing a candidate mechanical trigger for the early Ca^{2+} release and depolarization noted above. Force magnitude alone, however, is difficult to reconcile with the primary sensory parameter: the gravitational forces acting on individual statoliths are extremely small (Zheng *et al.*, 2015), responses do not scale with statolith weight (Limbach *et al.*, 2005), and they track inclination angle rather than gravity intensity (Chauvet *et al.*, 2016).

Position-sensing models instead propose that statocytes detect the spatial localization of statoliths, analogous to a clinometer measuring inclination angle (Moulia *et al.*, 2019). This view is supported at the molecular level by LAZY1-LIKE (LZY) proteins. Following gravistimulation, LZY proteins are carried with the sedimenting amyloplasts to the lower plasma membrane, a relocalisation driven by MKK5-MPK3-dependent phosphorylation. Their

accumulation precedes detectable auxin asymmetry and recruits D6 protein kinase, which directs PIN-mediated auxin efflux toward the lower flank (Nishimura *et al.*, 2023; Chen *et al.*, 2023).

Current evidence favors statolith position over force magnitude as the primary signal, yet the two are best regarded as complementary rather than mutually exclusive (Chauvet *et al.*, 2016; Moulia *et al.*, 2019; Nishimura *et al.*, 2023). Cortical microtubules have been proposed as a parallel mechanosensory component: lateral auxin transport is suppressed both by microtubule elimination and by taxol-induced stabilization, dissociating their sensory role from their later function in cellulose deposition (Gutjahr and Nick, 2006; Nick, 2013). The relative contributions of these mechanisms remain still unresolved. Regardless of which sensing mechanism predominates, the proposed routes ultimately converge on a single downstream event that translates the perceived reorientation into a growth response.

1.2.3 Auxin Redistribution and the Establishment of the Auxin Gradient

The classical Cholodny–Went hypothesis posits that lateral redistribution of auxin from the upper to the lower flank of a gravistimulated organ drives differential growth. This hypothesis remains the conceptual basis of current models of gravitropic auxin asymmetry (Digby and Firn, 1976; Gutjahr *et al.*, 2005). The asymmetric redistribution of auxin is the central hormonal event linking gravity perception in the root cap to differential growth in the elongation zone (Boonsirichai *et al.*, 2002; Su *et al.*, 2017).

The directionality of this flux arises from polar auxin transport mediated by PIN efflux carriers and AUX1 influx carriers. The mechanism is best characterized in *Arabidopsis* roots, where PIN3 and PIN7 relocalise toward the lower membranes of the columella cells after gravistimulation and redirect auxin toward the lower flank of the root cap (Su *et al.*, 2017; Xu *et al.*, 2023). From there, AUX1- and PIN2-dependent transport carries auxin through the lateral root cap and epidermis into the elongation zone. The functional importance of this transport is evident in loss-of-function mutants of either carrier, which show strongly reduced gravitropic curvature (Marchant *et al.*, 1999; Su *et al.*, 2017). Direct evidence for the resulting asymmetry was provided by Ottenschläger *et al.*, (2003), who detected asymmetric signal in the distal lateral root cap approximately 1.5 h after gravistimulation.

The gradient is further regulated by feedback on PIN abundance and trafficking and by auxin homeostasis. SCF^TIR1/AFB-dependent regulation, asymmetric gibberellin signaling, and the GOLVEN–ROOT GROWTH FACTOR INSENSITIVE (GOLVEN–RGI) pathway adjust PIN2

stability and plasma-membrane abundance (Baster *et al.*, 2013; Löfke *et al.*, 2013; Xu *et al.*, 2023). In parallel, Indole-3-acetic acid (IAA) carboxyl methyltransferase 1 (IAMT1)–mediated methylation of IAA in the endodermis restricts polar auxin transport to a concentration range permitting asymmetric distribution. In contrast, methyl esterase 17 (MES17)–mediated demethylation on the lower flank amplifies the active gradient through an Auxin Response Factor 7 (ARF7)–dependent feedback loop (Abbas *et al.*, 2018; Zhang *et al.*, 2022). The transcriptional response to the auxin gradient is mediated by the Auxin Response Factor (ARF) family. ARF proteins bind auxin response elements in the promoters of auxin-responsive genes and either activate or repress their transcription, depending on the individual factor (Ulmasov *et al.*, 1997; Chandler, 2016). Auxin Response Factor 1 (ARF1) was the first member of this family to be characterized as a direct auxin-response-element-binding factor (Ulmasov *et al.*, 1997) and was selected in the present work as a marker to monitor auxin signaling activity.

Once established, this gradient must be converted into a physical response. The cellular machinery that translates unequal auxin distribution into the differential elongation underlying curvature is the subject of the following section.

1.2.4 Differential Growth Response

Differential cell elongation in the elongation zone represents the final effector phase of gravitropism. In roots, auxin accumulation on the lower side inhibits cell elongation relative to the upper side, which results in downward curvature. In shoots, higher auxin levels generally stimulate elongation on the lower side and thereby promote upward bending (Boonsirichai *et al.*, 2002; Löfke *et al.*, 2013; Su *et al.*, 2017; Xu *et al.*, 2023; Figure 2). This organ-specific difference reflects distinct auxin dose–response relationships in root and shoot tissues.

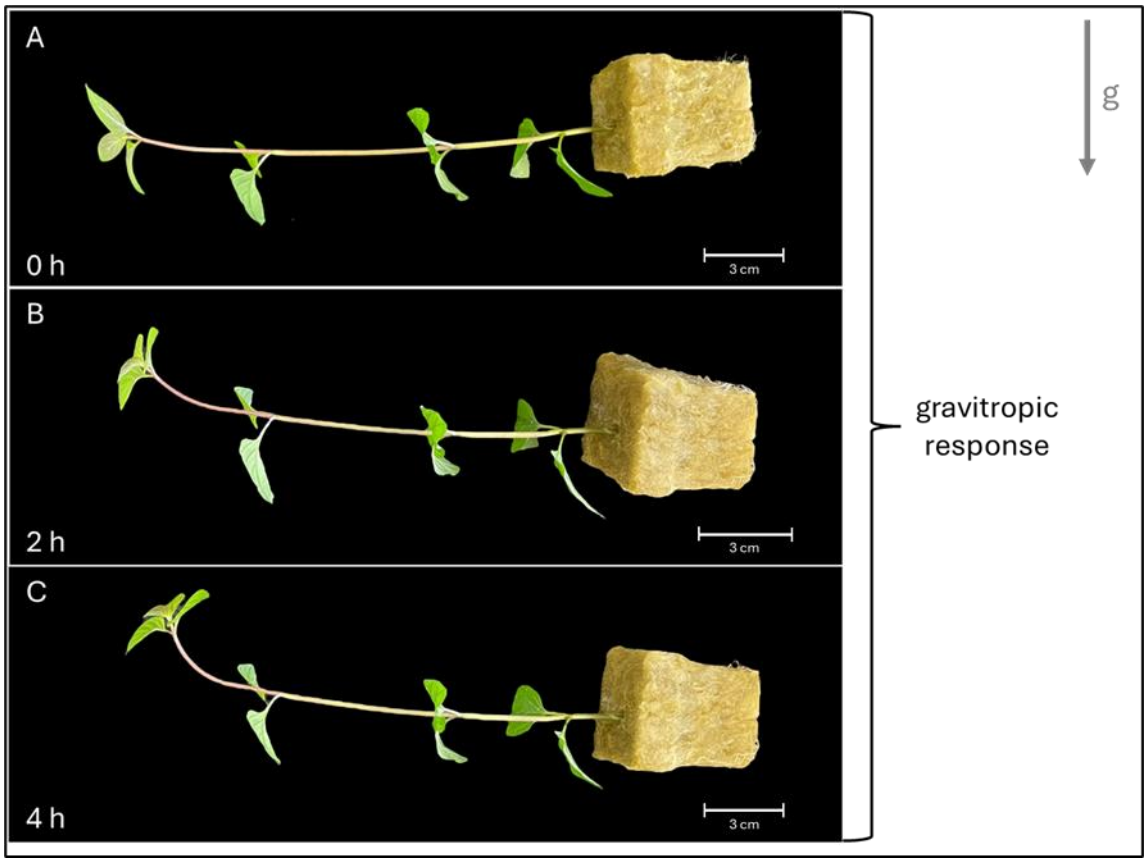

Figure 2 Shoot gravitropic response of *Mentha* × *piperita* following gravistimulation. *(A) Immediately after 90° reorientation (0 h), the shoot is horizontally positioned. (B) After 2 h, an upward curvature of the shoot apex becomes apparent. (C) After 4 h, the shoot has largely reestablished a vertical growth orientation. The direction of gravity (g) is indicated by the arrow. Scale bars = 3 cm.*

At the cellular level, differential elongation is mediated by the orientation of cellulose microfibrils in the cell wall. Cellulose synthase complexes move within the plasma membrane along tracks defined by cortical microtubules. They deposit microfibrils parallel to the underlying microtubule array (Paredez *et al.*, 2006; Li *et al.*, 2012). A predominantly transverse orientation of microfibrils relative to the cell's long axis reinforces the wall laterally. At the same time, it permits longitudinal extension under turgor pressure. This orientation is therefore characteristic of actively elongating cells (Burk and Ye, 2002; Crowell *et al.*, 2011). Auxin asymmetry translates into differential growth in part by sustaining transverse microtubule orientation on the elongating flank. This sustained orientation maintains the wall architecture required for continued cell extension (Nick *et al.*, 1990a). The link between cell elongation and cellulose orientation is also developmental. In elongating apical tissues, microfibrils on the inner cell wall face are deposited transversely. In contrast, mature, non-elongating basal tissues show predominantly longitudinal orientation (Takeda and Shibaoka, 1981; Kerstens and Verbelen, 2002). This orientation pattern can be visualized in situ by polarization microscopy.

The method exploits the birefringence of crystalline cellulose to reveal the net microfibril direction (Verbelen and Stickens, 1995).

The auxin gradient alone, however, is quantitatively insufficient to account for the differential growth it is thought to drive. The lateral difference in auxin concentration between the two flanks is comparatively modest, whereas the resulting difference in growth rate is far larger (Digby and Firn, 1976; Gutjahr *et al.*, 2005). Because cell elongation scales approximately with the logarithm of auxin concentration, the gradient cannot produce a growth differential of this magnitude on its own. This discrepancy implies that the auxin gradient must be amplified by a second gradient, namely one of tissue sensitivity to auxin (Brauner and Hager, 1958; Salisbury *et al.*, 1988; Rorabaugh and Salisbury, 1989). Jasmonic acid (JA) has been identified as a candidate modulator of this responsiveness (Gutjahr *et al.*, 2005), and its role is examined in the following section.

1.2.5 The Role of Jasmonic Acid in Gravitropism

In rice coleoptiles, Gutjahr *et al*., (2005) showed that gravitropic stimulation induces both an overall rise in jasmonate content and the formation of a JA gradient oriented opposite to the auxin gradient. The higher JA levels coincided with the upper, growth-inhibited flank. Split-segment assays in the same study demonstrated that gravistimulation alters the responsiveness of the two flanks to exogenous auxin. The lower flank continues to respond normally. In contrast, the upper flank loses its capacity to react. This spatial pattern is consistent with a localized JA-mediated inhibition of auxin responsiveness in the upper flank. Importantly, the JA gradient still formed when lateral auxin transport was blocked by N-1-naphthylphthalamic acid (NPA). This indicates that JA accumulation is induced independently of the auxin gradient, rather than as a downstream consequence of it. Functionally, JA is not strictly required for gravitropic bending. The JA-deficient rice mutant *hebiba* still curves, albeit with a marked delay. Exogenous flooding with methyl jasmonate also delays the onset of bending (Gutjahr *et al.*, 2005). JA therefore acts as an accelerator and amplifier of the gravitropic response by sharpening the effective growth differential between the two flanks. It is not an indispensable signal.

A complementary role for jasmonate has been described in root gravitropism. Sun *et al.*, (2011) showed that methyl jasmonate affects PIN2 endocytosis and plasma membrane abundance in *Arabidopsis* roots. It also impairs the formation of the asymmetric DR5rev:GFP reporter pattern after gravistimulation. This suggests that JA can influence root gravitropic responses through modulation of PIN2-dependent auxin redistribution. Taken together, jasmonate appears to

modulate gravitropic curvature through at least two mechanistically distinct routes: modulation of auxin responsiveness in shoots and modulation of polar auxin transport in roots. This dual role is consistent with a general function of JA as a tuning signal of the gravitropic response.

Taken together, these mechanisms describe a complete sensory pathway. Gravity is perceived through statolith sedimentation in the statocytes, transduced into a lateral auxin gradient whose effect is sharpened by a gradient of tissue sensitivity, and executed as differential elongation in growth-competent tissue. Crucially, this pathway is not a single-use developmental switch but a system that is re-engaged each time the organ is reoriented. This raises the possibility that reorientation might be applied not merely as an experimental probe of plant movement, but as a deliberate and repeatable input - a perspective developed in the following section.

1.3 From Gravitropic Response to Gravitropic Stimulation

The preceding sections describe gravitropism as the plant's response to displacement. The same pathway, however, can be read in the opposite direction - as a system that can be driven deliberately by imposing controlled, repeated reorientation.

If reorientation is treated as an input rather than a disturbance, the relevant question becomes what that input changes. For any cultivation purpose, two outputs matter: the quantity of plant material a crop produces and its chemical composition. Both are demonstrably sensitive to the gravitational environment. Changes in gravitational orientation consistently promote biomass accumulation across diverse experimental paradigms, with clinorotation increasing hypocotyl and root dry weight in *Veronica arvensis* (Driss-Ecole *et al.*, 1994) and hypergravity increasing total dry mass in *Arabidopsis thaliana* (Ohara *et al.*, 2024). Secondary metabolite responses are less uniform but equally real, with small secondary metabolites tending to accumulate under microgravity and profiles shifting under hypergravity, reflecting both mechanical loading and gravity-related changes in the cellular environment (Tuominen *et al.*, 2009). At the molecular level, exposure to microgravity reprograms gene expression in a manner that predominantly affects defense systems against abiotic stress (Medina *et al.*, 2023), suggesting that a changed gravitational input is routed in part through the stress-responsive signaling closely tied to secondary metabolite production.

Gravitropism has not gone unexploited as an agronomic lever, yet the ways in which it has been harnessed are revealing. It is manipulated as a breeding target, where the gravitropic set-point angle (GSA) controlled by the IGT gene family (LAZY, DEEPER ROOTING 1, and TILLER ANGLE CONTROL 1) is altered to optimize root system architecture and nutrient acquisition

on marginal soils (Waite and Dardick, 2021; Chin and Blancaflor, 2022). It is a process to be suppressed, as in the postharvest handling of cut flowers, where gravitropic bending of horizontally stored stems represents a major commercial problem to be prevented (Philosoph-Hadas, 1999). And it is a constraint to be engineered around, as in space farming, where the orienting function of gravity must be replaced by other cues such as light (Medina *et al.*, 2023). In each case gravitropism is treated as a trait to select, a problem to eliminate, or a constraint to circumvent. Its use as a controllable stimulus, applied under normal gravity to deliberately enhance the metabolic output of a crop, remains essentially unexplored.

Testing this possibility requires a model system in which both output axes are not only measurable but agronomically meaningful - a crop whose commercial value resides directly in a secondary metabolite profile that quality demands hold to a defined standard. Peppermint, a plant prized for an essential oil whose commercial worth depends on a composition that is highly sensitive to growing conditions, is such a candidate.

1.4 Peppermint as a Model Medicinal and Aromatic Plant

Peppermint (*Mentha* × *piperita* L.) is a member of the Lamiaceae and one of the most widely used medicinal and aromatic plants. It is grown for the pharmaceutical, food, and cosmetic industries (Mahendran and Rahman, 2020; Wei *et al.*, 2023). Its economic value comes almost entirely from its essential oil and the oil's main constituent, menthol. The global peppermint oil market exceeds USD 220 million, and menthol holds a large share of the flavor and fragrance trade (Song *et al.*, 2026). This demand has driven interest in higher oil yields and in chemotypes with tailored chemical profiles (Gupta *et al.*, 2023).

Peppermint is a natural hybrid of watermint (*Mentha aquatica* L.) and spearmint (*Mentha spicata* L.). It is propagated predominantly vegetatively via stolons and stem cuttings (Rita and Animesh, 2011; Ahkami *et al.*, 2015). Two features of this biology suit the present study. First, the plant is sterile and hexaploid (2n = 72), which severely limits classical breeding. Non-genetic approaches such as environmental control and elicitation therefore become the practical route to improving oil traits (Lange *et al.*, 2011; Fuchs *et al.*, 2022). Second, vegetative propagation produces clonally uniform plants. This removes genotypic variation that would otherwise confound a controlled stimulation experiment.

The essential oil is the main commercial product. It is made and stored in specialized epidermal glandular trichomes (Lange *et al.*, 2011). The oil consists mainly of oxygenated p-menthane monoterpenes. Menthol is the principal component and gives peppermint its characteristic

cooling and olfactory properties (Kalemba and Synowiec, 2020). Oil quality is set by regulatory standards. These prescribe a minimum menthol content and strict upper limits for pulegone and menthofuran, both of which are hepatotoxic (Mahmoud and Croteau, 2003; European Medicines Agency, 2016). This composition is not fixed. Abiotic stress consistently shifts it toward menthofuran and away from menthol (Fuchs *et al.*, 2022; Khameneh *et al.*, 2025). Oil yield and oil composition are therefore plastic traits. Together with the trichomes that produce them, they are the measurable outputs through which a stimulus such as gravitropic reorientation could act.

1.5 Glandular Trichomes and Essential Oil as Response Traits

1.5.1 Glandular Trichomes and Oil Yield

Peppermint essential oil is produced and stored in glandular trichomes on the aerial surfaces of the plant, predominantly on the leaves (Lange *et al.*, 2011). Two trichome types occur, peltate and capitate, but the peltate glands account for the bulk of monoterpene biosynthesis and oil storage in *Mentha × piperita* (McConkey *et al.*, 2000; Turner *et al.*, 2000; Ahkami *et al.*, 2015). In these glands the oil is synthesized in a small cluster of secretory cells and accumulates in a subcuticular storage cavity. The number and density of trichomes on a leaf are directly quantifiable, which makes them a convenient structural readout of the plant's oil-producing apparatus.

Trichome formation is developmentally programmed. New peltate glands are initiated only while the leaf is still expanding, and initiation ceases once expansion stops (Turner *et al.*, 2000). Because leaf maturation proceeds basipetally, gland production halts first near the apex, while the younger basal regions remain active in initiation. Trichome number is therefore tightly coupled to leaf age and to the progress of leaf expansion. Density is further modulated by the environment and by hormonal signals. Photoperiod alters the number and size of peltate glands (Kılıç and Tarakci, 2018), light intensity co-regulates trichome density and oil content (Souza *et al.*, 2016), and exogenous epibrassinolide increases both trichome density and menthol yield (Parrey *et al.*, 2023).

Oil yield is not set by trichome number alone. It reflects two largely independent levers: how many trichomes a leaf carries, and the biosynthetic capacity of each individual gland. Monoterpene biosynthesis rate has been identified as the principal factor controlling oil accumulation, with enzyme activity inside the gland cells as the key regulatory level (Gershenzon *et al.*, 2000). Consistent with this, trichome number and oil productivity are

positively correlated across genotypes and peak together during rapid leaf expansion (Mishra *et al.*, 2017; Mishra *et al.*, 2021). Mathematical modeling separates the two outputs cleanly: oil yield is most sensitive to trichome density and distribution, whereas oil composition depends more on the concentrations of the biosynthetic enzymes within the glands (Rios-Estepa *et al.*, 2010). Trichome number, per-trichome biosynthetic capacity, and composition are therefore three separate output axes, each open to modulation by a stimulus.

1.5.2 Essential Oil Composition and the Biosynthetic Branch Point

The chemical composition of the oil is its second quantifiable output, and the one that determines commercial quality. Peppermint oil consists mainly of oxygenated p-menthane monoterpenes. Menthol is the principal constituent and typically makes up 30–70 % of the oil. It is accompanied by menthone, menthyl acetate, and menthofuran, together with smaller amounts of limonene, pulegone, Pinene, Eucalyptol and related compounds (Kalemba and Synowiec, 2020; Hudz *et al.*, 2023). This profile is not static during leaf development. Young leaves are richer in menthone, while menthol accumulates later as the leaf matures (McConkey *et al.*, 2000; Kalemba and Synowiec, 2020). The shift reflects the temporal order in which the biosynthetic enzymes reach peak activity, with the menthol-forming step engaged later than the upstream reactions (McConkey *et al.*, 2000).

The monoterpenes are assembled along a well-characterized pathway that is distributed across several subcellular compartments within the secretory cells (Croteau *et al.*, 2005). The universal precursor geranyl diphosphate (GPP) is cyclized to limonene and then converted through a series of oxidation and reduction steps to the central intermediate pulegone. The complete sequence of enzymatic reactions and their compartmentalization is shown in Figure 3.

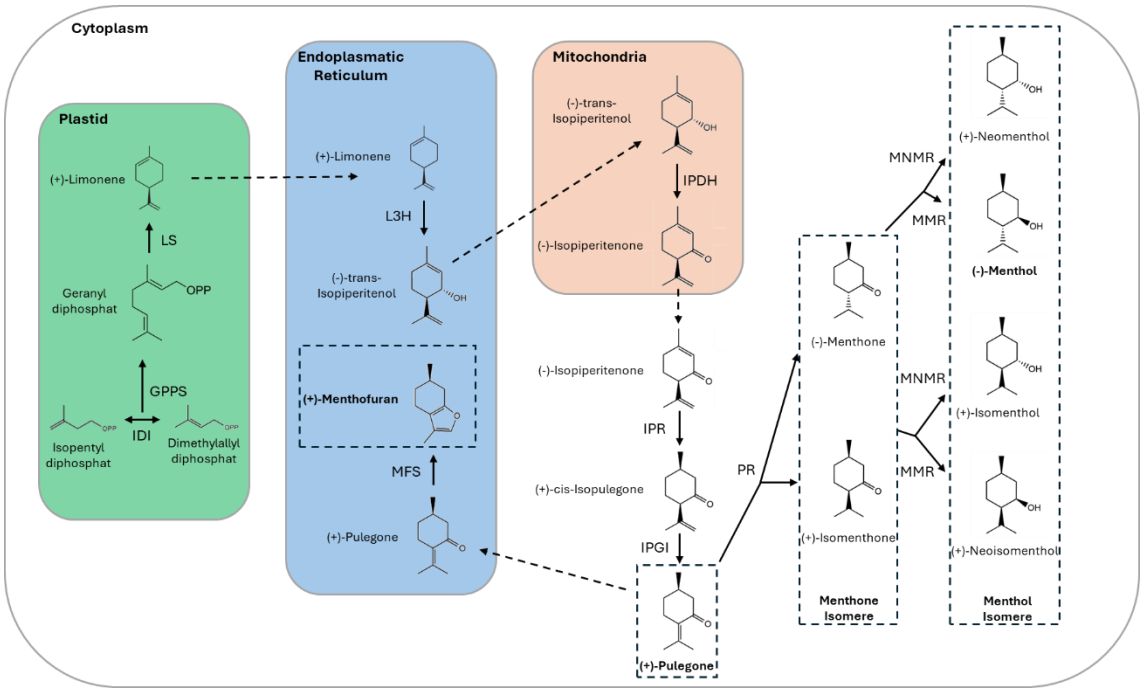

Figure 3 Biosynthetic pathway of (−)-menthol in peppermint *(Mentha × piperita)*. *The pathway proceeds from the universal monoterpene precursors isopentenyl diphosphate (IPP) and dimethylallyl diphosphate (DMAPP) through eight enzymatic steps distributed across four subcellular compartments. Solid arrows indicate enzymatic reactions. Dashed arrows indicate transport between compartments. The branch-point intermediate (+)-pulegone is highlighted by a dashed box. From this branch point, one route leads via menthofuran synthase (MFS) to the undesirable by-product (+)-menthofuran, which is also marked by a dashed box. The main reductive branch proceeds via pulegone reductase (PR) toward (−)-menthol as the principal end product. Abbreviations: IDI, isopentenyl diphosphate isomerase; GPPS, geranyl diphosphate synthase; LS, limonene synthase; L3H, limonene-3-hydroxylase; IPDH, isopiperitenol dehydrogenase; IPR, isopiperitenone reductase; IPGI, isopulegone isomerase; PR, pulegone reductase; MFS, menthofuran synthase; MMR, menthone:menthol reductase; MNMR, menthone:neomenthol reductase.*

Pulegone occupies the decisive position in the pathway. It is a branch point at which two competing enzymes determine the fate of the oil. Pulegone reductase (PR) directs flux along the main reductive route toward menthone and ultimately menthol, the desirable end product. Menthofuran synthase (MFS) diverts pulegone toward menthofuran, the toxicologically undesirable by-product (Mahmoud and Croteau, 2003; Figure 3). The relative activity of these two enzymes therefore sets the balance between the compounds that define oil quality. A superior oil is high in menthol and low in pulegone and menthofuran (Nair, 2001; Mahmoud and Croteau, 2003). Any factor that shifts the PR/MFS balance changes the commercial value of the product directly. Oil composition is thus not only a measurable trait but a sensitive reporter of the metabolic state of the gland.

1.5.3 Jasmonate as the Link between Stimulus and Metabolic Response

The trichome and oil traits described above share a common regulator: jasmonic acid (JA), the phytohormone introduced earlier as an amplifier of the gravitropic response. In peppermint, JA acts directly on these output axes. Exogenous methyl jasmonate (MeJA) increases peltate

trichome density and raises essential oil production several-fold at millimolar concentrations (Cappellari *et al.*, 2019). It also reaches into the compositional branch point. MeJA induces the transcription of both PR and MFS, with PR responding earlier than MFS (Afkar *et al.*, 2013; Afkar and Karimzadeh, 2025). Because the relative activity of these two enzymes sets the menthol-to-menthofuran balance, JA governs oil composition as well as oil quantity. The same signal therefore reaches all three output axes defined above.

These responses rest on a conserved signaling mechanism. JA is a lipid-derived compound produced through the octadecanoid pathway. The pathway begins with the release of α-linolenic acid from membrane lipids and its conversion by lipoxygenase (LOX), the first committed step, through a series of reactions to JA. JA is then conjugated to isoleucine to form jasmonoyl-L-isoleucine (JA-Ile), the bioactive ligand of the canonical pathway. JA can also be methylated to methyl jasmonate (MeJA), a volatile derivative that is largely reconverted to JA after uptake into plant tissue and therefore feeds into the same signaling pathway (Wasternack and Song, 2017; Ruan *et al.*, 2019). Signaling proceeds by depression. In the absence of bioactive jasmonate, JASMONATE ZIM-DOMAIN (JAZ) proteins repress downstream transcription factors. When JA-Ile accumulates, it promotes the binding of JAZ to the F-box receptor CORONATINE INSENSITIVE 1 (COI1), after which the JAZ repressors are degraded by the 26S proteasome. This releases the transcription factors, including the MYB- and bHLH-type factors that link JA signaling to trichome development, and switches on JA-responsive genes (Chini *et al.*, 2007; Thines *et al.*, 2007; Pauwels and Goossens, 2011; Chalvin *et al.*, 2020). The JAZ genes are themselves induced by this activation, so JAZ transcript level rises with pathway activity and serves as a reliable marker of JA signaling (Chini *et al.*, 2007; Thines *et al.*, 2007).

JA thus sits at the convergence of the stimulus and its measurable outputs, and it can be probed pharmacologically from both directions. Exogenous MeJA activates the pathway and tests whether JA signaling is sufficient to reproduce a given response. Phenidone does the opposite. By inhibiting lipoxygenase, the first committed step, it lowers endogenous JA and tests whether JA biosynthesis is necessary (Engelberth, 2011). Together these two tools allow the contribution of JA to be dissected in either direction.

Directing these traits through a single signaling pathway is only useful, however, if the cultivation environment is controlled tightly enough to apply the stimulus reliably and to reproduce its effect.

1.6 Controlled environment agriculture and high-value crops

Controlled environment agriculture (CEA) addresses this by decoupling production from external conditions. Temperature, humidity, light, and nutrient supply are managed precisely, across systems that range from climate-controlled greenhouses to fully enclosed plant factories and vertical farms (Touliatos *et al.*, 2016; Reimann *et al.*, 2018; Dsouza *et al.*, 2025). These systems differ mainly in how water and nutrients reach the roots. In soil- or substrate-based systems, the roots are anchored in a solid medium that holds the nutrient solution. In hydroponic systems, the roots sit directly in a circulating nutrient solution. In aeroponic systems, the roots hang freely in air and are supplied by intermittent mist cycles (Hayden *et al.*, 2004; Giurgiu *et al.*, 2017).

For medicinal plants, CEA has to deliver on two fronts at once. The optimized conditions accelerate growth, increase biomass, and shorten production cycles (Giurgiu *et al.*, 2017; Gaja *et al.*, 2023). At the same time, they yield phytochemically consistent material from batch to batch (Zobayed *et al.*, 2005; Reimann *et al.*, 2018). Indoor cultivation is only worthwhile when a crop grows both faster and to a more reliable quality than in the field. The same precise control also turns the environment into a tool. Defined stress or elicitor treatments can be applied deliberately and repeatably. Moderate abiotic stress, for example, often raises the concentration of pharmacologically relevant compounds (Naik and Al–Khayri, 2016; Shil and Dewanjee, 2022).

This level of control is expensive. High capital investment, together with the operating costs of artificial lighting and climate management, makes CEA difficult to justify economically (Engler and Krarti, 2021; Bhattarai *et al.*, 2025). The systems that dominate the sector today grow leafy greens such as lettuce and microgreens. These crops have very short production cycles, which lets them turn over quickly and absorb the high running costs (Dsouza *et al.*, 2023). High-value medicinal and aromatic plants are a more difficult case. Their cycles are typically much longer, so each cycle must return more to remain viable. This makes the economics work only where cultivation delivers both a strong yield and a premium quality that the open field cannot match (Stutte, 2016; Gill *et al.*, 2025). Their value rests on exactly the quality and reproducibility that controlled cultivation can provide, yet they remain comparatively underexplored in CEA research (Dsouza *et al.*, 2023)(Dsouza *et al.*, 2023). Making them viable depends on strategies that modulate metabolite profiles reliably, ideally without the residues and regulatory burden that chemical elicitors carry.

1.7 Gravitropic stimulation as a non-chemical elicitation strategy in CEA

The preceding sections bring together the elements of a single hypothesis. Gravitropic reorientation transiently raises the endogenous JA content of the affected organs (Section 1.2; Gutjahr *et al.*, 2005). JA, in turn, regulates both glandular trichome development and monoterpene biosynthesis in peppermint (Section 1.5). Placed side by side, these two findings point to a direct route. Controlled, repeated reorientation could activate the same JA-dependent metabolic responses as an exogenous elicitor, but through an entirely endogenous signal. Gravitropic stimulation therefore emerges as a candidate non-chemical elicitation strategy.

Peppermint is well suited to test this idea. Its commercial value rests on an essential oil whose two measurable outputs, yield and composition, are precisely the traits that JA controls. CEA supplies the other half of the requirement. It can deliver a defined, repeatable gravitropic stimulus while holding every other growth variable constant. This is the condition for attributing any observed change specifically to the stimulus rather than to confounding variation (Reimann *et al.*, 2018). Of the three cultivation systems described above, however, only one is compatible with repeated tilting. Soil and substrate shift when the container is reoriented, and hydroponic solution spills. Aeroponics avoids both problems. The roots hang freely and are misted in cycles that do not depend on orientation, so the plant can be tilted at will without interrupting the nutrient supply (Hayden *et al.*, 2004).

Two features make the approach particularly attractive. Because the stimulus acts through an endogenous signal, it leaves no residue in the plant or the system, and it avoids the regulatory clearance that a chemical elicitor would require. And because reorientation is purely mechanical, it can be automated and scaled within an existing CEA facility. Despite this combination, gravitropic stimulation has not been investigated as a deliberate elicitation strategy for medicinal plant production.

1.8 Aims of the Study

The present doctoral project investigates the potential of gravitropic stimulation as a non-invasive elicitation strategy for medicinal plant production in CEA. Several research questions were addressed:

- **How does *Mentha* × *piperita* perceive and respond to gravitropic stimulation?** The gravitropic response chain should be characterized specifically for peppermint. This includes statolith-mediated gravity perception, signal transduction, and differential shoot growth. The analysis should also identify which internodes retain gravitropic competence and determine the kinetics of shoot reorientation.
- **Can targeted gravitropic stimulation enhance biomass accumulation and secondary metabolite production in peppermint under CEA conditions?** Custom-built aeroponic tilting modules should be used to systematically vary key stimulation parameters. These parameters include tilt angle, duration, frequency, and light conditions. Their effects should be determined on plant morphology, biomass, glandular trichome density and number, essential oil yield, and oil composition with respect to menthol, menthone, and menthofuran.
- **Is jasmonic acid the causal mediator of gravitropism-induced changes in secondary metabolism?** The role of JA should be tested pharmacologically. Exogenous MeJA application should assess whether the gravitropic hormonal signal alone is sufficient to replicate the observed effects. Phenidone-mediated inhibition of JA biosynthesis should determine whether endogenous JA production is required for the gravitropic induction of glandular trichome formation and essential oil changes.

Figure 4 summarizes the conceptual framework and the experimental strategy of this work, from the gravitropic stimulus applied under CEA, through the proposed biological response layers, to the measured biomass, trichome and oil traits and the pharmacological tests of jasmonate involvement.

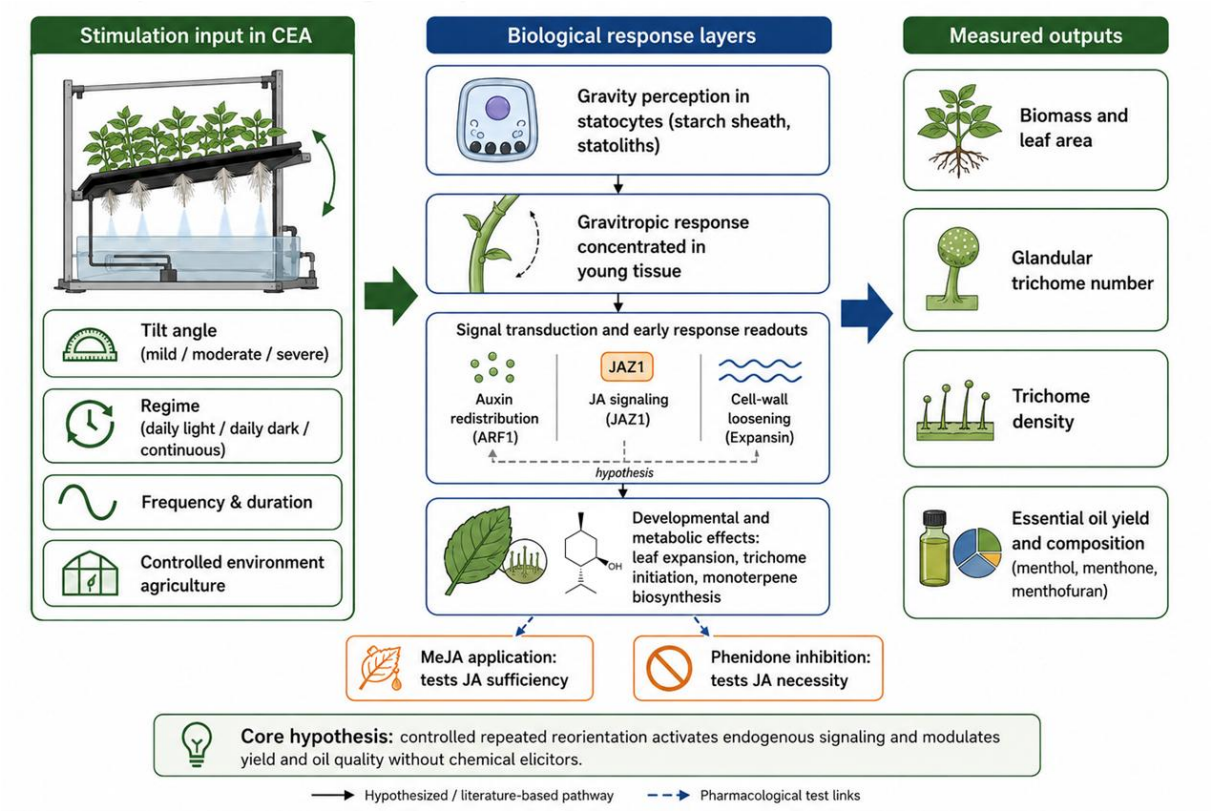

Figure 4 Conceptual framework of this work: gravitropic stimulation as a non-chemical elicitor in *Mentha* × *piperita*. *Repeated reorientation is applied as a controllable input under controlled environment agriculture (CEA), defined by tilt angle, regime, frequency and duration (left). The stimulus is proposed to act through successive biological response layers (centre): gravity perception in statocytes, a gravitropic response concentrated in young tissue, and a signal transduction step read out through three markers, auxin redistribution (ARF1), JA signaling (JAZ1) and cell-wall loosening (Expansin). These converge on developmental and metabolic effects, including leaf expansion, glandular trichome initiation and monoterpene biosynthesis, which are quantified as the measured outputs of biomass and leaf area, glandular trichome number and density, and essential oil yield and composition (right). The role of jasmonic acid is tested pharmacologically, with methyl jasmonate (MeJA) probing sufficiency and phenidone probing necessity. Solid arrows denote the hypothesized, literature-based pathway rather than relationships established in this work. Dashed blue arrows indicate the pharmacological test points.*

2 Materials and Methods

2.1 Plant Material and Propagation

All experiments were conducted with *Mentha* × *piperita* (KIT accession no. 5393, origin: JKIP KIT), maintained as mother plants in the greenhouse of the Botanical Garden of the Karlsruhe Institute of Technology (KIT). For cutting preparation, shoots were severed directly above the fourth apical leaf pair and transferred into a water mixture of Karlsruhe tap water and deionized water adjusted to an electrical conductivity (EC) of approximately 0.25 mS/cm.

Two rooting supports were used over the course of the project. In the rockwool setup, the lower portion of the shoot was fully embedded up to the next leaf pair, with the block standing directly in the water mixture and supplying the plant by capillary action. The neoprene plug setup held only a small section of the shoot directly below the next leaf pair, leaving the remainder freely

suspended above the water surface. Both methods resulted in comparable plant growth. Rockwool was used in initial experiments but subsequently replaced by reusable neoprene plugs, owing to the considerably higher energy demands associated with its production and disposal.

After one week of rooting in the greenhouse, cuttings were transferred to the experimental modules. The anatomical organization of the shoot, including the positions of apical leaf pairs and internodes used for tissue sampling and curvature measurements, is shown in Figure 5.

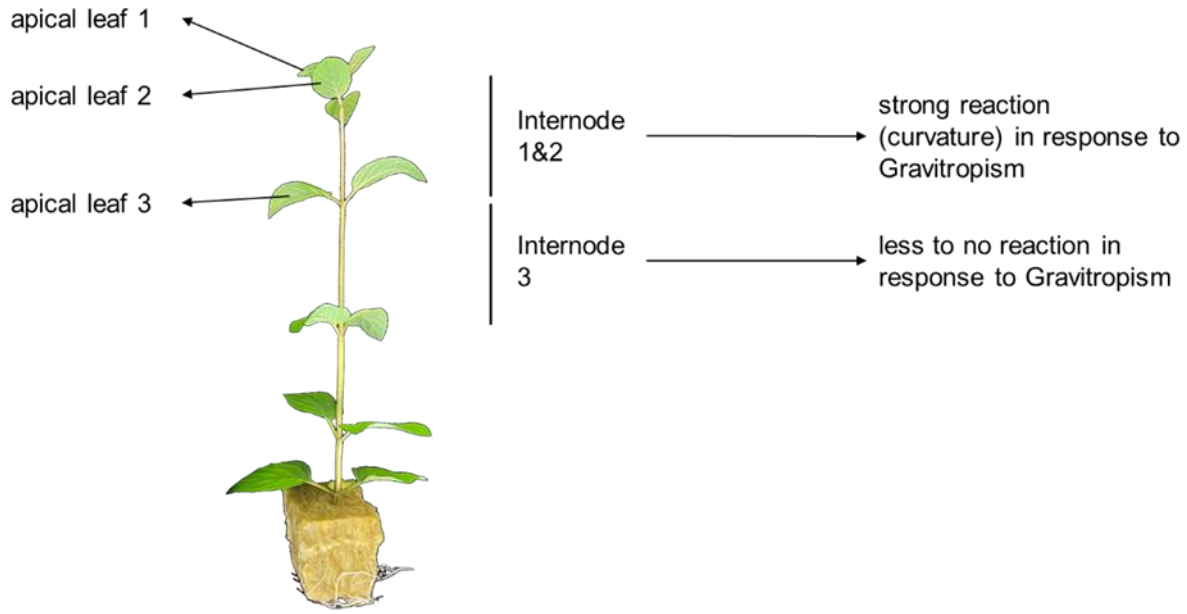

Figure 5 Schematic overview of *Mentha* × *piperita* shoot anatomy and gravitropic responsiveness. *Apical leaf pairs (lp1–3) and internodes (1&2 and 3) are indicated. Internodes 1 and 2 show a strong curvature response to gravitropic stimulation . Internode 3 shows little to no response.*

2.2 Aeroponic tilting modules

Following the rooting phase, plants were transferred to custom-built aeroponic tilting modules designed for controlled environment agriculture (CEA). Each module consisted of a deep Eurobox (60 × 40 × 42 cm, L × W × H) serving as the root and nutrient chamber, topped by a shallower Eurobox (60 × 40 × 7 cm) whose lid contained 11 evenly distributed circular openings (diameter 5 cm). Plants held in 3D-printed pots with either rockwool blocks or neoprene plugs were inserted into these openings. The overall module design is shown in Figure 6.

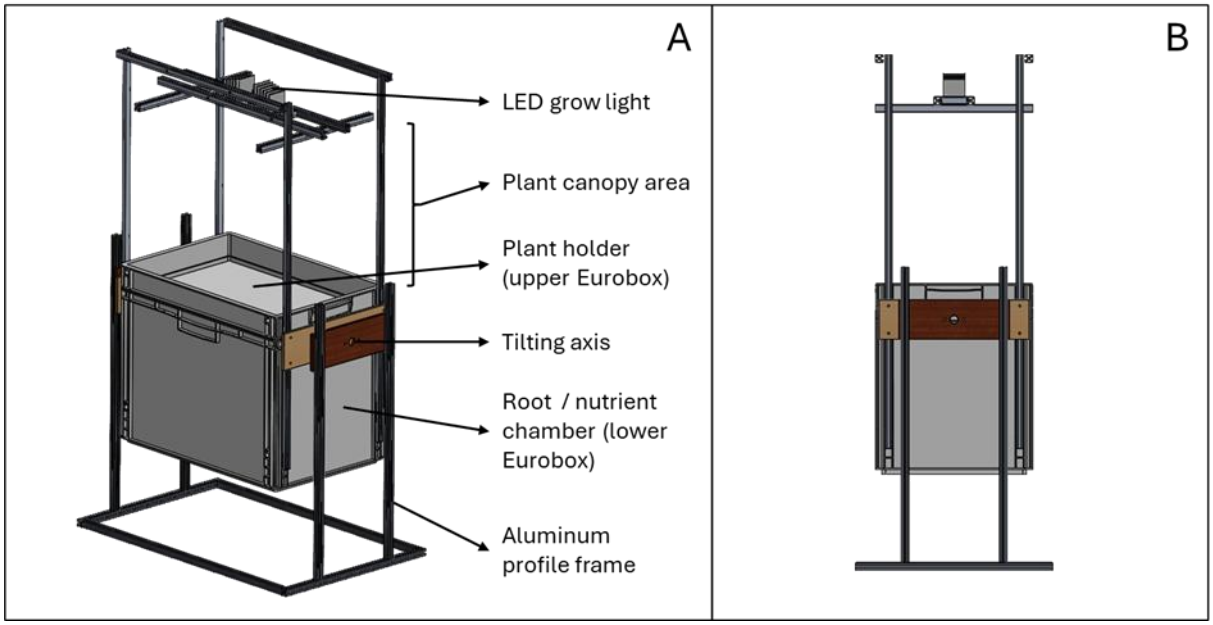

Figure 6 CAD design of the custom-built CEA tilting module in upright position. *(A) Isometric view with key components labelled: LED grow light, plant canopy area, plant holder (upper Eurobox), tilting axis, root/nutrient chamber (lower Eurobox), and aluminum profile frame. (B) Front view. The module is driven by a stepper motor-controlled tilting mechanism. This mechanism allows positioning at defined angles between 0° and 90°.*

Six Netafim Coolnet spray nozzles (flow rate 7.5 l/h) were mounted on the floor of the lower chamber to deliver the nutrient solution aeroponically. Tilting was controlled by a stepper motor driven by an Arduino-based system, allowing the module to be positioned at any angle between 0° and 90° in increments of 15°. The LED grow light (SanLight Q1W DIM EU) was structurally connected to the module frame and tilted together with the plants, ensuring consistent illumination from the adaxial side at all tilt angles (Figure 7).

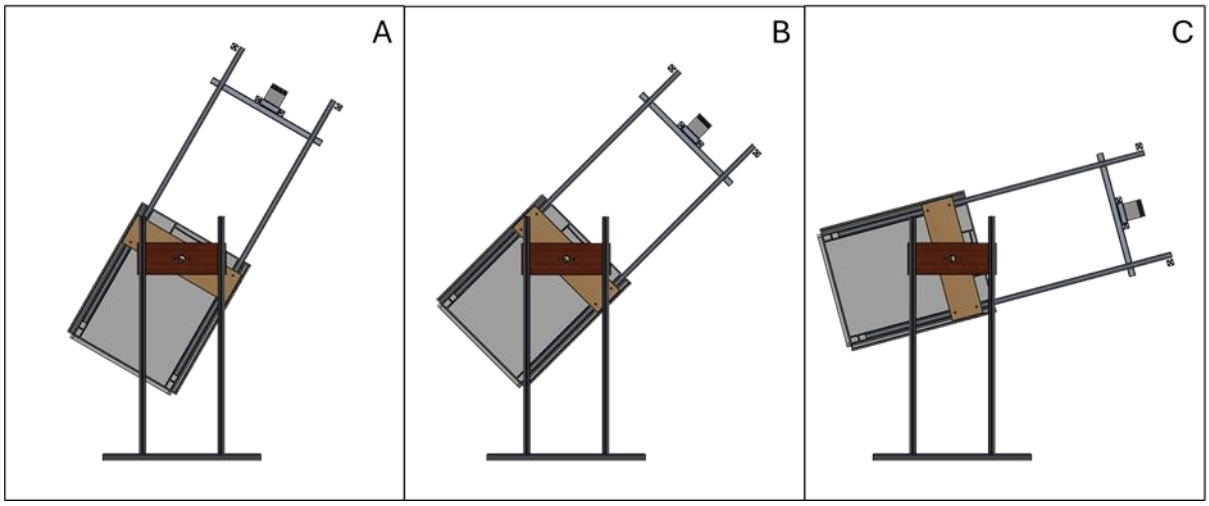

Figure 7 CAD front views of the CEA tilting module at the three experimental tilt angles. *(A) 30° , (B) 45° and (C) 75° from the vertical axis. Negative angles (−30°, −45°, −75°) are mirror images of the respective positive angles. The Eurobox and LED grow light tilt together. The aluminum profile frame remains stationary.*

Over the course of the doctoral project, the setup was iteratively refined. Modifications included adjustments to spray nozzle number, the addition of white reflective panels for more homogeneous light distribution, changes in lamp distance, and optimization of tilting duration, angle, and frequency. Earlier iterations employed angles including 54°, which appear in selected experiments reported throughout this work.

2.3 Controlled-environment cultivation conditions

The modules were housed in a climate-controlled room maintained at 24 °C. Plants received 16 hours of light per day from a dedicated LED grow light (SanLight Q1W DIM EU) mounted approximately 50 cm above the plant canopy, providing a light intensity of approximately 150 µmol/m²/s and a daily light integral (DLI) of 8.64 mol/m²/d. The nutrient solution was prepared using deionized water supplemented with Terra Aquatica TriPart fertilizer according to the vegetative growth schedule (1.8 ml/l Grow, 1.2 ml/l Micro, 0.6 ml/l Bloom), with the pH adjusted to 6.0–6.5. Irrigation cycles ran for 30 seconds every 10 minutes at approximately 4 bar.

2.4 Experimental overview

This study comprised two complementary lines of investigation. The first examined the effects of gravitropic stimulation on plant growth, glandular trichome formation, and essential oil composition using the aeroponic tilting system described above. The second line tested whether jasmonic acid acts as a mediator of these gravitropic effects, through both exogenous hormone application and pharmacological inhibition of JA biosynthesis. Both lines of investigation used the same plant material and cultivation conditions, with differences in treatment design described in the respective sections below. The general timeline of the experimental procedure, comprising a one-week rooting phase, a one-week acclimatization phase in the tilting modules, and a two-week experimental phase, is shown in Figure 8.

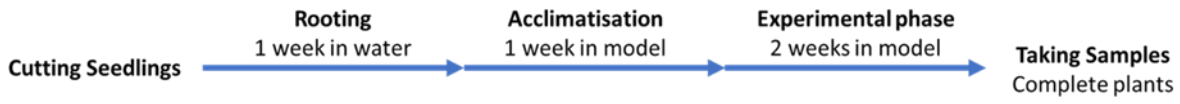

Figure 8 Timeline of the experimental procedure. *Cuttings were rooted for one week in water. This was followed by a one-week acclimatization phase in the tilting module. A two-week experimental phase concluded the procedure, after which complete plants were harvested*

2.5 Gravitropic stimulation experiments

Four tilt angles were used to impose defined levels of gravitropic stress: mild (27°/30°), moderate (45°/54°), severe (75°), and extreme (90°), as illustrated in Figure 9. After the one-week acclimatization period in the tilting modules, the two-week experimental phase commenced.

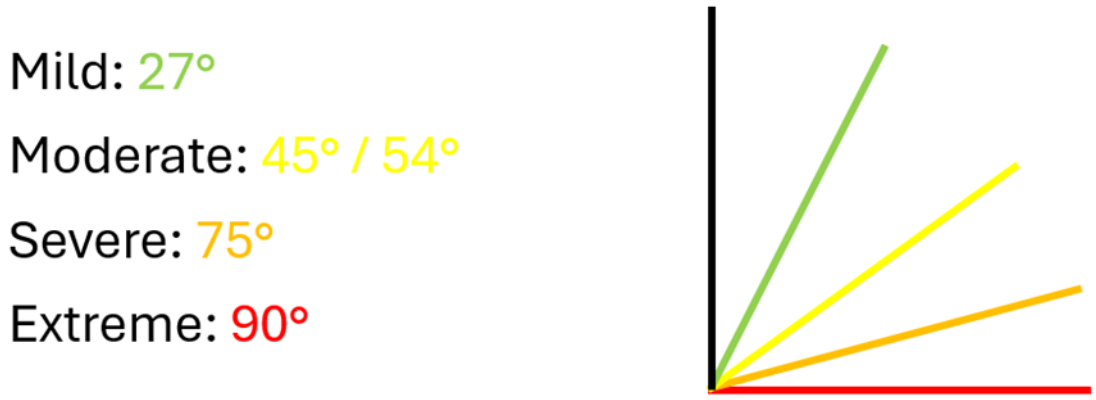

Figure 9 Gravitropic stress levels and corresponding tilt angles used in this study. *Tilt angles are categorized as mild (27°/30°), moderate (45°/54°), severe (75°) and extreme (90°) gravitropic stress. The visual representation shows the respective angles relative to the vertical axis.*

Three tilting protocols were applied across separate experimental runs, differing in the timing and continuity of the gravitropic stimulus.

In the standard protocol (daily tilting in light), plants were tilted to one side for 4 hours and then to the opposite side for 4 hours during the light phase, before returning to the upright position for the remaining hours of the daily cycle. This alternating scheme was repeated daily throughout the two-week period and is illustrated in Figure 10.

In the second protocol (daily tilting in darkness), the same alternating scheme of 4 hours per side was applied during the 8-hour dark phase, while plants remained upright throughout the light phase. This protocol applied the gravitropic stimulus in the absence of light, allowing the effect of the light environment during stimulation to be assessed.

In the third protocol (continuous tilting), plants were tilted alternately to opposite sides every 4 hours without returning to an upright resting position, continuously across both the light and dark phases of the day–night cycle. This protocol served to assess the effect of constant gravitropic stimulation on plant development.

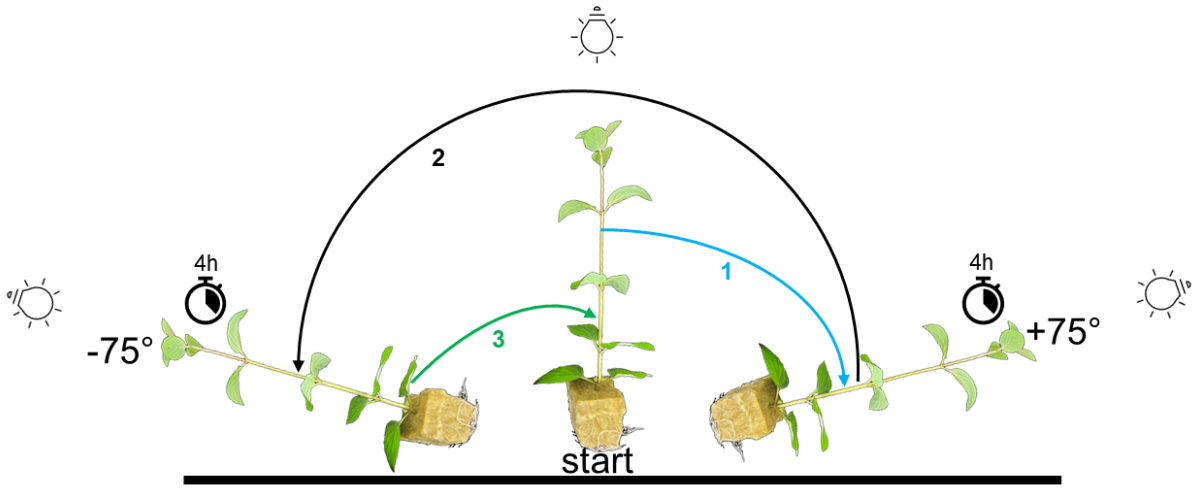

Figure 10 Schematic of the alternating tilting scheme used for gravitropic curvature measurements. *Starting from the upright position (start), plants were first tilted to +75° (1, blue arrow) and held for 4 hours under illumination from the adaxial side. Plants were then tilted to −75° (2, black arrow) for a further 4 hours. They were then returned towards the upright position (3, green arrow). The light source tilted together with the plants throughout the experiment.*

Preliminary short-term curvature experiments were conducted prior to transfer to the CEA modules to characterize the basic gravitropic response under simplified conditions. Plants held in rockwool blocks were placed in darkened cardboard boxes without active irrigation and tilted to either 90° or 45°. These experiments provided initial data on curvature kinetics and gravitropic adaptation before proceeding to the full CEA setup.

Tilting to 90° was not feasible in the aeroponic modules, as the nutrient solution could not drain back into the reservoir at that angle. Experiments at 90° were therefore conducted separately over a single day without irrigation.

2.6 Jasmonic acid intervention experiments

Two complementary pharmacological approaches were used to investigate the role of jasmonic acid in mediating the gravitropic response: exogenous application of methyl jasmonate (MeJA) to assess whether JA pathway activation is sufficient to replicate gravitropic effects, and application of the lipoxygenase inhibitor phenidone to assess whether suppression of endogenous JA biosynthesis attenuates them.

2.6.1 Methyl jasmonate treatment

MeJA treatment was conducted as part of a Master's thesis under the author's supervision (Burkard, 2023). As MeJA is volatile and transfers readily through the air, the aeroponic tilting modules could not be used. Instead, three cuttings per cylindrical glass container were rooted for 7 days in deionized water, followed by a 7-day acclimatization phase in Murashige and

Skoog (MS) medium (Duchefa Biochemie B.V., Haarlem, Netherlands; 0.143 g/400 ml) supplemented with 0.4 g/400 ml MES (Carl Roth GmbH + Co. KG, Karlsruhe, Germany) and adjusted to pH 5.8 with 1 N potassium hydroxide (Carl Roth GmbH + Co. KG, Karlsruhe, Germany) in a ventilated incubator. The experimental setup is shown in Figure 11.

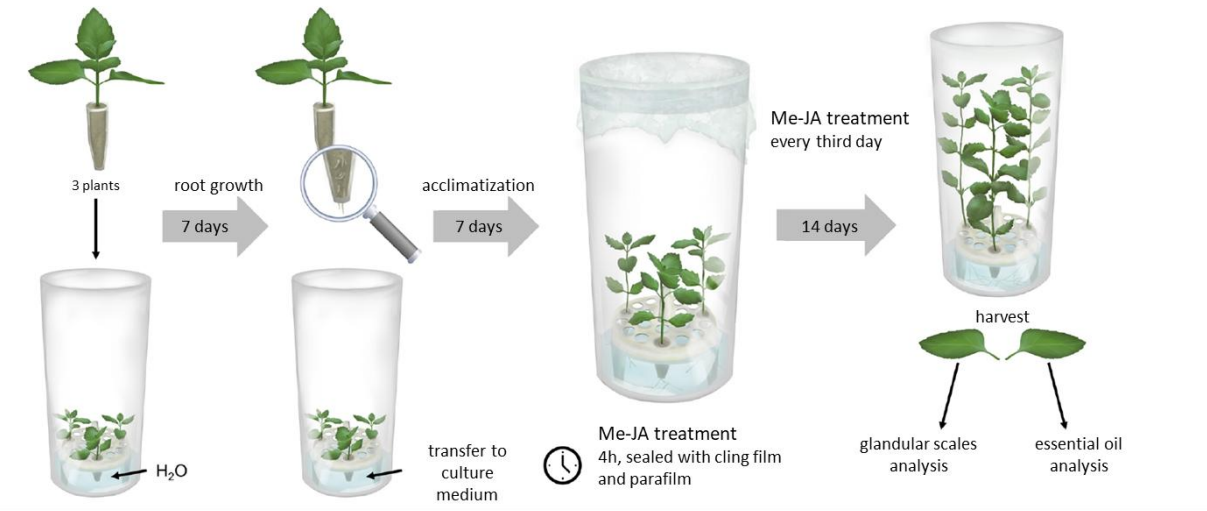

Figure 11 Schematic overview of plant cultivation and MeJA treatment procedure. *Three cuttings per container were rooted for 7 days in water. This was followed by a 7-day acclimatization phase in culture medium. During the subsequent 14-day treatment phase, plants were sprayed with MeJA solution every third day and sealed with cling film and Parafilm for 4 hours after each application. At harvest, one leaf per open leaf pair was used for glandular trichome analysis and one for essential oil analysis. Adapted from Burkard (2023).*

During the subsequent two-week treatment phase, plants were sprayed with a 100 µM MeJA solution every three days. The stock solution was prepared by dissolving MeJA (95% purity; VWR International GmbH, Darmstadt, Germany) in absolute ethanol (99.96%; Merck KGaA, Darmstadt, Germany) to 10 mM, then diluted to 100 µM in ultrapure water. Control plants received an equivalent ethanol dilution in ultrapure water. Immediately after each spray application, containers were sealed with cling film and Parafilm for 4 hours to ensure sufficient exposure while preventing transfer to control plants, then unsealed and ventilated for one hour. The nutrient medium was renewed weekly. At harvest, one leaf per open leaf pair was used for glandular trichome analysis and one for essential oil extraction in hexane with camphor as an internal standard, analyzed by GC-MS as described in section 2.12. A full description of the experimental procedure is provided in Burkard (2023).

2.6.2 Phenidone treatment

Phenidone (1-phenyl-3-pyrazolidinone; Sigma-Aldrich, Merck KGaA, Darmstadt, Germany), a lipoxygenase inhibitor that blocks JA biosynthesis, was applied to gravitropically stimulated plants to test whether endogenous JA is required for the observed responses. As phenidone is

non-volatile, plants could be cultivated in the standard aeroponic tilting modules. Four treatment groups were established: an untilted control and a tilted group (45°), each receiving either a solvent spray or a 2 mM phenidone solution prepared in ultrapure water with 0.1% Tween 20 (Sigma-Aldrich, Merck KGaA, Darmstadt, Germany) as a surfactant.

Plants were sprayed every three days throughout the two-week experimental phase. To minimize the risk of leaf burn from surfactant residue under direct light, illumination was switched off for 1.5 hours after each application before tilting commenced.

2.7 Gravitropic curvature measurement

To monitor the gravitropic response over time, plants were positioned on their side with the adaxial surface facing upward and photographed from directly above at defined time points after tilting: 0, 10, 30, 60, 120, 240, 250, 270, 300, 360, and 480 minutes, with denser sampling around the 240-minute mark to capture the response to reorientation. A ruler was placed alongside each plant in every photograph as a scale reference.

Curvature angles were measured from the photographs using ImageJ. For each image, two angles were determined relative to the same vertical reference line. The first was measured along the shoot baseline, defined as the stem axis from approximately the third to fourth internode from the apex, representing the non-curved portion of the shoot. The second was measured along a line connecting the midpoint between the two uppermost apical leaves, representing the orientation of the shoot tip at the first internode. The difference between these two angles yielded the curvature value for each time point, expressed as the change relative to t = 0 min.

To allow repeated gravitropic stimulation while minimizing cumulative stem torsion, plants were tilted to one side for 240 minutes and then to the opposite side for a further 240 minutes, as described in section 2.5. This alternating scheme maintained an approximately upright growth orientation and ensured continued optimal light interception.

Curvature experiments were conducted under two light conditions. In darkness, the pure gravitropic response could be assessed independently of phototropic effects. Under adaxial illumination, the light source tilted together with the plants, ensuring consistent light interception regardless of tilt angle. This second condition was introduced after preliminary experiments showed that static overhead lighting during tilting led to negligible biomass accumulation, likely due to suboptimal light interception.

2.8 Histology and microscopy

To investigate the anatomical basis of gravitropic perception, the first four apical internodes of *Mentha* × *piperita* shoots were harvested and processed for light microscopy. Internodal segments of approximately 0.5 cm length were cut on a wax dish, immediately transferred into labelled microcentrifuge tubes containing 1 ml of freshly prepared fixative, and fixed for 30 minutes in a 30% formaldehyde solution. Formaldehyde was chosen over paraformaldehyde (PFA) to avoid the hazardous heating steps required for PFA preparation. After fixation, samples were washed three times for 10 minutes each in PIPES wash buffer (50 mM PIPES, pH 6.0) and dehydrated through a graded ethanol series (30%, 50%, 70%, 90%, 100%). Following two overnight incubations in 100% xylene, samples were gradually infiltrated with paraffin through a xylene/paraffin series (1:1, then 1:2 overnight), with residual xylene evaporated over approximately 6 hours. Final embedding in pure paraffin for 24 hours was followed by casting in silicone molds to form paraffin blocks.

Sections of 10 µm thickness were cut from the paraffin blocks using a rotary microtome, with the blade treated with Roti®-Histol to facilitate clean sectioning. Both transverse and longitudinal sections were prepared from all four internodes, collected onto chromium-gelatin-coated glass slides (76 × 26 mm; 0.15% gelatin, 0.015% chrome alum; DIAGONAL), and dried overnight in a dust-free environment.

PAS staining

To visualize starch-containing statoliths, sections were deparaffinized through xylene, isopropanol, and a graded ethanol series down to distilled water, then stained using the Periodic Acid–Schiff (PAS) reaction according to Gerlach (1977). Sections were incubated for 5 minutes in 0.5% periodic acid solution, rinsed with tap and distilled water, incubated in Schiff's reagent for 30–60 minutes, and washed three times for 15 minutes each in SO_2 water (prepared from $K_2S_2O_5$ and 1N HCl) under a fume hood. After rinsing with tap water, sections were dehydrated through an ascending ethanol and isopropanol series, cleared in xylene, and mounted with Entellan for permanent preparation. The PAS reaction selectively stains polysaccharides, including starch grains, in magenta, allowing identification and localization of statoliths within the shoot tissue.

Polarization microscopy

To assess cellulose microfibril orientation, additional unstained sections from the same embedded material were examined under polarized light using a red gypsum compensator plate

(lambda plate). The birefringence of cellulose microfibrils produces characteristic color shifts under polarized light, allowing the relative orientation of cell wall cellulose to be compared across internode positions.

All sections were examined using a Leica DM750 light microscope (Leica Microsystems, Wetzlar, Germany) equipped with a Leica FLEXACAM C5 camera, with a polarization filter set mounted for polarization microscopy. Images were captured at a resolution of 1920 × 1080 pixels.

2.9 Gene expression analysis

Gene expression analyses were conducted as part of a dedicated single-day experiment, separate from the two-week tilting experiments described in section 2.5. Plants were cultivated and tilted according to the standard protocol, but harvested at defined time points within a single day rather than at the end of a two-week period. At each time point, shoot segments of internodes 1–2 and 3, as well as apical leaf pairs 1 and 2, were collected, immediately frozen in liquid nitrogen, and stored at −80 °C until RNA extraction. The anatomical positions of the sampled tissues are shown in Figure 5. Whole internodes were processed without separating upper and lower flanks, meaning that differential expression confined to one flank would not be resolved by this approach. The primers used for all gene expression analyses are listed in Table 1.

Table 1 Primer sequences and annealing temperatures. *Primers were used for semi-quantitative RT-PCR and RT-qPCR analyses of JAZ1, ARF1, Expansin and the reference genes Actin and 18S rRNA.*

Primer name	Sequence 5’ – 3’	Annealing temp.
Actin_MP2-fw	ACTACGAGAATGAGATCGAGACAG	58 °C
Actin_MP2-rv	AGGGCACCGGAATCTCTCA	58 °C
JAZ1_MP-fw	CAGGCAAAGTGTTGGTGTT	58 °C
JAZ1_MP-rv	CCACAAGAAATCTGGGAGC	58 °C
18SMP-fw	CTTCGGGATCGGAGTAATGA	58 °C
18SMP-rv	GCGGAGTCCTAGAAGCAACA	58 °C
ARF1_qPCR_fw	CAAGGTGTTCTTGGAGTCGGA	58 °C
ARF1_qPCR_rv (ARF1ex2 rv)	GCTTGGTTTCATAAGAATAGTCAATC	58 °C
Expansin fw	GCGGGGTGGAATTAGGTTCA	58 °C
Expansin rv	GACAAGCTTTGCCCGTTGAG	58 °C

2.9.1 RNA extraction and quality control

Total RNA was extracted from frozen plant tissue using the NucleoSpin® RNA kit (Macherey-Nagel, Düren, Germany) following the manufacturer's protocol (Rev. 18, December 2019) with the modifications described below. Frozen tissue was first homogenized with liquid nitrogen

and a mortar and pestle, then disrupted mechanically in a TissueLyser (30 seconds, 22 Hz). Cell lysis was performed by adding 353 µl of a master mix of Buffer RA1 and β-mercaptoethanol per sample. On-column DNA digestion used RNase-free DNase I (QIAGEN GmbH, Hilden, Germany) instead of the kit-supplied rDNase, with 5 µl DNase I and 35 µl RDD buffer per sample incubated for 20 minutes at 37 °C. RNA was eluted in 30 µl of RNase-free water pre-warmed to 65 °C.

Concentration and purity were assessed using a NanoDrop Lite Plus spectrophotometer (Thermo Fisher Scientific, Karlsruhe, Germany), with absorbance ratios at 260/280 nm and 260/230 nm evaluated for protein and solvent contamination. RNA integrity was verified by agarose gel electrophoresis (1.5% agarose, 0.5× TAE buffer, 100 V, 25 minutes; Mupid® One chamber, Advance/Mupid Co., Tokyo, Japan), with nucleic acids visualized using Midori Green Xtra (Nippon Genetics Europe GmbH, Düren, Germany). Intact RNA was confirmed by the presence of two distinct ribosomal RNA bands (25S and 18S rRNA). Only samples with acceptable purity ratios and clear ribosomal bands were used for cDNA synthesis.

2.9.2 cDNA synthesis

RNA samples were diluted to 500 ng in 14.6 µl nuclease-free water. First-strand cDNA synthesis was performed in a two-step reaction. In the first step, 1 µl of 10 mM dNTPs and 0.4 µl of 100 µM Oligo $d(T)_{18}$ primers (both New England Biolabs, Frankfurt, Germany) were added, and the mixture was incubated at 65 °C for 5 minutes in a Primus 96 advanced® thermal cycler (PEQLAB, Erlangen, Germany) to denature secondary structures, then immediately transferred to ice. A second master mix of 2 µl 10× reverse transcriptase buffer, 1.25 µl nuclease-free H_2O (Biozym, Hessisch Oldendorf, Germany), 0.5 µl RNase inhibitor, and 0.25 µl MuLV reverse transcriptase (all New England Biolabs, Frankfurt, Germany) was then added, and cDNA synthesis was carried out at 42 °C for 60 minutes, followed by enzyme inactivation at 90 °C for 10 minutes. The resulting cDNA was diluted 1:10 in nuclease-free water and stored at −20 °C.

2.9.3 Semi-quantitative RT-PCR

Prior to quantitative analysis, semi-qPCR was performed on all cDNA samples to confirm amplification quality and the presence of intact template. Each 10 µl reaction contained 1× Thermopol Buffer, 0.2 mM dNTPs, 0.2 µM each of forward and reverse primer (Table 1), 0.01 U/µl Taq DNA polymerase (all New England Biolabs, Frankfurt, Germany), 2.5 µl of 1:10 diluted cDNA, and nuclease-free H_2O (Biozym, Hessisch Oldendorf, Germany). PCR was

performed in a FlexCycler thermal cycler (Analytik Jena AG, Jena, Germany) with the following program: 95 °C for 2 minutes, then 35 cycles of 94 °C for 30 seconds, 58 °C for 30 seconds, and 68 °C for 30 seconds, with a final elongation at 68 °C for 5 minutes. Products were analyzed by agarose gel electrophoresis as described above, and only samples yielding a single distinct band of the expected size were used for RT-qPCR.

2.9.4 RT-qPCR

Transcript levels were quantified in 20 µl reactions containing 1× GoTaq® Buffer, 200 µM dNTPs, 0.2 µM each primer (Table 1), 2.5 mM $MgCl_2$ (USB Corporation, Cleveland, OH, USA), 0.5× SYBR™ Green (Thermo Fisher Scientific Inc., Waltham, MA, USA), 0.5 units GoTaq® polymerase (Promega GmbH, Mannheim, Germany), 1 µl of 1:10 diluted cDNA, and nuclease-free H_2O (Biozym, Hessisch Oldendorf, Germany). Reactions were run on a CFX96 Touch™ Real-Time PCR Detection System (Bio-Rad Laboratories GmbH, Munich, Germany) with the following program: 95 °C for 3 minutes, then 39 cycles of 95 °C for 15 seconds and 58 °C for 40 seconds, followed by a melting curve from 65 °C to 95 °C in steps of 0.5 °C per 5 seconds.

Data analysis was performed using Bio-Rad CFX Manager™ 3.1 software. Technical replicates with a Ct deviation exceeding 0.5 or an incorrect melting peak were excluded. Relative gene expression of JAZ1, ARF1, and Expansin was calculated using the 2^(−ΔCt) method (Livak and Schmittgen, 2001), with the ΔCt derived by subtracting the geometric mean Ct of the two reference genes 18S rRNA and Actin from the target gene Ct. Because the resulting values were very low, they were multiplied by a factor of 10^3 for clarity of presentation. This scaling factor was applied uniformly to all samples and does not affect the relative comparison between groups. Statistical significance was assessed by one-way ANOVA using IBM SPSS Statistics 28.0 (IBM, Armonk, NY, USA).

2.10 Harvest, growth, and root architecture analysis

Morphological parameters were recorded at the start of the two-week experimental phase and immediately prior to harvest. Plant height was measured from the substrate surface to the shoot apex, while leaf number and shoot number were counted per plant. Shoot width was measured manually using a caliper at the second to third apical internode, the region most responsive to gravitropic stimulation. Root length, defined as the length of the longest root per plant, was recorded at harvest. Morphological responses are reported as the relative change between the two measurement time points.

At harvest, all plants were photographically documented before dissection into individual organs. Fresh weights of leaves, shoots, roots, and the whole plant were recorded, after which shoots and roots were dried completely for dry weight determination. Leaves were divided into three portions, one for dry weight determination, one for glandular trichome analysis and essential oil profiling, and one for essential oil extraction. The analytical methods applied to each fraction are described in the respective sections below.

Root architectural parameters were analyzed using WinRhizo software (Regent Instruments, version 2022a). As plants were cultivated aeroponically, roots required no removal from substrate and were only briefly rinsed before scanning. Two-dimensional images of the root systems were captured using a flatbed scanner (Epson Expression 12000XL) and subsequently analyzed by the software. Background noise such as shoot remnants or debris was removed manually using the software's editing function, and the region of interest was selected as a rectangular area. For samples with very fine or pale roots, the "Very pale roots" detection setting was enabled to improve recognition accuracy.

The following parameters were extracted for each sample: total root length (cm), root surface area (cm^2), average root diameter (mm), and root volume (cm^3). Three topology parameters were additionally recorded: root tips (terminal ends of root segments), forks (branching points where a root splits into two daughter roots), and crossings (points where two roots visually overlap without forming a true branch). Data were exported in text format and imported into the associated Excel extension XLRhizo for further analysis. Topology parameters should be interpreted with caution, as they are derived from a two-dimensional projection of a three-dimensional root system and may be affected by root density and overlap.

2.11 Glandular trichome analysis.

To determine glandular trichome density and total number per leaf, four to ten microscopic images were acquired from both the adaxial and abaxial leaf surfaces using a Keyence microscope, alongside one whole-leaf photograph taken with a smartphone camera. The number of images per leaf was adjusted according to leaf size and followed a standardized sampling scheme that ensured representative coverage of the surface (Figure 12). This scheme accounted for the known spatial variation in trichome density, which is higher near the midrib and stem attachment and lower towards the leaf tip.

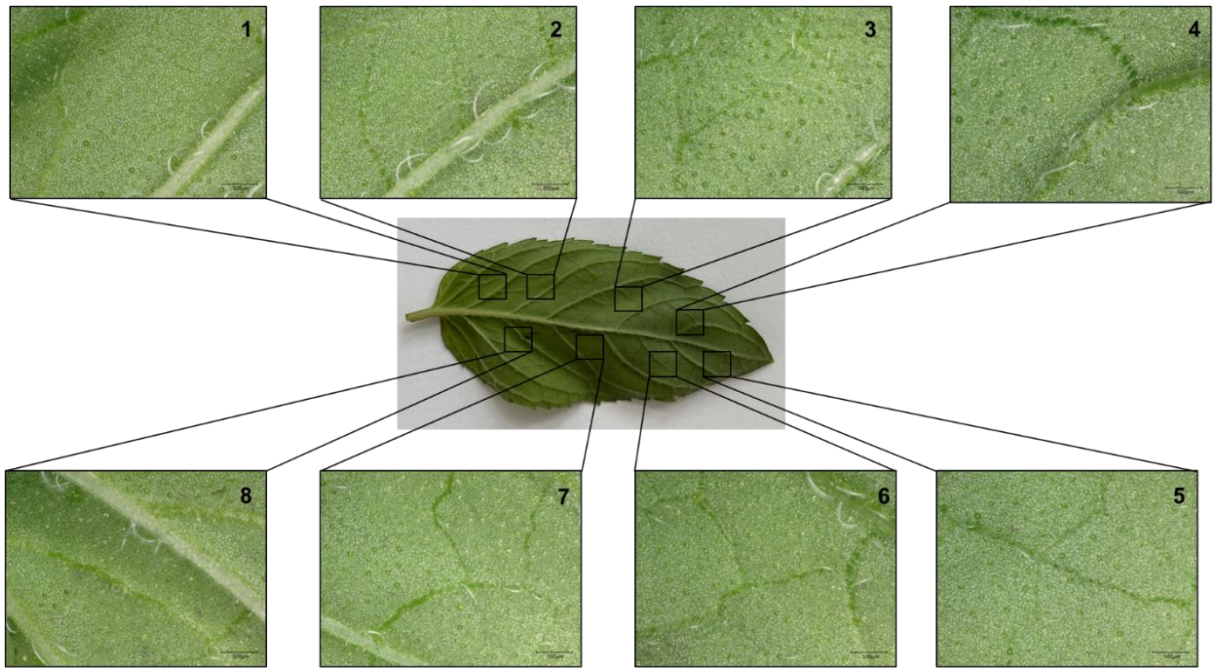

Figure 12 Standardized sampling scheme for microscopic imaging of glandular trichomes. *Depending on leaf size, between four and ten sampling positions were distributed across the leaf surface of* Mentha × piperita *to ensure representative coverage and account for spatial variation in glandular trichome density. The central image shows the complete leaf with the corresponding sampling positions indicated. Surrounding panels show representative microscopic images from each sampling position acquired using a Keyence microscope at 100× magnification.*

Whole-leaf photographs were analyzed in ImageJ to determine leaf surface area, while the microscopic images were processed for trichome count using the AI-based detection system described below. Trichome density per mm² was calculated by dividing the average trichome count per image by the area captured in a single image. Multiplying this density by the total leaf surface area then yielded an estimate of the total number of glandular trichomes per leaf.

AI-based trichome detection. Glandular trichomes were quantified automatically using a custom object detection system, developed jointly with a collaborator at Vertical Farm Tech GmbH, where the author was employed during this doctoral project. The system was based on the convolutional neural network YOLOv8 (You Only Look Once, version 8), adapted to a trichome-specific dataset by transfer learning. Approximately 1,000 manually annotated images of peppermint leaves were used for training, labelled with the annotation software CVAT (Computer Vision Annotation Tool). To improve detection of these small-scale structures, each original image was divided into four equal sub-images during data preparation, and the model was trained over 100 epochs.

The system was validated by comparing automated counts with manual counts across several hundred images, yielding an agreement of approximately 95%. The validated model was then used without further modification for all analyses in this work. Detection was performed

through a graphical user interface that output the number of trichomes per image as a CSV summary.

2.12 Essential oil and volatile analysis

2.12.1 Hydro-distillation

Essential oils were extracted from fresh peppermint leaves by hydro-distillation, using between 8 and 20 g of fresh leaf material per distillation depending on harvest yield. The material was briefly crushed in liquid nitrogen to rupture the oil cavities of the glandular trichomes and facilitate oil release, then placed in a round-bottomed flask filled to half its height with distilled water. After adding further distilled water to the apparatus for reflux and activating the water-cooling system, the material was heated to 100 °C and distilled for 1 hour. The extracted oil was quantified using a glass burette, collected in glass vials, and stored at 4 °C until analysis. Depending on available plant material and growth performance, one to three distillations were performed per treatment at each harvest.

2.12.2 GC-MS analysis

Immediately after extraction, each oil was split into two portions and stored at −20 °C. One portion was kept undiluted, while the second was diluted 1:500 in hexane (2 µl oil in 998 µl hexane) for GC-MS injection. Diluted samples were analyzed within two weeks, as longer storage led to noticeable volatilization even under freezing conditions. Two injection methods were used depending on sample type, with an identical temperature program throughout.

For bulk oil composition, 1 µl of the diluted oil was injected at a split ratio of 25:1. For individual leaves and internodes, solid-phase microextraction (SPME) was used. Each leaf sample was crushed in liquid nitrogen and stored in a sealed glass vial at 4 °C until measurement, with either the whole leaf or a representative portion used depending on size. Before extraction, vials were equilibrated to at least room temperature to allow sufficient volatilization into the headspace. A DVB/PDMS SPME fiber (65 µm/10 mm) was then exposed to the headspace for approximately 60 seconds and injected in splitless mode at 250 °C and 9.15 psi. This approach allowed the oil composition of the first four leaf pairs to be analyzed individually.

All analyses were performed on an Agilent 8860 GC System coupled to an Agilent 5977C GC/MSD mass selective detector (Agilent Technologies, Santa Clara, CA, USA), equipped with an HP-5 capillary column (30 m × 0.25 mm I.D. × 0.25 µm film thickness) and helium as

carrier gas at a constant flow rate of 1.2 ml/min. The temperature program comprised an isothermal phase at 40 °C for 1 min, a first ramp at 5 °C/min to 60 °C (held for 4 min), a second ramp at 3 °C/min to 170 °C, and a final ramp at 30 °C/min to 270 °C (held for 10 min). Mass spectra were recorded in electron ionization (EI) mode at 70 eV over a mass range of 25–300 m/z. Compounds were identified by their characteristic retention times and mass spectra, with data acquired and processed in Agilent MassHunter Quantitative Analysis software.

For oils obtained by hydro-distillation, a linear calibration curve was established for each reference substance: (–)-limonene, (–)-pulegone, (+)-menthofuran, (–)-menthone, and (–)-menthol (all Sigma-Aldrich, Steinheim, Germany), using a concentration series from 12.5 to 750 ng/µl. All curves showed excellent linearity, with R^2 values of 0.990 for (–)-limonene, 0.993 for (–)-pulegone, 0.989 for (+)-menthofuran, 0.995 for (–)-menthone, and 0.998 for (–)-menthol. Compound concentrations in the extracted oils were calculated from these calibrations.

2.13 Statistical analysis

Statistical analyses were performed using two approaches depending on the comparison of interest. Pairwise comparisons between two treatment groups were assessed by a two-tailed Student's t-test assuming unequal variances in Microsoft Excel (Microsoft Corporation, Redmond, WA, USA). Comparisons across multiple treatment groups were assessed by one-way ANOVA followed by Tukey's honest significant difference (HSD) post-hoc test in OriginPro 2023 (OriginLab Corporation, Northampton, MA, USA).

The number of biological replicates varied between experiment types. Preliminary curvature kinetics experiments used five biological replicates per tilt angle. Growth, morphological, and biomass measurements used 11 plants per module, each plant representing one biological replicate. For glandular trichome analyses, individual leaves served as biological replicates. Essential oil composition in the tilting experiments was based on three independent hydro-distillations per treatment, each treated as one biological replicate, whereas in the MeJA and phenidone experiments oils were analyzed per leaf, with each leaf treated as one biological replicate. Gene expression analyses used three independent biological replicates per time point and treatment.

Results are presented as means ± standard error (SE), with differences considered statistically significant at $p \leq 0.05$. In Figures, asterisks without brackets indicate significant differences compared to the untilted control, while asterisks with brackets indicate significant differences

between the groups indicated by the bracket. Different letters above bars indicate significant differences between all pairwise group combinations as determined by Tukey's HSD post-hoc test.

2.14 Use of artificial intelligence tools

In the preparation of this thesis, artificial intelligence tools were used as writing and research aids. Claude (Anthropic, version Opus 4.7) and ChatGPT (OpenAI, version GPT-4o) assisted with translation, formulation, and stylistic refinement of text passages, and Elicit (Ought) supported the literature search over the course of the doctoral project. All content, scientific interpretations, and conclusions are the sole responsibility of the author.

3 Results

3.1 Peppermint perceives gravity, but bending competence is developmentally restricted

The Results are structured to first establish whether *Mentha* × *piperita* is gravitropically competent and to characterize the underlying response mechanisms. The standard elicitation protocol — daily tilting in light — is then evaluated in detail for its effects on growth, trichome formation and essential oil traits. A separate comparison chapter tests whether the effects observed under the standard protocol depend specifically on the light and stimulation context, or whether they represent a generic response to mechanical reorientation. Finally, pharmacological experiments test the role of jasmonate signaling as a mediator of these effects.

3.1.1 Gravity-perceiving cells are present throughout the shoot, but elongation capacity declines with internode age

Before gravitropic stimulation can be applied as an elicitation strategy, it must be established that peppermint shoots possess the anatomical basis for gravity perception and that the response is not restricted to a single developmental zone. Histological sections of internodes 1–4 were therefore examined for the presence of statolith-containing statocytes and for developmental changes in cell morphology.

Statolith-containing statocytes were detected in all four internodes examined (Figures 13 and 14). The gravisensory apparatus is therefore structurally present throughout the shoot axis and is not lost with increasing internode age.

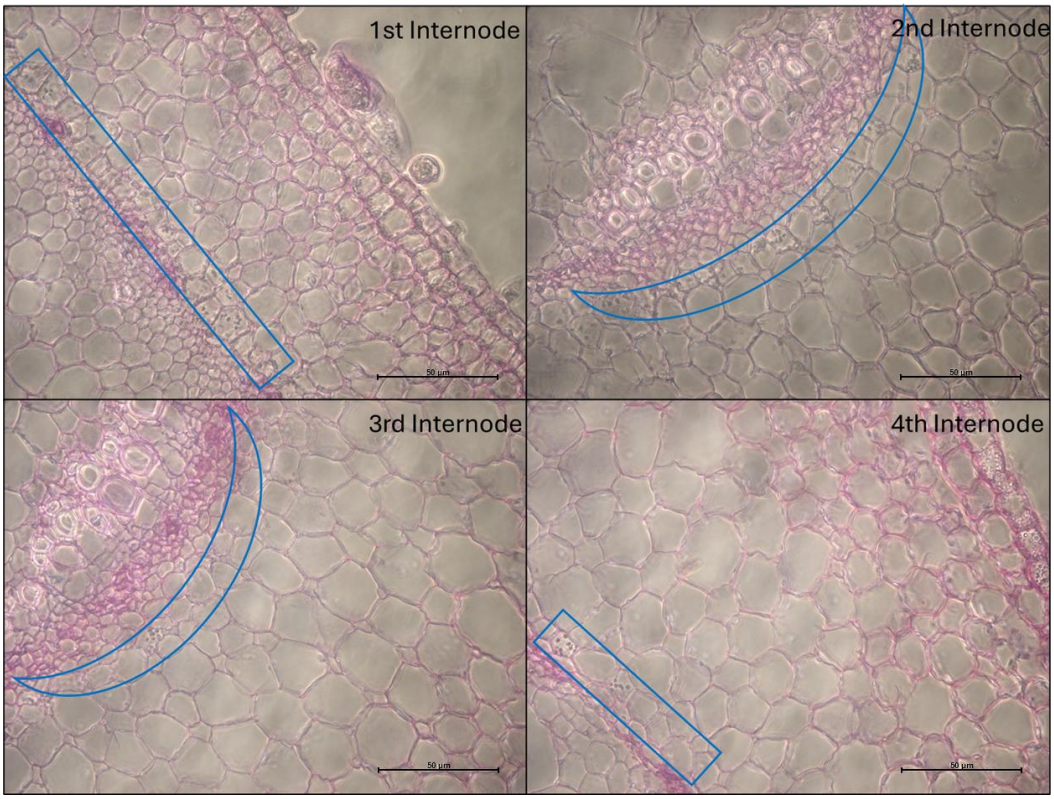

Figure 13 Cross-sections of internodes 1–4 of *Mentha* × *piperita* shoots stained with PAS. *Internode 1 represents the first apical (youngest) internode. Blue outlines indicate statocytes containing starch-filled statoliths. Scale bar = 50 µm.*

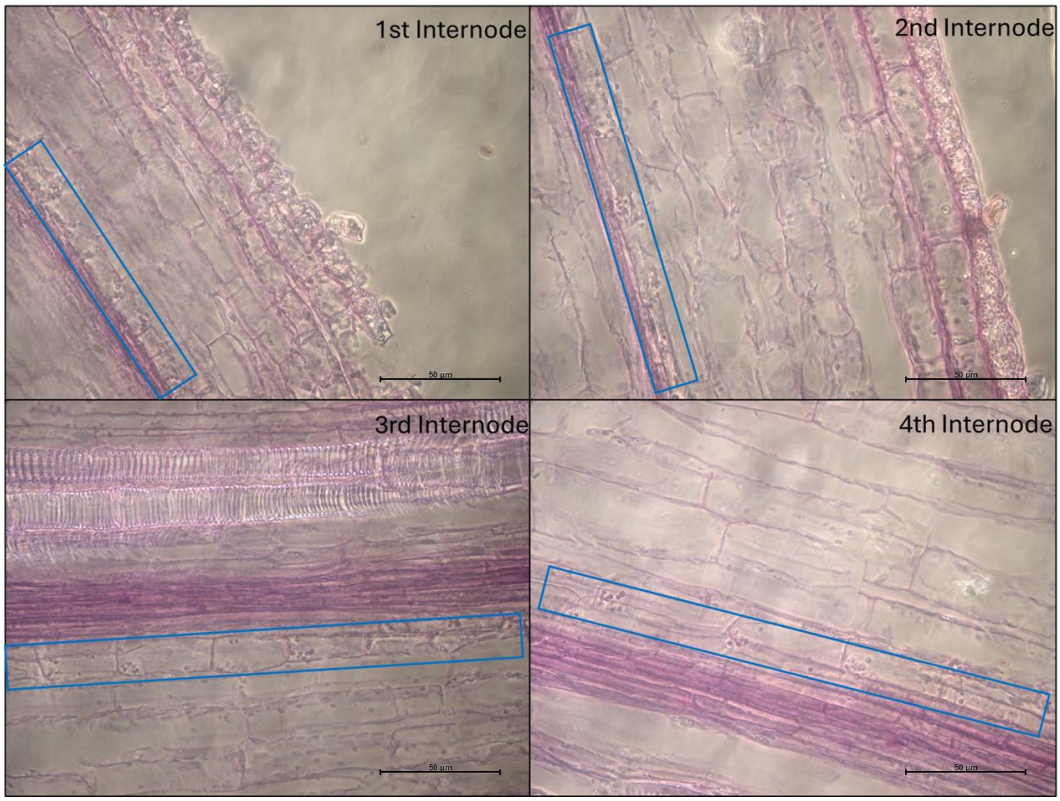

Figure 14 Longitudinal sections of internodes 1–4 of *Mentha* × *piperita* shoots stained with PAS. *Internode 1 represents the first apical (youngest) internode. Blue outlines indicate statocytes containing starch-filled statoliths. Scale bar = 50 µm.*

Cross-sections further revealed a progressive increase in cell size from internode 1 to internode 4. Longitudinal sections corroborated this observation and additionally showed increasingly elongated cells in internodes 3 and 4 compared to the younger internodes. Gravitropic bending in response to reorientation was observed predominantly in internodes 1 and 2 (Figure 2, Introduction). Older internodes showed little to no curvature response. To test whether this loss of bending competence is associated with differences in cellulose microfibril orientation, polarization microscopy was performed on internodes 1 and 4. However, the absence of a consistent cotton fiber reference standard precluded a reliable comparison between internodes (Figure A1, Appendix).

Together, these results show that the gravisensory apparatus is structurally intact throughout the shoot, while bending competence is restricted to the younger internodes.

3.1.2 Repeated gravitropic stimulation weakens the gravitropic response in darkness but enhances it under light

Having confirmed that gravity-perceiving cells are present throughout the shoot, the curvature response of *Mentha* × *piperita* shoots was characterized in terms of onset, magnitude, reversibility and adaptive behavior. Experiments were first conducted in darkness to isolate the gravitropic response, then repeated under the light conditions used in the CEA elicitation protocol.

Shoots tilted to 90° in darkness showed a slight downward deflection within the first 30 minutes, followed by a statistically significant upward curvature first detected between 30 and 60 minutes (figure 15A). Curvature continued to increase, reaching approximately 12° at 240 minutes. Following reversal, the maximum of approximately 13° was reached within the first 10 minutes, then declined significantly between 120 and 240 minutes. Full realignment to t_0 had not occurred within the observation period. At 45°, the same general pattern was observed with reduced magnitude and delayed onset (Figure 15B). Significant curvature was first detected between 60 and 120 minutes, reaching approximately 7° at 240 minutes. Following reversal, curvature peaked at approximately 8° at 30 minutes before declining to approximately 1.5° relative to t_0 by the end of the experiment.

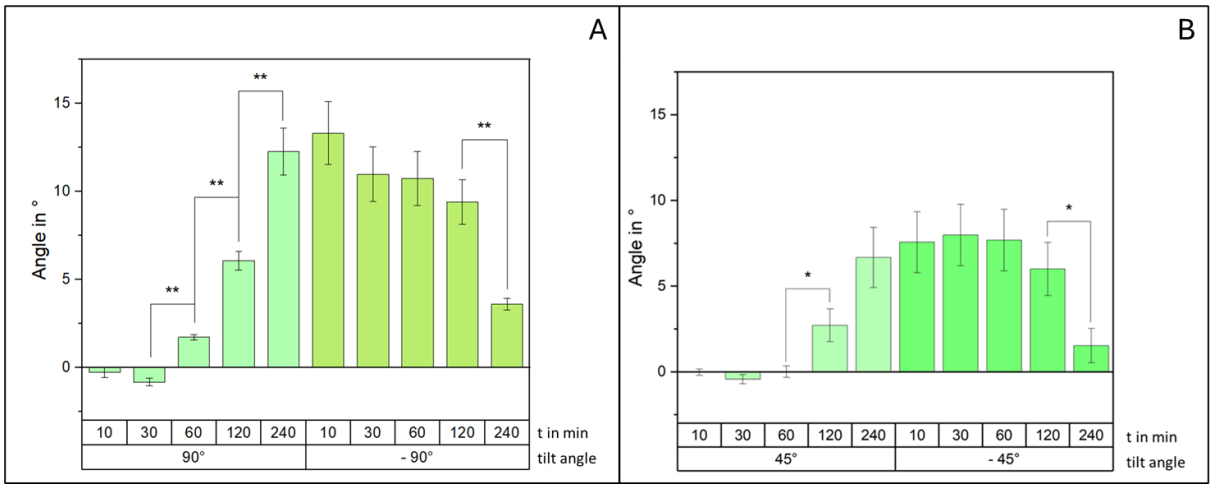

Figure 15 Gravitropic curvature response of *Mentha* × *piperita* shoots upon tilting in darkness at two stress levels. *(A) Extreme stress (90°): angle difference relative to t_0 is shown at 10, 30, 60, 120 and 240 min after tilting to 90° (left) and after tilting back to −90° (right). (B) Severe stress (45°): angle difference relative to t_0 is shown at 10, 30, 60, 120 and 240 min after tilting to 45° (left) and after tilting back to −45° (right). Data represent means ± SE (n = 5). Asterisks indicate statistically significant differences between consecutive time points (* p < 0.05, ** p < 0.01).*

Repeated tilting over consecutive days revealed a dissociation between response onset and response magnitude (Figure 16). At 90° over five days, the initial downward deflection decreased from approximately −2.5° on days 1–2 to approximately −0.5° on day 5. The maximum curvature declined progressively from approximately 13° on day 1 to approximately 7° on day 5. At 45° over two days, the initial downward deflection present on day 1 was largely absent on day 2, and the maximum curvature decreased from approximately 8° to approximately 5.5°. Despite this reduction in amplitude, the onset of upward curvature occurred earlier on successive days at both angles.

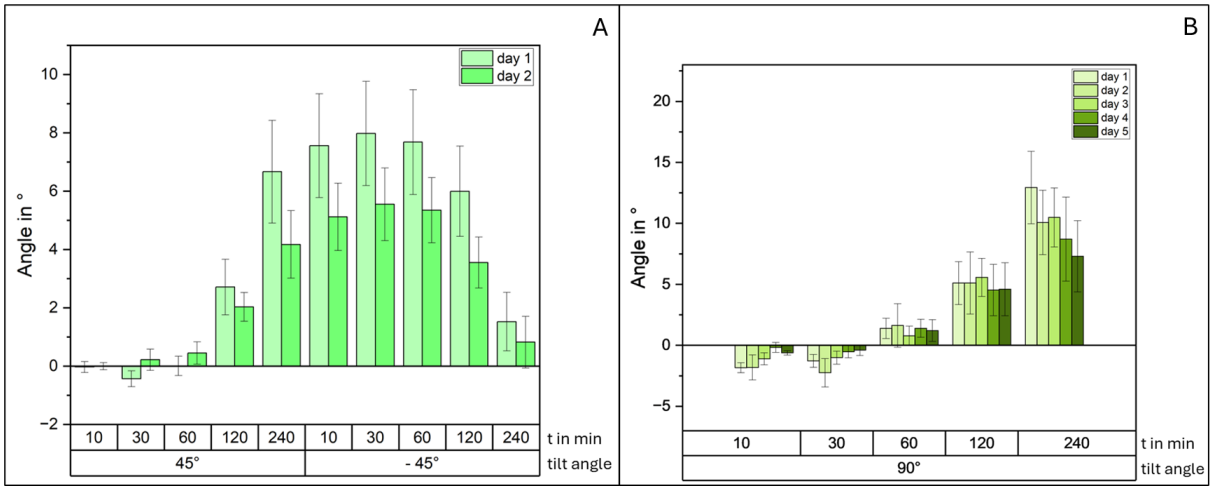

Figure 16 Gravitropic curvature response of *Mentha* × *piperita* shoots upon repeated tilting in darkness over consecutive days. *(A) Repeated severe stress (45°) over two consecutive days: angle difference relative to t_0 is shown at 10, 30, 60, 120 and 240 minutes after tilting to 45° (left) and after tilting back to −45° (right). (B) Repeated extreme stress (90°) over five consecutive days: angle difference relative to t_0 is shown at 10, 30, 60, 120 and 240 minutes after tilting to 90°. Data represent means ± SE (n = 5). Different shades of green indicate consecutive tilting days.*

The response pattern differed fundamentally under the light conditions of the CEA tilting modules. A single tilting event at 54° produced only a weak response: a slight downward deflection during the first 60 minutes was followed by an upward curvature of approximately 1° at 240 minutes (Figure 17). Following reversal, the maximum reached approximately 2° within the first 10 minutes. No statistically significant differences between consecutive time points were detected.

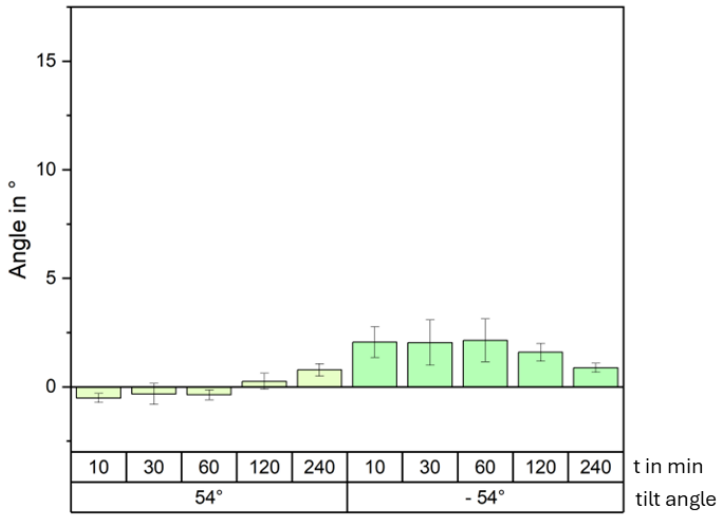

Figure 17 Gravitropic curvature response of *Mentha* × *piperita* shoots upon 54° tilting under light conditions. *Angle difference relative to t_0 is shown at 10, 30, 60, 120 and 240 minutes after tilting to 54° (left) and after tilting back to −54° (right). Data represent means ± SE (n = 11). No statistically significant differences between consecutive time points were detected.*

Repeated tilting over ten days produced a strikingly different outcome from the dark experiments. At both angles, response speed and magnitude increased progressively across days (Figure 18). At 54°, upward curvature was first detectable at 240 minutes on day 1 but already at 60 minutes on day 10, with the maximum after reversal increasing from approximately 2° to approximately 9°. On day 10, the shoot tip continued beyond t_0 following reversal, reaching approximately −3° at 240 minutes. At 75°, the progression was more pronounced: the onset shifted from 240 minutes on day 1 to within the first 10 minutes on day 10, and the maximum curvature increased from approximately 6° to approximately 16°.

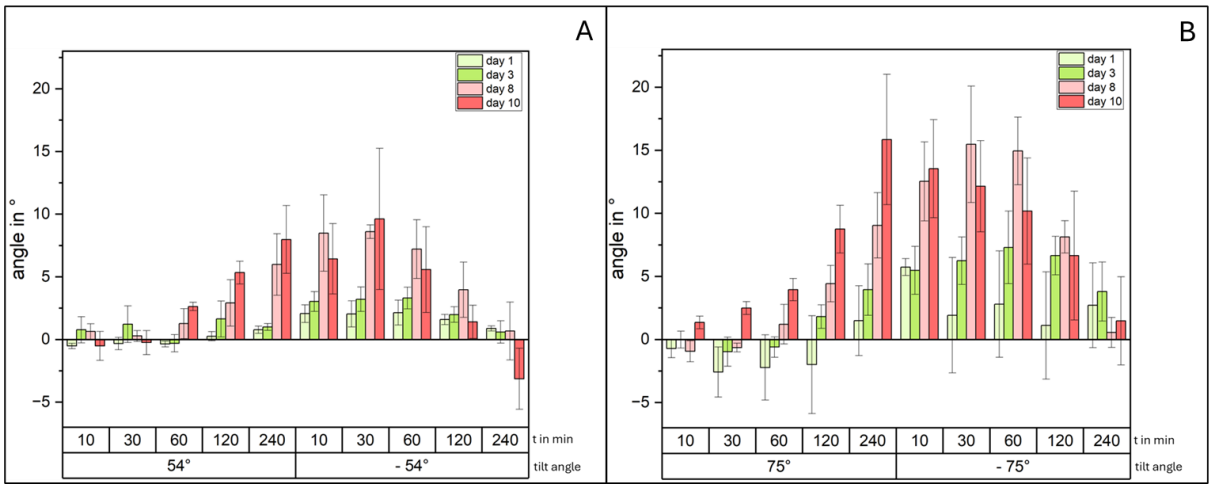

Figure 18 Gravitropic curvature response of *Mentha* × *piperita* shoots upon repeated tilting under light conditions over ten days. *(A) Moderate stress (54°): angle difference relative to t_0 is shown at 10, 30, 60, 120 and 240 minutes after tilting to 54° (left) and after tilting back to −54° (right). (B) Severe stress (75°): angle difference relative to t_0 is shown at 10, 30, 60, 120 and 240 minutes after tilting to 75° (left) and after tilting back to −75° (right). Measurements were taken on days 1, 3, 8 and 10. Data represent means ± SE (n = 11). No statistically significant differences between consecutive time points were detected. Different shades of green and red indicate the four measurement days.*

Together, these results show that *Mentha* × *piperita* shoots mount a clear, angle-dependent gravitropic curvature response. In darkness, repeated stimulation progressively reduced response amplitude while accelerating response onset. Under light conditions, ten days of repeated stimulation enhanced both speed and magnitude.

3.1.3 Gravitropic stimulation activates JA, auxin and cell wall remodeling markers in a tissue- and phase-specific manner

Section 3.1.2 showed that gravitropic stimulation produces a curvature response in the young internodes. To investigate the signaling underlying this response, the expression of three marker genes was analyzed following stimulation at 75° under light conditions. JAZ1 was analyzed as a marker for jasmonic acid (JA) signaling, the candidate pathway linking gravitropic stimulation to secondary metabolism. ARF1 was included as a marker for auxin signaling, to test whether the JAZ1 response is triggered by an auxin signal travelling basipetally along the shoot. Expansin was analyzed as a marker for cell wall remodeling, to assess whether JA signaling is also associated with cell wall loosening during the response. Four tissue types were sampled across the tilt and reversal phases - internodes 1-2, internode 3, apical leaf 1 and apical leaf 2.

JAZ1 expression remained low across all tissues during the initial tilt phase (Figure 19). At t0, treatment expression was significantly lower than control in internodes 1-2 and internode 3, although expression levels in both groups were comparably low at this time point. A pronounced upregulation in the treatment group developed from 240 minutes onwards in internodes 1-2,

peaking at 30 minutes after reversal before gradually declining, with significant differences at multiple time points during this period. In internode 3, a similar but attenuated pattern was observed, with treatment expression increasing from 240 minutes and reaching a maximum at 120 minutes after reversal. In the apical leaves, upregulation occurred predominantly during the reverse phase, peaking at 60 minutes after reversal in both apical leaf 1 and apical leaf 2.

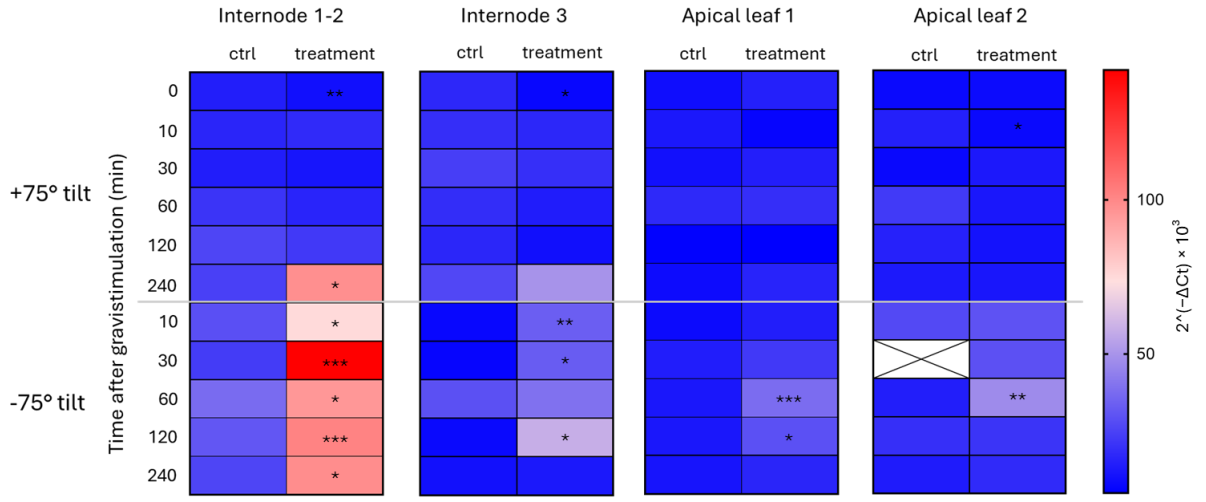

Figure 19 Heatmap of relative JAZ1 gene expression in internodes 1–2, internode 3, apical leaf 1 and apical leaf 2 following gravitropic stimulation at 75° under light conditions. *Relative expression values (2^(−ΔCt) × 10³) are shown for control (ctrl) and gravitropically stimulated (treatment) plants at 0, 10, 30, 60, 120 and 240 minutes after tilting to +75° and at 10, 30, 60, 120 and 240 minutes after reversal to −75°. The color scale ranges from blue (low expression) to red (high expression). Asterisks indicate statistically significant differences between control and treatment at the respective time point (* $p < 0.05$, ** $p < 0.01$, *** $p < 0.001$; one-way ANOVA followed by Tukey's HSD post-hoc test). The crossed-out field indicates a sample for which RNA extraction was not possible across all biological replicates. Data represent means of 4 biological replicates with 3 technical replicates each. Absolute expression values with standard errors are provided in the Appendix [Figure A2].*

ARF1 expression showed no coherent treatment-specific pattern in internodes 1-2 or internode 3 (Figure 20). Both control and treatment groups showed sporadic increases and decreases across the time course, without a consistent direction of regulation. The isolated significant differences that were detected pointed in both directions - treatment was higher than control at some time points but lower at 120 minutes of the tilt phase in internodes 1-2. In contrast, a clear and directional upregulation in the treatment group was observed in the apical leaves during the reverse phase, with treatment expression peaking at 60 minutes after reversal in both apical leaf 1 and apical leaf 2.

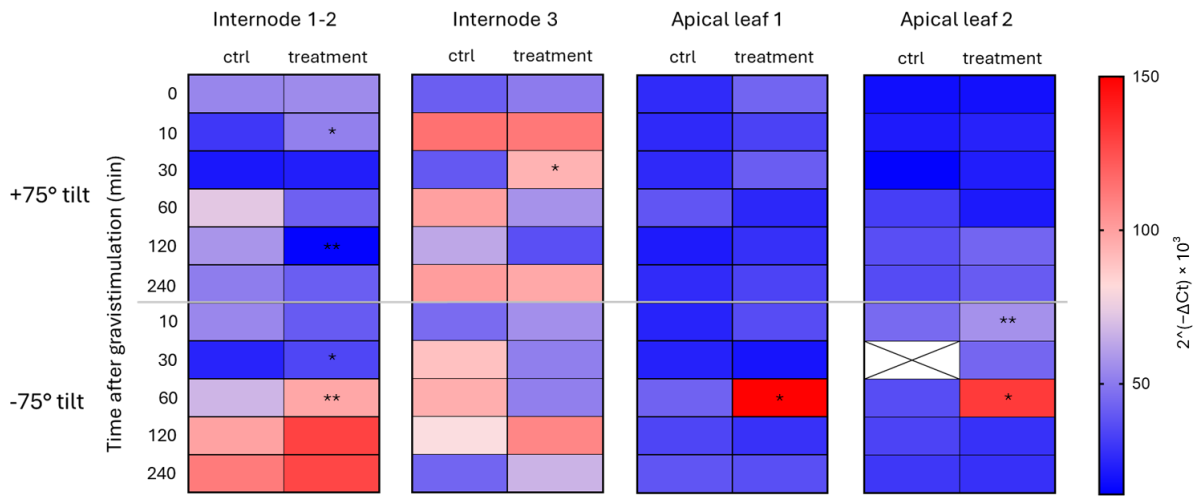

Figure 20 Heatmap of relative ARF1 gene expression in internodes 1–2, internode 3, apical leaf 1 and apical leaf 2 following gravitropic stimulation at 75° under light conditions. *Relative expression values (2^(−ΔCt) × 10³) are shown for control (ctrl) and gravitropically stimulated (treatment) plants at 0, 10, 30, 60, 120 and 240 minutes after tilting to +75° and at 10, 30, 60, 120 and 240 minutes after reversal to −75°. The color scale ranges from blue (low expression) to red (high expression). Asterisks indicate statistically significant differences between control and treatment at the respective time point (* $p < 0.05$, ** $p < 0.01$; one-way ANOVA followed by Tukey's HSD post-hoc test). The crossed-out field indicates a sample for which RNA extraction was not possible across all biological replicates. Data represent means of 4 biological replicates with 3 technical replicates each. Absolute expression values with standard errors are provided in the Appendix [Figure A3].*

Expansin expression levels were markedly lower overall than those of JAZ1 and ARF1, but showed distinct tissue-specific patterns (Figure 21). In internodes 1-2, expression was reduced in the treatment group at 30 minutes after tilting, followed by a sustained increase above control during the late tilt and reverse phase. In internode 3, treatment expression was elevated above control during the late tilt and early reverse phase. In apical leaf 1, expression remained uniformly low in both groups, with treatment slightly elevated only at isolated time points and no coherent response overall. In apical leaf 2, treatment expression was reduced relative to control during the early tilt phase but showed a pronounced increase at 60 minutes after reversal.

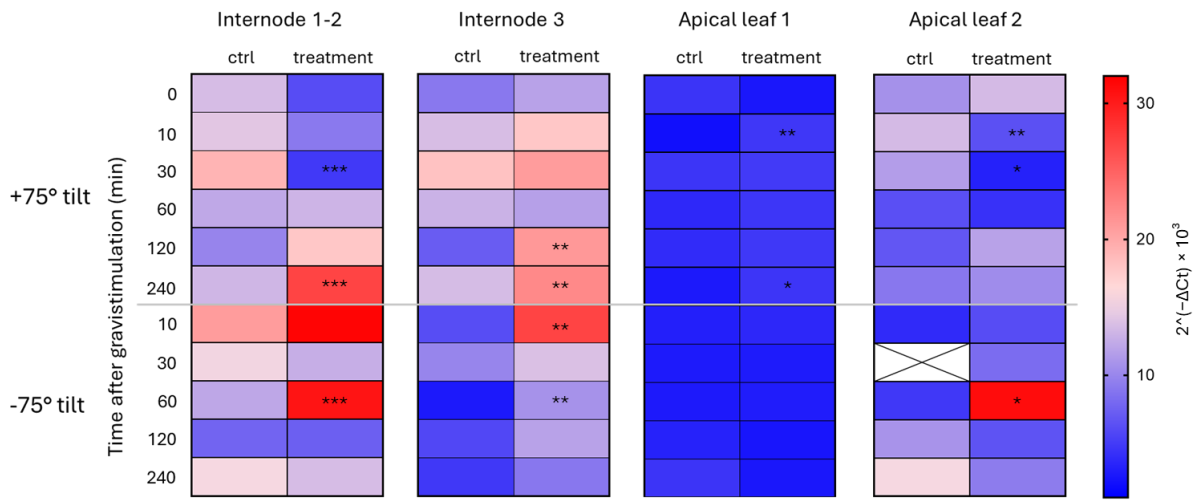

Figure 21 Heatmap of relative Expansin gene expression in internodes 1–2, internode 3, apical leaf 1 and apical leaf 2 following gravitropic stimulation at 75° under light conditions. *Relative expression values (2^(−ΔCt) × 10³) are shown for control (ctrl) and gravitropically stimulated (treatment) plants at 0, 10, 30, 60, 120 and 240 minutes after tilting to +75° and at 10, 30, 60, 120 and 240 minutes after reversal to −75°. The color scale ranges from blue (low expression) to red (high expression). Note that the color scale differs from that of Figures 19 and 20 owing to the markedly lower overall expression levels. Asterisks indicate statistically significant differences between control and treatment at the respective time point (* p < 0.05, ** p < 0.01, *** p < 0.001; one-way ANOVA followed by Tukey's HSD post-hoc test). The crossed-out field indicates a sample for which RNA extraction was not possible across all biological replicates. Data represent means of 4 biological replicates with 3 technical replicates each. Absolute expression values with standard errors are provided in the Appendix [Figure A4].*

Together, these results show that gravitropic stimulation activates all three signaling markers, but in a tissue- and phase-specific manner. JAZ1 was consistently upregulated across all four tissues, with the strongest response in internodes 1-2 and peaking predominantly after reversal of the tilt direction. ARF1 showed a directional treatment response only in the apical leaves during the reverse phase, with no coherent regulation in the internodes. Expansin upregulation in the internodes coincided temporally with the JAZ1 response in the same tissues.

3.2 Gravitropic stimulation in light modifies growth, trichome formation and essential oil traits

The following sections present the effects of the standard elicitation protocol - daily tilting under light - on shoot morphology, root architecture, biomass accumulation, glandular trichome parameters and essential oil yield and composition. This protocol was the primary focus of the study because it produced the most consistent responses across all measured traits.

3.2.1 Gravitropic stimulation in light affects biomass allocation more than overall morphology

Having established that peppermint responds to gravitropic stimulation at the level of curvature and gene expression, the next question was whether repeated daily tilting under the standard

protocol translates into measurable changes at the whole-plant level. Shoot morphology, root architecture and biomass allocation were assessed over the two-week experimental period.

Morphology

Plant height and leaf number showed slight non-significant increases at mild (27°) and moderate stress (54°), while plant height tended to decrease at severe stress (75°) (Figure 22). Shoot number decreased slightly at mild stress and increased at moderate and severe stress, with a significant difference between mild and the two higher stress levels. Root length, measured here as the length of the longest root per plant, was not affected by stress level.

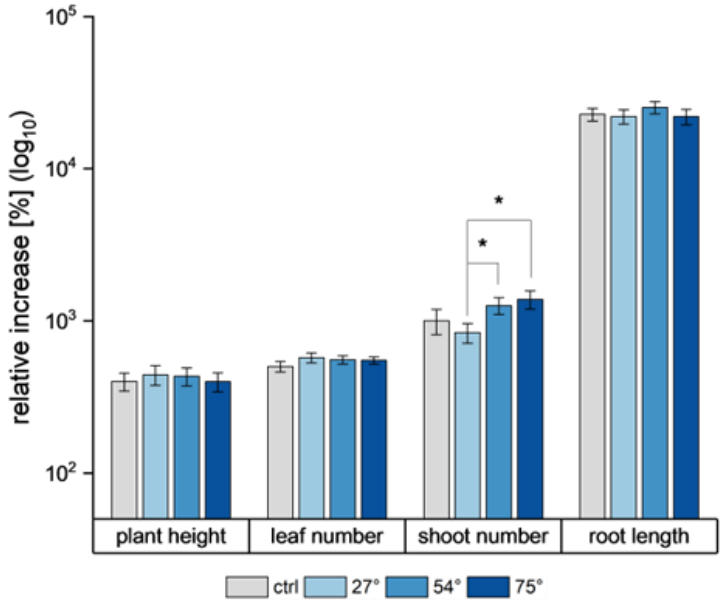

Figure 22 Relative growth of plant organs under increasing gravitropic stimulation during daily tilting in light. *Relative increase (%) from experiment start to end is shown on a log_{10} scale for plant height, leaf number, shoot number and root length. Tilting angles of 27°, 54° and 75° are compared to untilted controls (ctrl). Data represent means ± SE (n = 11). Asterisks with brackets indicate statistically significant differences between the indicated groups (* $p < 0.05$).*

Root architecture

A detailed analysis of the root system distinguished total root length - the summed length of all roots - from the single-root measurement above. Total root length decreased progressively with increasing stress level, with the most pronounced reduction at severe stress (Figure 23A). Root volume showed slight increases at mild and moderate stress before decreasing at severe stress (Figure 23B). Average root diameter was slightly higher in all tilted groups compared to the control (Figure 23C). The number of root tips decreased progressively with stress level, reaching significance at severe stress (Figure 23D). At mild and moderate stress, root tip number

decreased while total root length remained comparable to control. At severe stress, both root tip number and total root length were reduced.

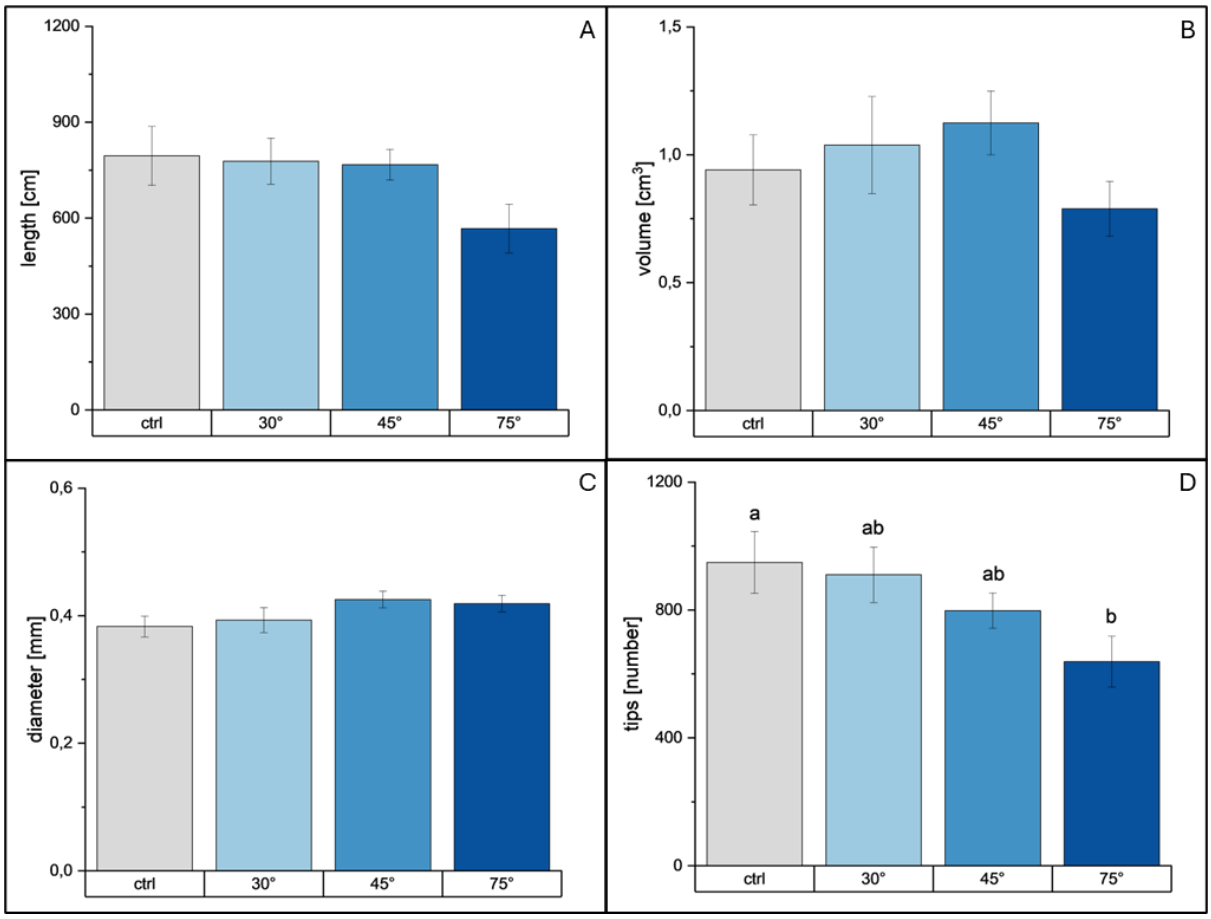

Figure 23 Root architecture parameters of *Mentha* × *piperita* under daily tilting in light at increasing gravitropic stress angles. *Total root length (A), root volume (B), average root diameter (C) and number of root tips (D) are shown for tilting angles of 30°, 45° and 75° compared to untilted controls (ctrl). Data represent means ± SE (n = 11). Different letters in panel D indicate statistically significant differences between groups as determined by one-way ANOVA followed by Tukey's HSD post-hoc test ($p < 0.05$).*

Biomass

Total dry biomass increased across all stress levels compared to the control, with the most pronounced increase at mild stress (Figure 24). This increase was driven mainly by leaf biomass, which was significantly elevated at mild stress and less pronounced at higher stress levels. Shoot biomass showed slight non-significant increases across all stress levels, and root biomass increased slightly at mild and moderate stress before returning to control levels at severe stress.

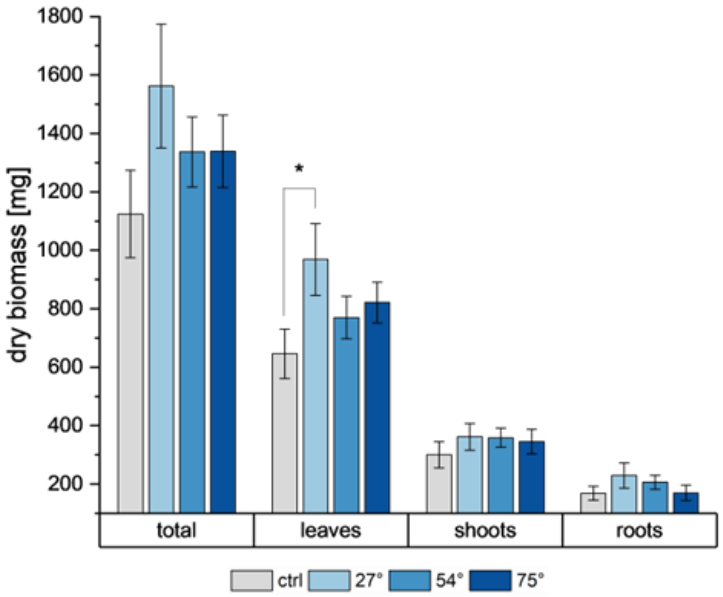

Figure 24 Dry biomass of total plant, leaves, shoots and roots under increasing gravitropic stimulation during daily tilting in light. *Dry biomass (mg) is shown for tilting angles of 27°, 54° and 75° compared to untilted controls (ctrl). Data represent means ± SE (n = 11). Asterisks with brackets indicate statistically significant differences between the indicated groups (* $p < 0.05$).*

Together, these results show that daily tilting in light had only minor effects on overall morphology and root architecture, but promoted biomass accumulation - most clearly in the leaves at mild stress.

3.2.2 Gravitropic stimulation in light increases glandular trichome formation and leaf surface area

Because glandular trichomes are the exclusive site of essential oil biosynthesis and storage, trichome formation was assessed as a direct indicator of the production capacity response to the standard protocol. Three parameters were measured per leaf pair - trichome density (trichomes per unit leaf area), leaf surface area, and total trichome count per leaf. Because density is expressed per unit area, a change in leaf size can alter density independently of any change in trichome number. Density, area and count are therefore presented together.

Trichome density

Averaged across all leaf pairs, glandular trichome density increased at mild stress, was only minimally higher than the control at moderate stress, and reached its highest value at severe stress, which was significantly different from the control (Figure A 5, Appendix). Because trichome density varies strongly with leaf position, the per-leaf-pair analysis is more informative and is shown here.

At the level of individual leaf pairs, density was highest in lp1 and lowest in lp3 across all treatments (Figure 25). In lp1, density was clearly elevated at mild and severe stress, with the increase at severe stress being stronger and significant relative to the control, while moderate stress showed only a minimal, non-significant increase. In lp2, the pattern was similar, but the elevation at mild stress was closer to that at severe stress and also reached significance, so that both mild and severe stress differed significantly from the control. In lp3, the same overall pattern was visible, although all values remained closer to the control, and only severe stress was significantly higher.

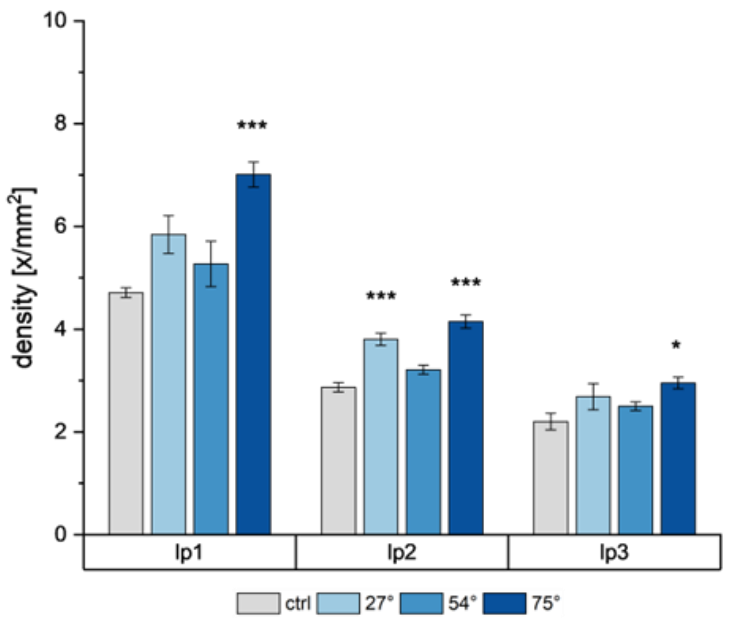

Figure 25 Glandular trichome density in individual leaf pairs under increasing gravitropic stress during daily tilting in light. *Density (x/mm²) is shown for leaf pairs (lp) 1–3, numbered from the apical (youngest) to the more basal (older) leaf pairs, for tilting angles of 27°, 54° and 75° compared to untilted controls (ctrl). Data represent means ± SE (n = 12 per leaf pair). Asterisks indicate statistically significant differences compared to the control (* $p < 0.05$, *** $p < 0.001$). In addition, 54° and 75° differed significantly in lp1, and 27° and 54° differed significantly in lp2.*

Leaf surface area

In lp1, leaf surface area was slightly increased at moderate stress and slightly reduced at mild and severe stress, with no significant differences from the control (Figure 26). In lp2, leaf surface area was significantly increased at moderate stress, while mild and severe stress were slightly below but close to the control. In lp3, leaf surface area was significantly increased at moderate stress. Mild stress was slightly elevated and close to the control, and severe stress was elevated more than mild but less than moderate, without reaching significance.

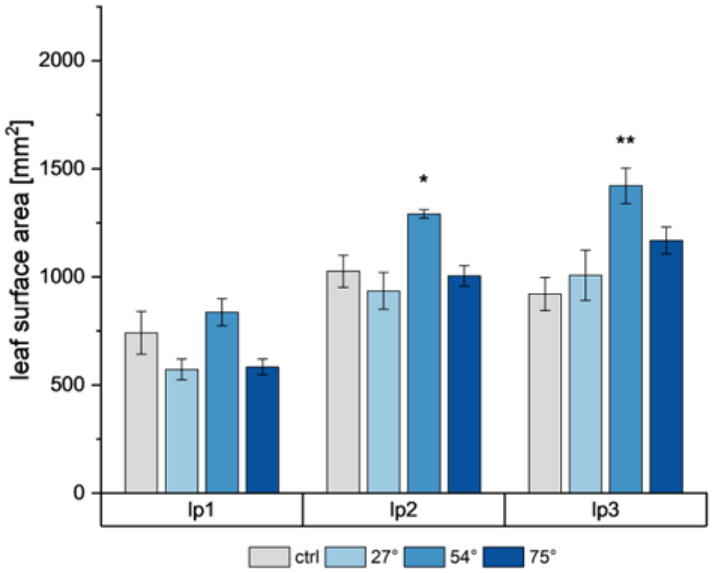

Figure 26 Leaf surface area in individual leaf pairs under increasing gravitropic stress during daily tilting in light. *Leaf surface area (mm²) is shown for leaf pairs (lp) 1–3, numbered from the apical (youngest) to the more basal (older) leaf pairs, for tilting angles of 27°, 54° and 75° compared to untilted controls (ctrl). Data represent means ± SE (n = 12 per leaf pair). Asterisks indicate statistically significant differences compared to the control (* $p < 0.05$, ** $p < 0.01$). In addition, 27° and 54° differed significantly in lp1, 54° differed significantly from both 27° and 75° in lp2, and 27° and 54° differed significantly in lp3.*

Total Trichome count

At the level of individual leaf pairs, total trichome count per leaf was elevated above the control across most stress levels, though the pattern differed between leaf pairs (Figure 27). In lp1, count rose at moderate and severe stress but did not reach significance relative to the control. In both lp2 and lp3, count increased up to moderate stress and was significantly higher than the control at moderate and severe stress, but did not rise further from moderate to severe stress, remaining at a comparable level.

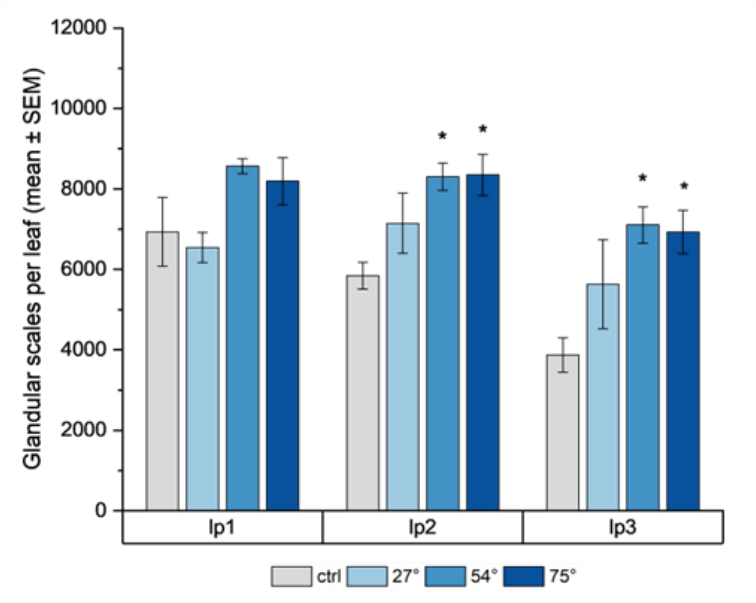

Figure 27 Total glandular trichome count per leaf in individual leaf pairs under increasing gravitropic stress during daily tilting in light. *Glandular trichome count per leaf is shown for leaf pairs (lp) 1–3, numbered from the apical (youngest) to the more basal (older) leaf pairs, for tilting angles of 27°, 54° and 75° compared to untilted controls (ctrl). Data represent means ± SE (n = 12 per leaf pair). Asterisks indicate statistically significant differences compared to the control (* p < 0.05).*

Averaged across all leaf pairs, total trichome count per leaf exceeded the control at all stress levels, reaching significance at moderate and severe stress. The mean count increased up to moderate stress and decreased slightly at severe stress, though it remained above the control (Figure 28).

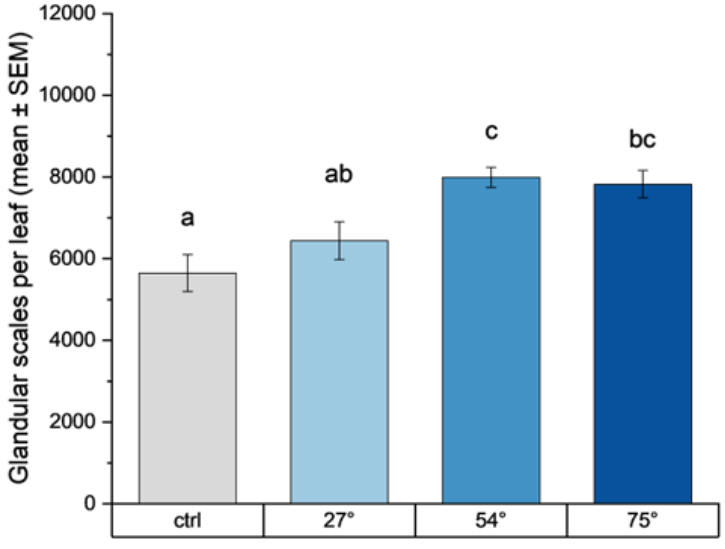

Figure 28 Mean total glandular trichome count per leaf under increasing gravitropic stress during daily tilting in light. *Glandular trichome count per leaf is shown as the mean across all measured leaf pairs for tilting angles of 27°, 54° and 75° compared to untilted controls (ctrl). Data represent means ± SE (n = 18). Different letters indicate statistically significant differences between groups as determined by one-way ANOVA followed by Tukey's HSD post-hoc test (p < 0.05).*

Together, these results show that daily tilting in light increased glandular trichome density and total trichome count across stress levels, with the response differing between moderate and severe stress. At moderate stress, leaf surface area in lp2 and lp3 increased while trichome density remained close to the control, and the total trichome count per leaf reached its highest values. At severe stress, leaf surface area in lp1 and lp2 was slightly below the control while trichome density was clearly elevated, most strongly in lp1, and the total count remained high without rising further.

3.2.3 Gravitropic stimulation in light increases oil yield while shifting composition

Because glandular trichome density and total trichome count changed in response to gravitropic stimulation, essential oil yield was assessed to determine whether these structural changes were reflected in oil production. Beyond total yield, the relative proportions and absolute quantities of the principal quality-determining components were analyzed, as both the amount of oil and its composition define the commercial value of peppermint oil.

Oil yield

Essential oil yield was determined by hydro distillation and expressed as oil volume per gram dry leaf mass. Gravitropic stimulation significantly increased oil yield at all stress levels compared to the control (Figure 29). The increase was largest at mild stress. Moderate stress showed a significantly smaller increase than mild stress, and severe stress lay between the mild and moderate values.

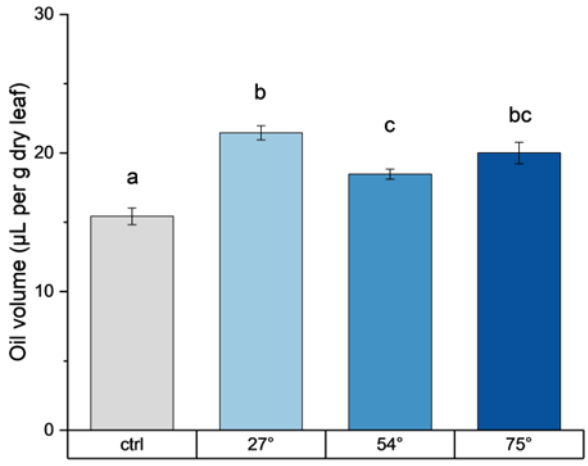

Figure 29 Essential oil volume per gram dry leaf mass under increasing gravitropic stress during daily tilting in light. *Oil volume (µL per g dry leaf) is shown for tilting angles of 27°, 54° and 75° compared to untilted controls (ctrl). Data represent means ± SE (n = 3). Different letters indicate statistically significant differences between groups as determined by one-way ANOVA followed by Tukey's HSD post-hoc test ($p < 0.05$).*

Relative Composition

The relative proportions of the three principal quality-determining components - menthol, menthone and menthofuran - were quantified by GC-MS. These components derive from the same biosynthetic branch point at pulegone, and their proportions were assessed to determine whether gravitropic stimulation shifts the balance between them (Figure 30). The percentages reflect the distribution among these three components only, not their absolute contribution to the total oil. Pulegone and limonene, also quantified by GC-MS, are reported in the Appendix (Figure A6). Pulegone showed no substantial variation across treatments, and limonene was present only in trace amounts.

At mild stress, the proportion of menthol decreased with a corresponding increase in menthone, while menthofuran decreased slightly. At moderate and severe stress, the proportion of menthofuran increased and menthol decreased, while menthone remained at the control level at these two stress levels.

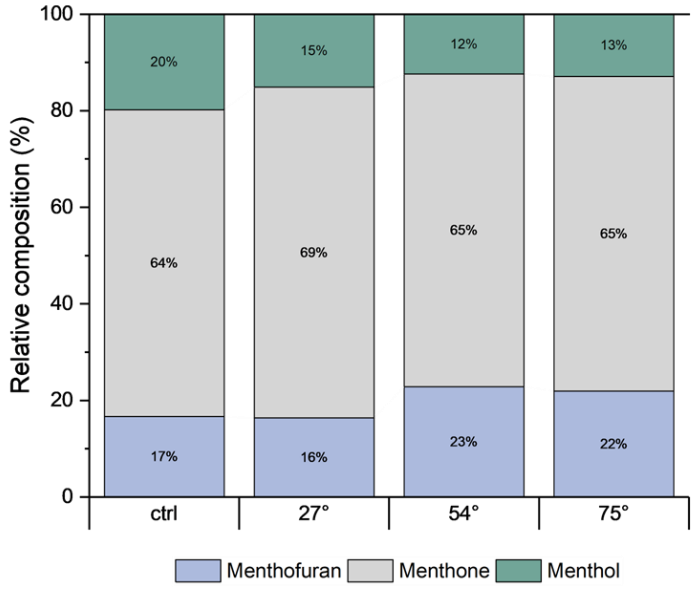

Figure 30 Relative composition of the three principal essential oil components under increasing gravitropic stress during daily tilting in light. *Relative proportions (%) of menthofuran, menthone and menthol are shown for tilting angles of 27°, 54° and 75° compared to untilted controls (ctrl). Data represent means (n = 3). Note that percentages reflect the relative distribution among these three components only and do not represent absolute contributions to total oil composition.*

Absolute quantities

To complement the relative proportions, the absolute quantities of the five principal components - limonene, pulegone, menthofuran, menthone and menthol - were determined by GC-MS as mg per gram dry leaf mass (Figure 31). The absolute quantity was significantly reduced at moderate stress compared to the control, while mild and severe stress did not differ significantly

from either the control or moderate stress. As already apparent from the relative composition, menthone dominated the quantitative profile across all treatments, and the changes affected primarily menthol and menthofuran.

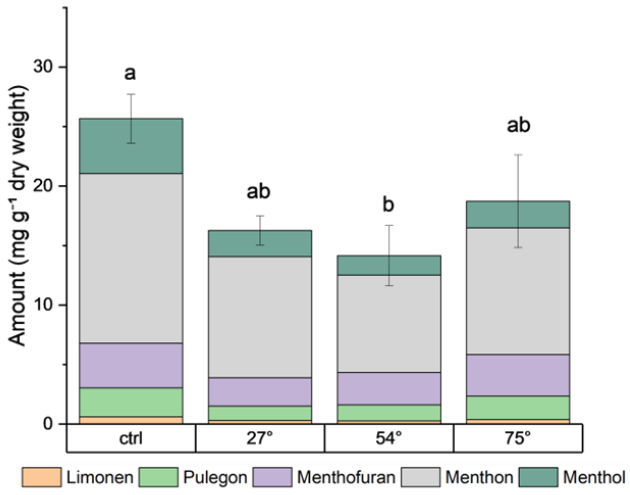

Figure 31 Absolute quantity of principal essential oil components per gram dry leaf mass under increasing gravitropic stress during daily tilting in light. *Combined amount (mg g⁻¹ dry weight) of limonene, pulegone, menthofuran, menthone and menthol is shown for tilting angles of 27°, 54° and 75° compared to untilted controls (ctrl). Data represent means ± SE (n = 3). Different letters indicate statistically significant differences between groups as determined by one-way ANOVA followed by Tukey's HSD post-hoc test (p < 0.05).*

Together, these results show that gravitropic stimulation increased essential oil yield at all stress levels, with the highest yield at mild stress, while shifting the relative composition toward menthofuran at moderate and severe stress. The absolute quantity of the five principal components was lowest at moderate stress and did not parallel the yield increase.

3.2.4 Summary: gravitropic stimulation in light

Across all measured traits, gravitropic stimulation under daily tilting in light affected peppermint at multiple levels. Biomass accumulation was promoted, most clearly in the leaves at mild stress, while overall morphology and root architecture changed only slightly. Leaf surface area increased at moderate stress, and the total glandular trichome count per leaf rose across stress levels, reaching its highest values at moderate stress. Essential oil yield was significantly elevated at all stress levels, with the highest yield at mild stress, while the relative oil composition shifted toward menthofuran at moderate and severe stress. The direction and magnitude of these responses varied with stress dose, with mild stress producing the highest oil yield and higher stress levels producing the shift toward menthofuran.

3.3 The response to gravitropic stimulation depends on light and continuity of the stimulus

The effects described in the previous section were obtained under daily tilting during the light phase. To assess whether they represent a general response to mechanical reorientation, or whether they depend on the timing and continuity of the stimulus, the same parameters were analyzed under two alternative protocols: daily tilting during the dark phase and continuous tilting throughout the day–night cycle. The results are presented as the percentage change relative to the untilted control of each protocol, with the daily-light data included for reference.

3.3.1 Growth, biomass and root architecture respond differently across protocols

Shoot morphology, dry biomass and root architecture were compared across the three protocols to determine whether the growth responses observed under gravitropic stimulation in light persisted under darkness or continuous gravitropic stimulation (Figure 32).

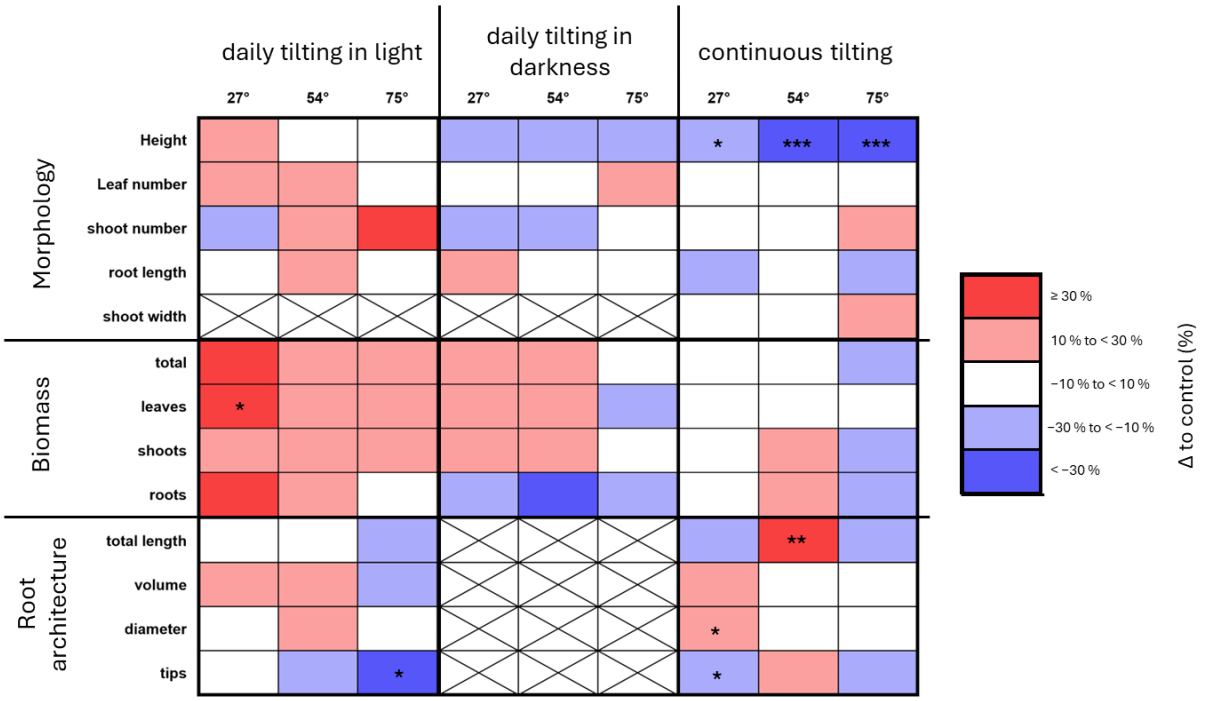

Figure 32 Effect of gravitropic stimulation on shoot morphology, biomass and root architecture across the three tilting protocols. *Percentage change relative to the untilted control of the respective protocol is shown for morphological parameters, dry biomass of plant fractions, and root architecture parameters, for tilting angles of 27°, 54° and 75°. Crossed-out fields indicate parameters not measured under the respective protocol: shoot width was recorded only under continuous tilting, and root architecture was not assessed under daily tilting in darkness. The color scale represents the percentage change relative to control, from blue (decrease) through white (no substantial change) to red (increase), in the categories indicated. Asterisks indicate statistically significant differences from the respective control (* $p < 0.05$, ** $p < 0.01$, *** $p < 0.001$). Data for daily tilting in light are shown for reference and correspond to the results presented in section 3.2.1. Detailed data for the rest is shown in Figures A7 -A9 (Appendix).*

Gravitropic stimulation in darkness

Plant height showed a slight decrease at all stress levels. Shoot number decreased slightly at mild and moderate stress and was unchanged at severe stress. Leaf number increased slightly at severe stress and was unchanged otherwise, while root length increased slightly at mild stress and was unchanged at the other levels. For biomass, total, leaf and shoot fractions increased slightly at mild and moderate stress. At severe stress these were unchanged, except for leaf biomass, which decreased. Root biomass decreased at all stress levels, slightly at mild and severe stress and more strongly at moderate stress. None of these changes were significant relative to the control. Root architecture was not assessed under this protocol, as the analysis equipment was not available during the darkness experiments.

Continuous gravitropic stimulation

Plant height was significantly reduced at all stress levels, with a stronger reduction at moderate and severe stress. Leaf number was unchanged, while shoot number and shoot width increased slightly at severe stress and were unchanged at mild and moderate stress. Root length decreased slightly at mild and severe stress and was unchanged at moderate stress. For biomass, leaf

biomass was unchanged across all stress levels, while shoot and root biomass were unchanged at mild stress, increased slightly at moderate stress and decreased slightly at severe stress. Total biomass was unchanged at mild and moderate stress and decreased slightly at severe stress. None of the biomass changes were significant relative to the control. For root architecture, total root length decreased slightly at mild and severe stress and increased significantly at moderate stress. Root volume and diameter increased slightly at mild stress, significantly so for diameter, and were unchanged at moderate and severe stress. Root tip number was significantly reduced at mild stress, decreased slightly at severe stress, and increased slightly at moderate stress.

Together, these results show that the growth response differed between protocols. Under gravitropic stimulation in darkness, morphology and biomass changed only slightly and never significantly. Under continuous gravitropic stimulation, plant height was significantly and progressively reduced, and root architecture responded mainly at mild and moderate stress, with a significant increase in total root length at moderate stress and significant changes in root diameter and tip number at mild stress.

3.3.2 Trichome parameters respond differently across protocols

Glandular trichome density, leaf surface area and total trichome count per leaf were compared across the three protocols to determine whether the trichome response observed under gravitropic stimulation in light occurred under darkness or continuous gravitropic stimulation (Figure 33). Because density is expressed per unit leaf area, the three parameters are described together.

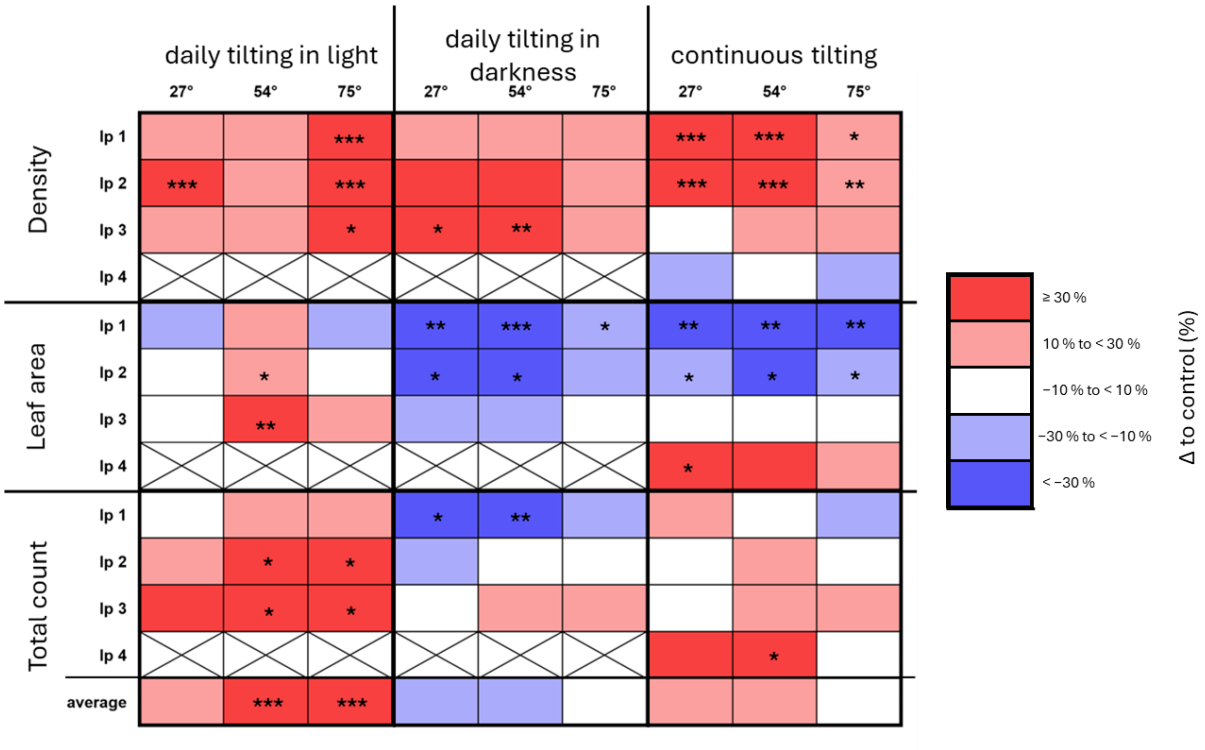

Figure 33 Effect of gravitropic stimulation on glandular trichome parameters across the three tilting protocols. *Percentage change relative to the untilted control of the respective protocol is shown for glandular trichome density, leaf surface area and total trichome count per leaf, resolved by leaf pair (lp) and as the average across leaf pairs, for tilting angles of 27°, 54° and 75°. For daily tilting in light and in darkness, leaf pairs 1–3 were analyzed; for continuous tilting, leaf pairs 1–4 were analyzed, so that the average values are based on three and four leaf pairs respectively. Crossed-out fields indicate leaf pairs not measured under the respective protocol. The color scale represents the percentage change relative to the respective control, from blue (decrease) through white (no substantial change) to red (increase), in the categories indicated. Asterisks indicate statistically significant differences from the respective control (* $p < 0.05$, ** $p < 0.01$, *** $p < 0.001$). Data for gravitropic stimulation in light are shown for reference and correspond to the per-leaf-pair results presented in section 3.2.2. Detailed data for the rest is shown in Figures A10 -A13 (Appendix).*

Gravitropic stimulation in darkness

Trichome density increased in all leaf pairs, with the strongest increase in lp3, where the values at mild and moderate stress were significant. In lp1 and lp2, leaf surface area was reduced at the same time, significantly in lp1 at all stress levels and in lp2 at mild and moderate stress, while in lp3 leaf surface area showed little to no reduction. Total trichome count per leaf was strongly and significantly reduced in lp1 at mild and moderate stress and slightly reduced at severe stress. In lp2, count was slightly reduced at mild stress and unchanged at moderate and severe stress. In lp3, count was unchanged at mild stress and slightly increased at moderate and severe stress. Averaged across leaf pairs, total trichome count was slightly reduced at mild and moderate stress and unchanged at severe stress, without reaching significance.

Continuous gravitropic stimulation

In the younger lp1 and lp2, trichome density increased significantly at all stress levels, more strongly at mild and moderate stress than at severe stress, while leaf surface area was significantly reduced at all stress levels. In lp3, density was unchanged at mild stress and

slightly increased at moderate and severe stress, with leaf surface area largely unchanged. In the oldest lp4, density decreased slightly at mild and severe stress, while leaf surface area increased, significantly at mild stress. Total trichome count per leaf was slightly increased or unchanged in lp1, lp2 and lp3, while lp4 showed a strong increase at mild and moderate stress, significant at mild stress. Averaged across leaf pairs, total trichome count was slightly increased at mild and moderate stress and unchanged at severe stress, without reaching significance.

Together, these results show that the trichome response differed between protocols both along the leaf axis and across the stress range. In both protocols, leaf surface area was reduced in the younger leaf pairs and recovered or increased in the older leaf pairs, with the increase occurring at lp4 under continuous stimulation, where lp3 was not yet affected. The clearest difference between protocols was found in trichome density. Under darkness it increased mainly in the older leaf pairs, whereas under continuous stimulation it increased mainly in the younger leaf pairs, similar to the pattern under gravitropic stimulation in light. Total trichome count followed a common spatial trend, decreasing or only slightly increasing in the younger leaf pairs and increasing in the older leaf pairs in both protocols. The two protocols also differed in their stress dependence. Under continuous stimulation the total count increase became smaller with increasing tilt angle, opposite to the increase seen under gravitropic stimulation in light, while under darkness the count reduction became smaller with increasing tilt angle.

3.3.3 Oil yield differs between protocols while composition shifts similarly

Essential oil yield was determined by hydro distillation, and the absolute quantity and relative proportions of the principal components were quantified by GC-MS. These parameters were compared across the three protocols to determine whether the responses observed under gravitropic stimulation in light occurred under darkness or continuous gravitropic stimulation.

Oil yield and absolute quantity

Under gravitropic stimulation in darkness, oil yield was slightly reduced at all stress levels, and the absolute quantity of the principal components was unchanged at mild stress and decreased with increasing tilt angle (Figure 34). Under continuous gravitropic stimulation, oil yield was slightly increased at mild and moderate stress and unchanged at severe stress, while the absolute quantity was unchanged at mild and severe stress and markedly increased at moderate stress. None of these changes were significant relative to the respective control.

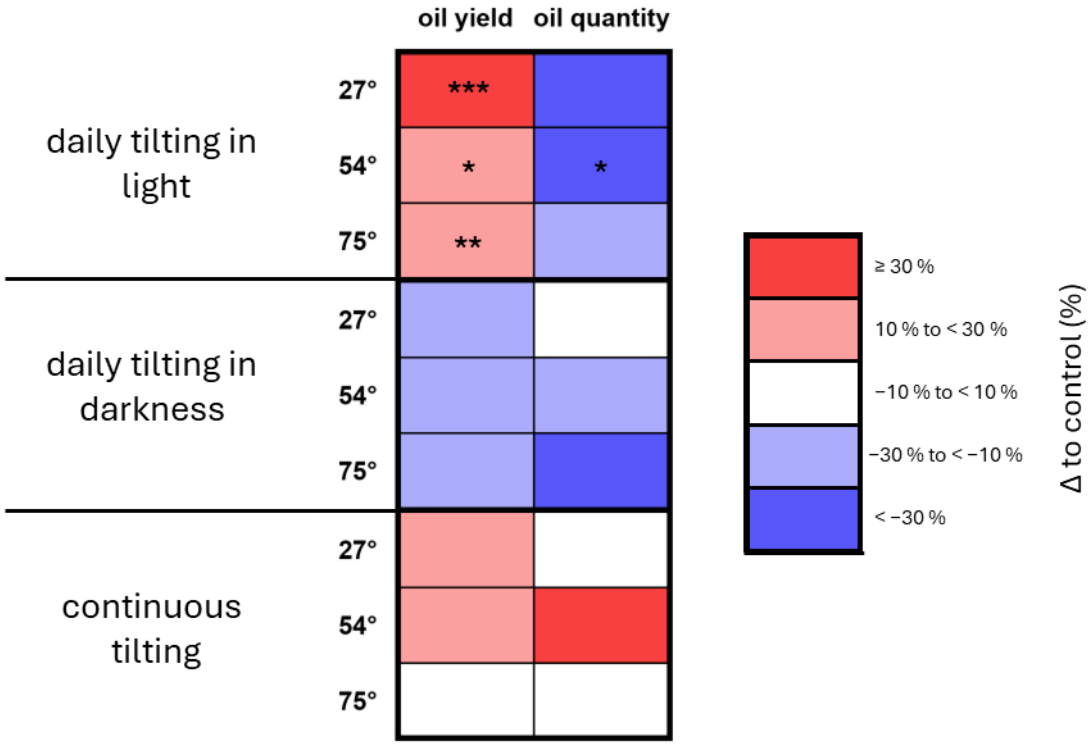

Figure 34 Effect of gravitropic stimulation on essential oil yield and absolute oil quantity across the three tilting protocols. *Percentage change relative to the untilted control of the respective protocol is shown for oil yield (oil volume per gram dry leaf mass) and oil quantity (combined absolute amount of the principal components per gram dry leaf mass), for tilting angles of 27°, 54° and 75°. The color scale represents the percentage change relative to the respective control, from blue (decrease) through white (no substantial change) to red (increase), in the categories indicated. Asterisks indicate statistically significant differences from the respective control (* $p < 0.05$, ** $p < 0.01$, *** $p < 0.001$). Data for gravitropic stimulation in light are shown for reference and correspond to the results presented in section 3.2.3. Detailed data for the rest is shown in Figures A14 -A15 (Appendix).*

Relative composition

Under gravitropic stimulation in darkness, oil composition at mild stress was comparable to the control (Figure 35). With increasing tilt angle, the proportion of menthofuran increased and menthol decreased, while menthone remained largely stable. Under continuous gravitropic stimulation, all groups including the control showed a high proportion of menthofuran and a low proportion of menthol. The proportion of menthofuran increased with increasing tilt angle, while menthone decreased.

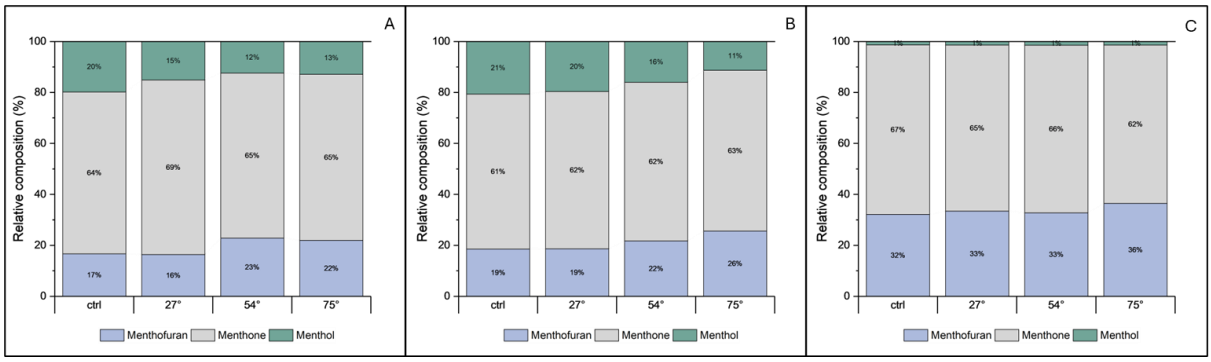

Figure 35 Relative composition of the three principal essential oil components across the three tilting protocols. *Relative proportions (%) of menthofuran, menthone and menthol are shown under gravitropic stimulation in light (A), in darkness (B) and under continuous gravitropic stimulation (C), for tilting angles of 27°, 54° and 75° compared to untilted controls (ctrl). Data represent means (n = 3). Percentages reflect the relative distribution among these three components only and do not represent absolute contributions to total oil composition. Panel A is included for reference and corresponds to the data presented in section 3.2.3. Pulegone and limonene, also quantified by GC-MS, are reported in the Appendix (Figure A6).*

Together, these results show that the oil response differed between protocols. The increase in oil yield seen under gravitropic stimulation in light was not reproduced under darkness, where yield was slightly reduced, or under continuous stimulation, where the increase was smaller and not significant. The shift toward menthofuran at higher stress levels occurred under both darkness and light, whereas under continuous stimulation the proportion of menthofuran was already high in the control and increased further with tilt angle.

Leaf-pair-resolved composition under continuous tilting (SPME)

The compositional analysis above was based on whole-plant samples obtained by hydro distillation and therefore did not resolve variation along the shoot. Since trichome parameters had shown distinct responses depending on leaf position, the relative monoterpene composition was additionally analyzed by leaf pair using solid-phase microextraction (SPME). This allowed the position-dependent trichome response to be examined at the level of oil composition, and addressed whether leaf age affects monoterpene synthesis in general and its response to gravitropic stimulation in particular. Because the SPME equipment was acquired late in the course of this work, this analysis was performed for continuous gravitropic stimulation only (Figure 36). In addition to the principal menthane monoterpenes, pinene and eucalyptol were included, as they were detectable and showed variation across leaf pairs and stress levels.

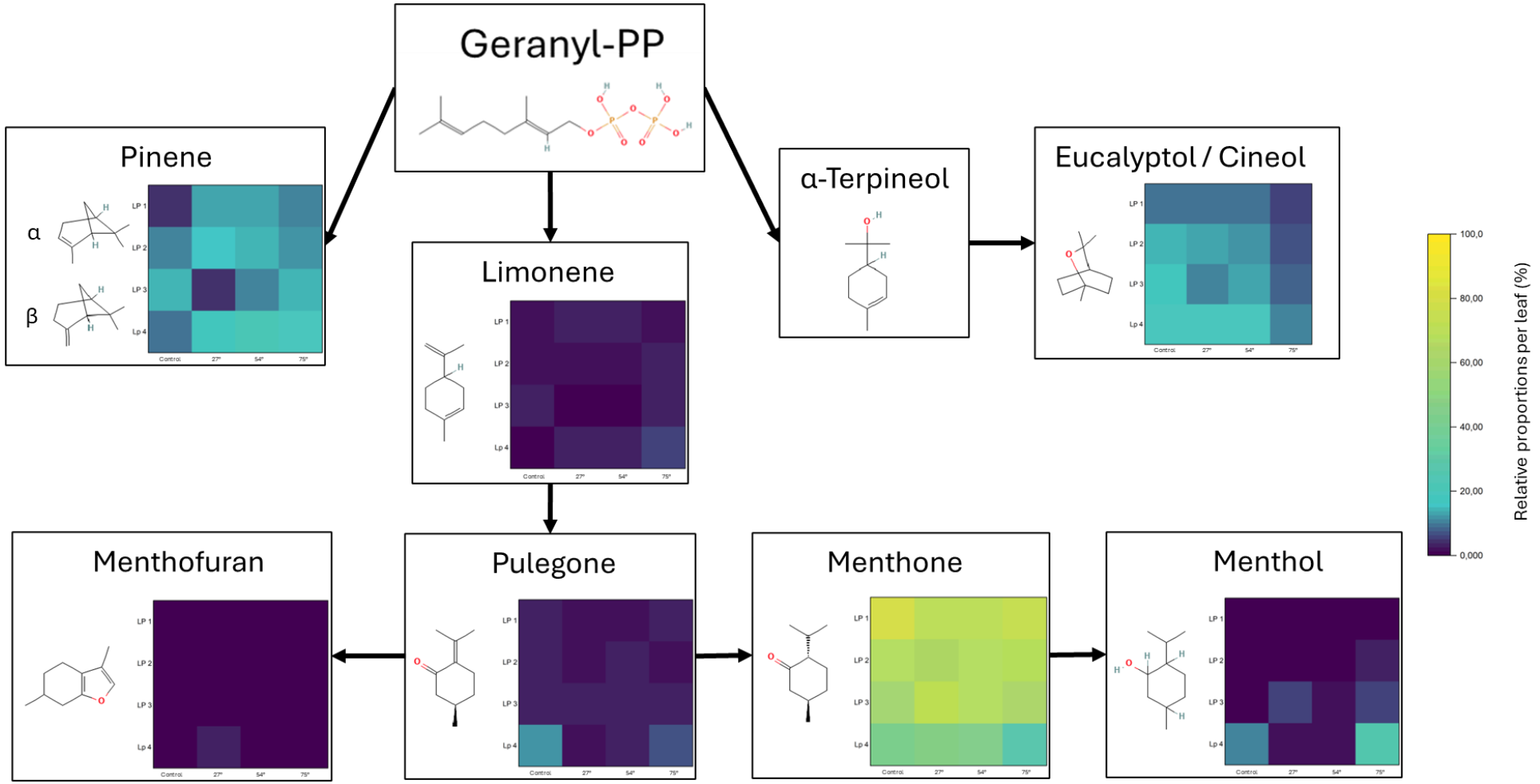

Figure 36 Relative monoterpene composition per leaf pair under continuous tilting at increasing tilt angles. *Relative proportions (%) of pinene, eucalyptol/cineol, limonene, pulegone, menthofuran, menthone and menthol are shown for leaf pairs 1–4 at tilting angles of 27°, 54° and 75° compared to untilted controls (ctrl). Data represent means of 3 leaves per leaf pair and treatment. The biosynthetic pathway from geranyl pyrophosphate (Geranyl-PP) to the individual components is indicated. The color scale ranges from dark purple (low relative proportion) to yellow (high relative proportion).*

Pinene showed a progressive increase with both increasing leaf age and increasing tilt angle. An exception was observed in the younger leaf pairs at severe stress, where a slight decrease occurred. Eucalyptol showed a similar increase with leaf age but was markedly reduced with increasing tilt angle. Limonene showed only a minor increase with both leaf age and tilt angle. The most notable elevation was observed in lp4 at severe stress. Pulegone was detectable primarily in lp4 of the control and in lp4 at severe stress. Negligible amounts were detected in all other conditions. Menthofuran was largely undetectable across all leaf pairs and tilt angles, with the exception of lp4 at mild stress. In contrast, menthofuran had been a major component in the hydro distillation-based analysis. Menthone decreased with increasing leaf age and showed a slight decrease with increasing tilt angle. Menthol increased with leaf age. Additional increases were observed at mild and severe stress, with the most pronounced elevation detected in lp4 at severe stress.

The SPME analysis showed that monoterpene composition varied strongly along the shoot axis. Menthol and pinene increased with leaf age, while menthone decreased, and several components responded to tilt angle in a leaf-position-dependent manner. The most pronounced changes under gravitropic stimulation occurred in the oldest leaf pair lp4.

3.3.4 Summary: alternative tilting protocols

Across all measured traits, the response to gravitropic stimulation differed markedly between protocols. Daily tilting in darkness produced weak, mostly non-significant growth and biomass responses and increased trichome density mainly in the older leaf pairs, while continuous tilting reduced plant height, increased trichome density mainly in the younger leaf pairs, and did not increase oil yield. The pronounced increase in oil yield seen under gravitropic stimulation in light was not reproduced by either alternative protocol. The compositional shift toward menthofuran at higher stress occurred under both light and darkness, whereas the oil yield increase was specific to light.

3.4 The role of jasmonic acid as a mediator of gravitropic effects

As shown in section 3.1.3, gravitropic stimulation induced expression of JAZ1, a marker of the jasmonic acid (JA) signaling pathway. To test whether JA is a causal mediator of the gravitropism-induced changes in glandular trichome parameters and essential oil composition described in section 3.2, two complementary pharmacological approaches were used. Exogenous methyl jasmonate (MeJA) was applied to test whether activation of the JA pathway

is sufficient to reproduce these changes, and the JA biosynthesis inhibitor phenidone was applied during gravitropic stimulation to test whether endogenous JA production is necessary.

3.4.1 Effects of exogenous MeJA on glandular trichomes and essential oil composition

To test whether exogenous activation of the JA signaling pathway is sufficient to reproduce the trichome and oil responses observed under gravitropic stimulation, plants were treated with methyl jasmonate (100 µM) over a two-week period. Because MeJA is volatile, the aeroponic tilting modules could not be used. Instead plants were cultivated in closed glass containers and sprayed at three-day intervals (section 2.6.1).

Trichome density

Glandular trichome density showed no significant difference between MeJA-treated and control plants, both as a mean across all leaf pairs and at the level of individual leaf pairs (Figure 37). A slight non-significant reduction was observed in lp3.

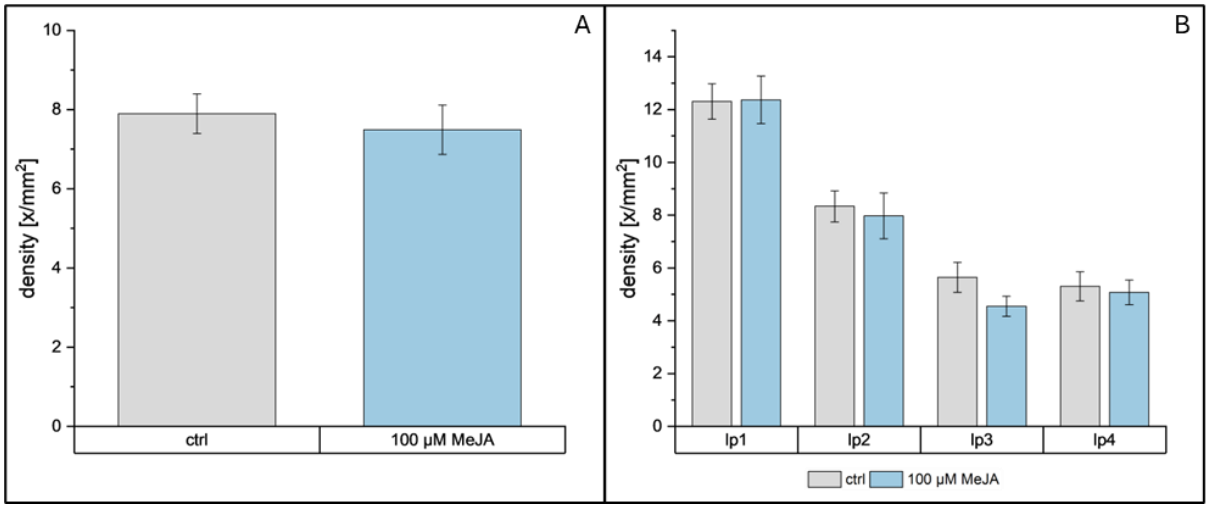

Figure 37 Glandular trichome density following MeJA treatment. *Mean density (x/mm²) across all leaf pairs (A) and per leaf pair (lp) 1–4 (B), numbered from the apical (youngest) to the more basal (older) leaf pairs, for untreated controls (ctrl) and 100 µM MeJA-treated plants. Data represent means ± SE. No statistically significant differences were detected.*

Leaf surface area

Leaf surface area was increased in MeJA-treated plants across lp1 to lp3, with significant increases in lp2 and lp3 (Figure 38). Leaf pair 4 showed no substantial change.

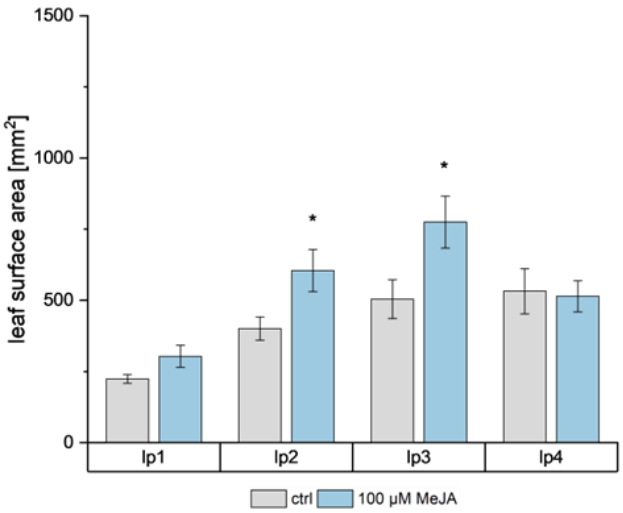

Figure 38 Leaf surface area per leaf pair following MeJA treatment. *Leaf surface area (mm²) is shown for lp 1–4, numbered from the apical (youngest) to the more basal (older) leaf pairs, for untreated controls (ctrl) and 100 µM MeJA-treated plants. Data represent means ± SE. Asterisks indicate statistically significant differences compared to the control (p < 0.05).*

Total trichome count per leaf

Total glandular trichome count per leaf was significantly higher in MeJA-treated plants than in the control (Figure 39). The increase was most pronounced in lp1 and lp2, where it was significant. Leaf pair 3 showed a non-significant increase, while leaf pair 4 remained unchanged.

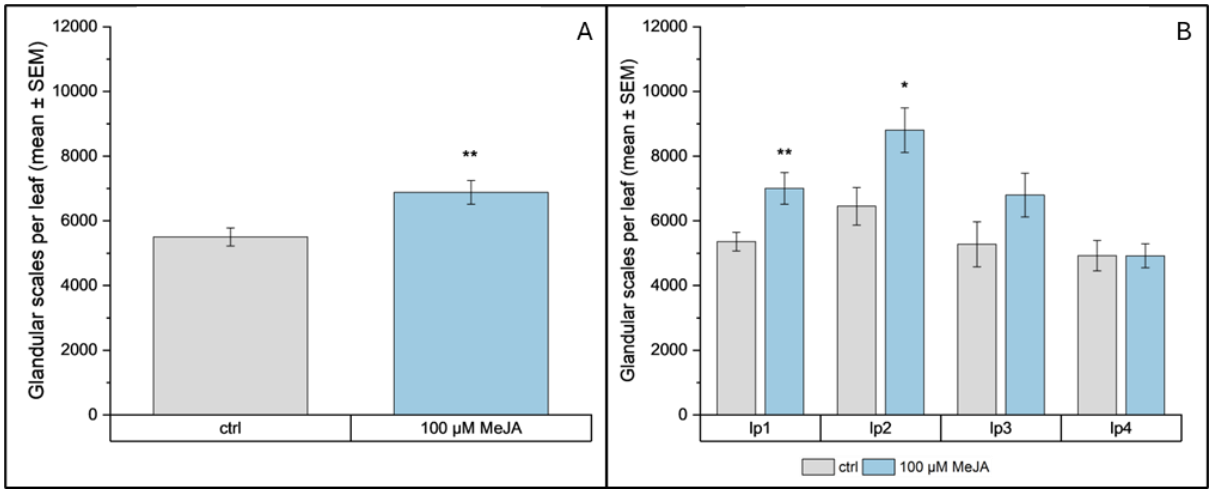

Figure 39 Total glandular trichome count per leaf following MeJA treatment. *Mean trichome count per leaf across all leaf pairs (A) and per lp 1–4 (B), numbered from the apical (youngest) to the more basal (older) leaf pairs, for untreated controls (ctrl) and 100 µM MeJA-treated plants. Data represent means ± SE. Asterisks indicate statistically significant differences compared to the control (p < 0.05, ** p < 0.01).*

Relative composition

The relative proportions of menthofuran, menthone and menthol in MeJA-treated plants resembled those observed under mild gravitropic stress during daily tilting in light (Figure 40). Under MeJA treatment, menthone increased while menthol and menthofuran decreased relative

to the solvent control. The oil composition for gravitropic stress treatments was determined by hydro distillation, while MeJA samples were extracted in hexane.

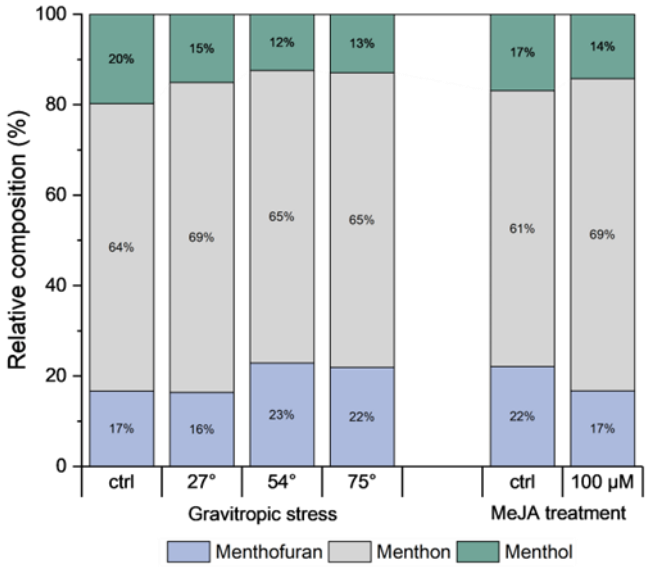

Figure 40 Relative composition of principal essential oil components under gravitropic stress and MeJA treatment. *Relative proportions (%) of menthofuran, menthone and menthol are shown for gravitropic stress treatments (ctrl, 27°, 54°, 75°; daily tilting in light) and MeJA treatment (ctrl, 100 µM MeJA). Note that percentages reflect the relative distribution among these three components only. Oil composition for gravitropic stress treatments was determined by hydro distillation. MeJA treatment samples were extracted in hexane (see Methods).*

Together, these results show that MeJA treatment increased total trichome count, most strongly in the youngest leaf pairs, and increased leaf surface area in lp2 and lp3, while trichome density was unchanged. The relative oil composition under MeJA resembled that under mild gravitropic stress, with a shift toward menthone.

3.4.2 Effects of phenidone-mediated JA inhibition on the gravitropic response

To test whether endogenous JA biosynthesis is required for the gravitropism-induced trichome and oil changes, the JA biosynthesis inhibitor phenidone (2 mM) was applied in combination with gravitropic stimulation at moderate stress (45°). Phenidone inhibits lipoxygenase, the first committed step of JA biosynthesis. Four groups were analyzed, all of which received spray treatment: the solvent-sprayed control (referred to as ctrl), the phenidone-sprayed control without tilting (ctrl + Ph), 45°-tilted plants with solvent spray (45°), and 45°-tilted plants with phenidone (45° + Ph). An additional untreated, unsprayed plant is shown for visual reference in Figure 41 but was not included in the analysis, as the spraying procedure itself reduced leaf and root development. All comparisons are therefore made within this experiment only.

Figure 41 Representative *Mentha* × *piperita* plants from the phenidone experiment. *From left to right: an untreated, unsprayed plant shown for visual reference, the solvent-sprayed control (ctrl), the phenidone-sprayed control without tilting (ctrl + Ph), 45°-tilted plants with solvent spray (45°), and 45°-tilted plants with phenidone (45° + Ph). The untreated plant illustrates the marked reduction in leaf and root development caused by the spraying procedure itself and was not included in the statistical analysis. Scale bar = 5 cm.*

Trichome density

Glandular trichome density was significantly higher in the 45° group compared to the control (Figure 42A). The phenidone-treated control (ctrl + Ph) showed a significant difference relative to all other groups. The 45° + Ph group showed intermediate density values, not significantly different from 45° alone but significantly higher than ctrl + Ph. When analyzed at the level of individual leaf pairs, density in lp1 was significantly higher in the 45° group compared to the control, and the 45° + Ph group showed a non-significant reduction compared to 45° alone (Figure 42B). A similar pattern was observed in lp2, where 45° showed higher density than the control and 45° + Ph showed a non-significant reduction compared to 45° alone. In lp3, the 45° group again showed higher density than the control, and the reduction in the 45° + Ph group compared to 45° alone reached statistical significance. In lp4, both 45° and 45° + Ph showed a non-significant increase in density compared to the control, with 45° + Ph slightly higher than 45° alone.

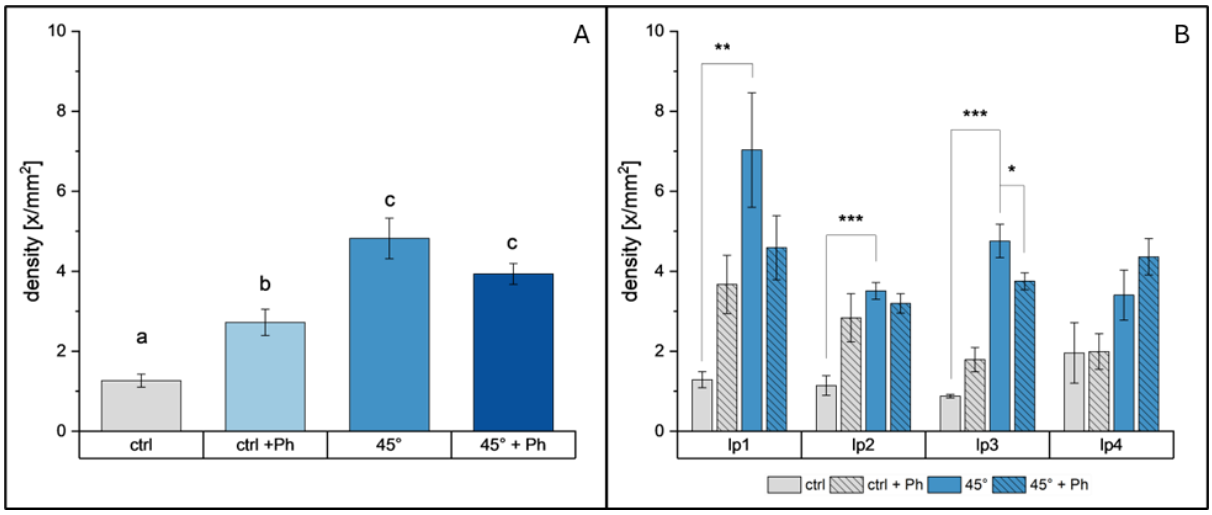

Figure 42 Glandular trichome density following phenidone treatment and gravitropic stimulation. *Mean density (x/mm²) across all leaf pairs (A) and per leaf pair (lp) 1–4 (B), numbered from the apical (youngest) to the more basal (older) leaf pairs, for solvent-sprayed controls (ctrl), phenidone-sprayed controls (ctrl + Ph), 45°-tilted plants with solvent spray (45°) and 45°-tilted plants with phenidone treatment (45° + Ph). Data represent means ± SE. Different letters in panel A indicate statistically significant differences between groups as determined by one-way ANOVA followed by Tukey's HSD post-hoc test ($p < 0.05$). Asterisks with brackets in panel B indicate statistically significant differences between the indicated groups ($p < 0.05$, ** $p < 0.01$, *** $p < 0.001$).*

Leaf surface area

Leaf surface area in the control group was the largest across almost all leaf pairs, the exception being lp3, where the 45° + Ph group showed the greatest leaf surface area (Figure 43). The 45° group showed reduced leaf surface area compared to the control across all leaf pairs, with significant differences in lp1 and lp2. In contrast, the 45° + Ph group consistently showed larger leaf surface area compared to 45° alone across all leaf pairs, reaching significance in lp2 and lp3.

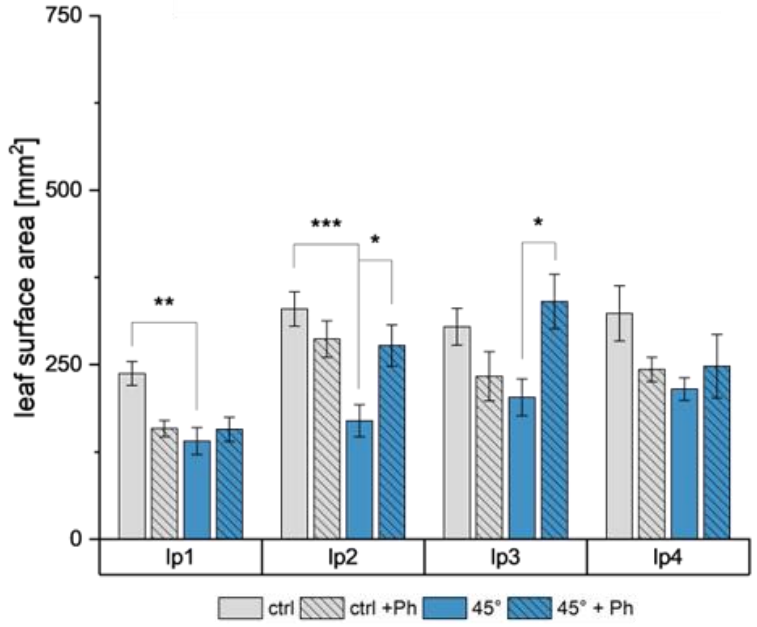

Figure 43 Leaf surface area per leaf pair following phenidone treatment and gravitropic stimulation. *Leaf surface area (mm²) is shown for lp 1–4, numbered from the apical (youngest) to the more basal (older) leaf pairs, for solvent-sprayed controls (ctrl), phenidone-sprayed controls (ctrl + Ph), 45°-tilted plants with solvent spray (45°) and 45°-tilted plants with phenidone treatment (45° + Ph). Data represent means ± SE. Asterisks with brackets indicate statistically significant differences between the indicated groups ($p < 0.05$, ** $p < 0.01$, *** $p < 0.001$). In lp1, ctrl differed significantly from both ctrl + Ph and 45° + Ph. In lp2, ctrl + Ph differed significantly from 45°.*

Total trichome count per leaf

Total glandular trichome count per leaf was significantly higher in both tilting groups (45° and 45° + Ph) compared to both control groups, with no significant difference between the two tilting groups (Figure 44A). At the level of individual leaf pairs, the 45° group showed higher trichome count compared to the control across all leaf pairs, with significant increases in lp1 and lp3 (Figure 44B). The 45° + Ph group showed an even higher trichome count than 45° alone in lp2 to lp4, though these differences did not reach significance, while in lp1 the 45° + Ph group showed a slightly lower count than 45° alone.

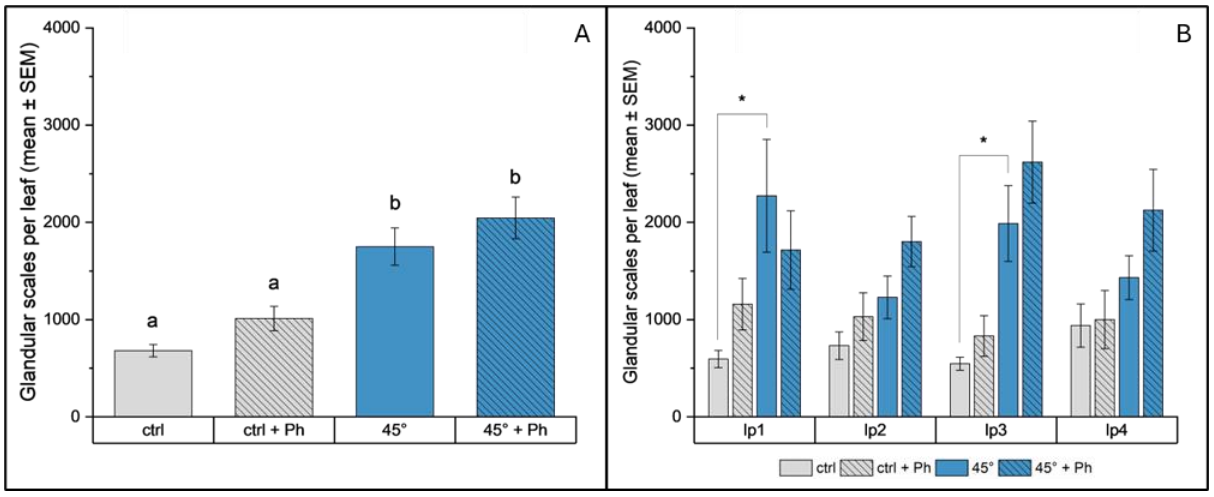

Figure 44 Total glandular trichome count per leaf following phenidone treatment and gravitropic stimulation. *Mean trichome count per leaf across all leaf pairs (A) and per lp 1–4 (B), numbered from the apical (youngest) to the more basal (older) leaf pairs, for solvent-sprayed controls (ctrl), phenidone-sprayed controls (ctrl + Ph), 45°-tilted plants with solvent spray (45°) and 45°-tilted plants with phenidone treatment (45° + Ph). Data represent means ± SE. Different letters in panel A indicate statistically significant differences between groups as determined by one-way ANOVA followed by Tukey's HSD post-hoc test ($p < 0.05$). In panel B, asterisks with brackets indicate statistically significant differences between the bracketed groups ($p < 0.05$). Additional significant differences not marked in the Figure for clarity: in lp2, 45° + Ph differed significantly from ctrl. In lp3, 45° + Ph differed significantly from both ctrl and ctrl + Ph. In lp4, 45° + Ph differed significantly from ctrl.*

Relative composition

Regarding whole-leaf essential oil composition, phenidone treatment in the absence of gravitropic stimulation (ctrl + Ph) resulted in a reduction of menthofuran and an increase in menthone compared to the control, while menthol decreased slightly (Figure 45). Under 45° tilting, menthofuran was lower than in the control, and menthone and menthol both increased. The combination of 45° tilting and phenidone treatment (45° + Ph) showed the lowest menthofuran proportion of all groups, with menthone further increased compared to 45° alone and menthol remaining comparable.

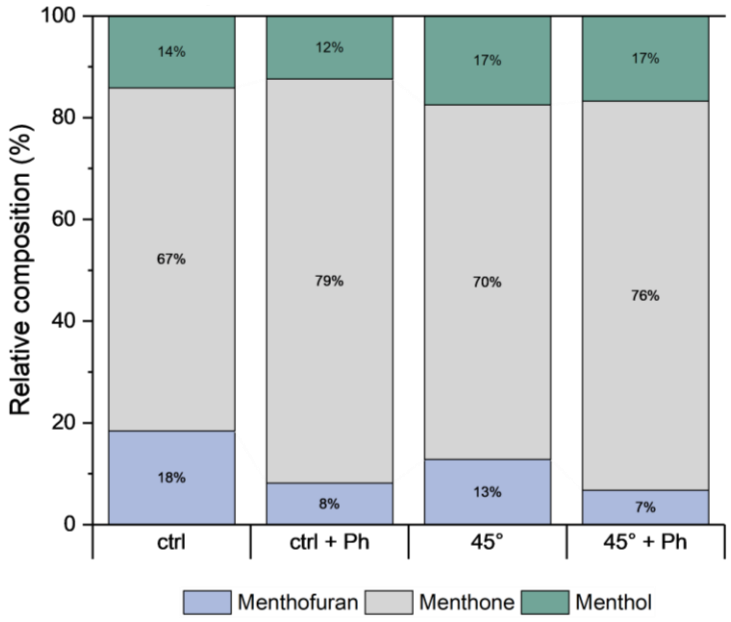

Figure 45 Relative composition of principal essential oil components following phenidone treatment and gravitropic stimulation. *Relative proportions (%) of menthofuran, menthone and menthol are shown for solvent-sprayed controls (ctrl), phenidone-sprayed controls (ctrl + Ph), 45°-tilted plants with solvent spray (45°) and 45°-tilted plants with phenidone treatment (45° + Ph). Note that percentages reflect the relative distribution among these three components only. Data represent means (n = 3). No statistical testing was performed.*

At the level of individual leaf pairs, the monoterpene composition showed distinct responses across individual components (Figure 46). Pinene showed a slight increase in the younger leaf pairs (lp1 and lp2) and a minor decrease in lp4 upon phenidone treatment of the control. Tilting at 45° markedly reduced pinene content, particularly in the younger leaf pairs, and the addition of phenidone to tilted plants partially recovered this reduction across all leaf pairs. Eucalyptol showed only a minor reduction in lp2 upon phenidone treatment of the control. Tilting at 45° increased eucalyptol content, particularly in the younger leaf pairs, and the addition of phenidone to tilted plants largely recovered this response to levels comparable to both control groups. Limonene showed no difference between the control and ctrl + Ph. Tilting at 45° reduced limonene in the younger leaf pairs (lp1–3) and increased it in lp4, and this effect was also recovered by phenidone addition. Pulegone was present in only very low proportions across all groups and leaf pairs, with no substantial differences between conditions. Menthofuran was reduced by phenidone treatment in the control group across all leaf pairs. Tilting at 45° also reduced menthofuran in the younger leaf pairs (lp1–2) and slightly increased it in lp4, and the combination of tilting and phenidone treatment further reduced menthofuran across all leaf pairs. Menthone increased upon phenidone treatment of the control across all leaf pairs. Tilting at 45° had little to no effect on menthone content, while the addition of phenidone to tilted plants again increased menthone, particularly in the younger leaf pairs (lp1–3). Menthol was slightly reduced in lp2 and lp3 upon phenidone treatment of the control. Tilting at 45° increased

menthol content, particularly in lp1 and lp2, and the addition of phenidone to tilted plants reduced menthol in the younger leaf pairs (lp1–2) and increased it in the older leaf pairs (lp3–4).

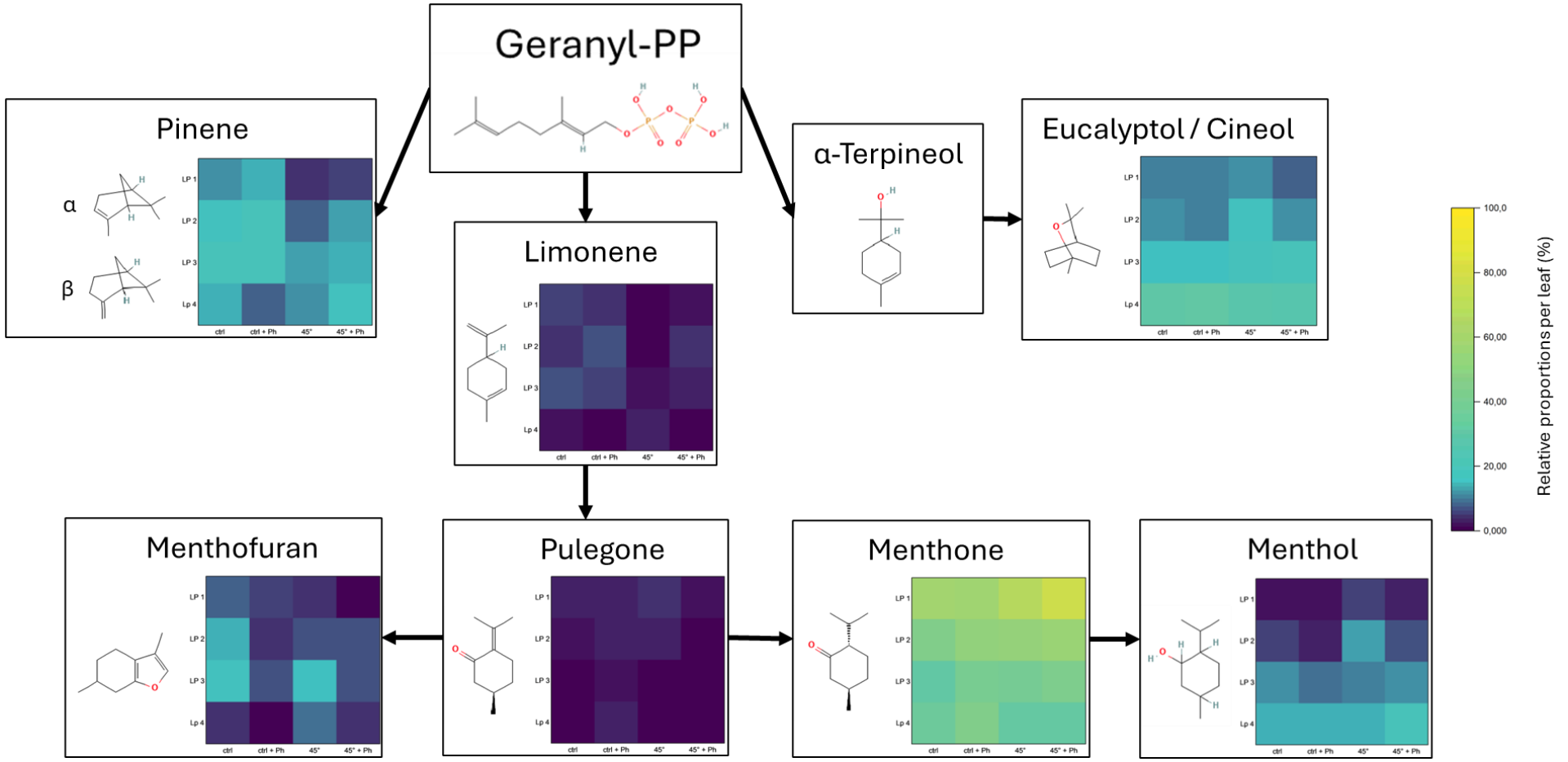

Figure 46 Relative monoterpene composition per leaf pair following phenidone treatment and gravitropic stimulation. *Relative proportions (%) of pinene, eucalyptol/cineol, limonene, pulegone, menthofuran, menthone and menthol are shown for lp 1–4, numbered from the apical (youngest) to the more basal (older) leaf pairs, for solvent-sprayed controls (ctrl), phenidone-sprayed controls (ctrl + Ph), 45°-tilted plants with solvent spray (45°) and 45°-tilted plants with phenidone treatment (45° + Ph). The biosynthetic pathway from geranyl pyrophosphate (Geranyl-PP) to the individual components is indicated. The color scale ranges from dark purple (low relative proportion) to yellow (high relative proportion). Data represent means of 3 leaves per leaf pair and treatment. No statistical testing was performed.*

Together, these results show that phenidone treatment did not fully suppress the gravitropism-induced increase in trichome count. Both 45° and 45° + Ph groups showed significantly higher trichome counts than the control groups, and at the level of individual leaf pairs the 45° + Ph group showed higher trichome counts than 45° alone in lp2 to lp4, with a slight reduction in lp1. Trichome density was reduced by phenidone in a leaf-pair-dependent manner, most strongly in lp3. Leaf surface area was reduced by tilting and partially restored by phenidone, with the 45° + Ph group showing the largest leaf surface area in lp3. In the oil composition, phenidone consistently reduced menthofuran and increased menthone both in the presence and absence of gravitropic stimulation. Gravitropic stimulation alone reduced pinene and limonene in the younger leaf pairs and increased eucalyptol there, and these effects were largely recovered by the addition of phenidone.

3.5 Summary of Results

Gravity Perception and Anatomy of Internodes

- Statolith-containing statocytes were detected in all four internodes examined, indicating that the gravisensory apparatus is structurally present throughout the shoot.
- Cell size and elongation increased progressively from internode 1 to internode 4, consistent with a developmental loss of elongation capacity in older internodes.

Gravitropic reaction: kinetics and adaptation

- *Mentha* × *piperita* shoots showed a clear gravitropic curvature response with kinetics and magnitude dependent on tilt angle and light conditions.
- Repeated tilting under darkness led to gravitropic adaptation, while repeated tilting under light over ten days progressively enhanced both the speed and magnitude of the response.

Signal transduction: JAZ, ARF1 and Expansin gene expression

- JAZ1 was consistently upregulated following gravitropic stimulation across all tissues, with the response most pronounced in internodes 1–2 and peaking after reversal of the tilt direction.
- ARF1 was consistently upregulated in the apical leaves during the reverse phase, with no coherent response in the internodes.

- Expansin showed distinct, tissue-specific patterns, with sustained upregulation in internodes 1–2 and internode 3 and a transient response in apical leaf 2. These changes largely coincided with the increased JAZ1 expression in the same tissues.

Growth, Morphology and Root Architecture

- Gravitropic stimulation had limited effects on overall morphology, with the most pronounced response observed under continuous tilting where plant height decreased significantly with increasing stress.
- Mild stress under daily tilting in light promoted biomass accumulation, while severe stress under continuous tilting negatively affected root biomass.
- Under continuous tilting, total root length increased significantly at moderate stress, while root diameter increased and root tip number decreased significantly at mild stress.

Glandular Trichomes and Leaf Surface Area

- Glandular trichome density and total trichome count were affected in a protocol- and leaf-pair-dependent manner, with the most pronounced increases under daily tilting in light at moderate and severe stress.
- Leaf surface area responses were also protocol- and leaf-pair-dependent, with continuous tilting reducing surface area in younger leaf pairs and daily tilting in darkness reducing surface area in younger leaf pairs at mild and moderate stress.

Essential Oil Yield and Composition

- Essential oil yield was significantly increased under daily tilting in light, while the absolute quantity of principal components was reduced.
- Gravitropic stimulation consistently shifted oil composition towards higher menthofuran proportions and lower menthol at moderate and severe stress.
- SPME-based leaf-pair analysis revealed differential effects on individual monoterpenes along the shoot axis, with particularly pronounced effects on pinene, eucalyptol and limonene in the older leaf pairs.

Role of Jasmonic Acid

- Exogenous MeJA application increased total trichome count and produced an oil composition comparable to mild gravitropic stress, but did not replicate the full pattern of gravitropic effects.

- Phenidone-mediated inhibition of JA biosynthesis did not suppress the gravitropism-induced increase in trichome count, but consistently reduced menthofuran proportions in the essential oil, both in the presence and absence of gravitropic stimulation.
- Phenidone also largely recovered the tilting-induced changes in pinene, eucalyptol and limonene.

4 Discussion

This discussion is structured along the three research questions of the thesis. The first part examines how *Mentha* × *piperita* perceives gravitropic stimulation and how the response unfolds. The second part evaluates whether daily tilting in light, used here as the reference protocol for the production-oriented assessment, can modulate growth and secondary metabolite production. Daily tilting in darkness and continuous tilting are then used as specificity and control treatments to test how far these effects depend on the light and timing of the stimulus. The final part asks whether jasmonic acid acts as a necessary or sufficient mediator of the observed effects.

Two terms are used in a defined sense throughout. Dose refers to the intensity of the stimulus, set by the tilt angle (mild, moderate, severe). Protocol refers to the light and timing condition under which tilting is applied (daily in light, daily in darkness, or continuous).

4.1 Gravitropic Competence and the Developmental Loss of Elongation Capacity along the Shoot Axis

A central observation from the histological analysis was that statolith-containing statocytes were present in all four internodes examined (Section 3.1.1), whereas gravitropic bending in response to reorientation was restricted to internodes 1 and 2 (Section 3.1.2). If the gravisensory apparatus is retained along the entire shoot, why does only the youngest tissue curve? The answer appears to lie downstream of perception. The structural apparatus is present throughout, while the capacity to translate the signal into curvature is lost in the older internodes. This pattern is consistent with prior reports that gravitropic sensitivity declines with tissue maturation (Li *et al.*, 2024) and that younger plants can re-erect after lodging while older ones cannot, despite both retaining functional statocytes (Blancaflor and Masson, 2003). The progressive increase in cell size and visibly elongated cell morphology in internodes 3 and 4 (section 3.1.1) indicates that these tissues have already largely completed their elongation program.

Mechanistically, gravitropic curvature depends on differential elongation between opposite flanks of the responding organ. This in turn requires that the responding cells retain the capacity for further wall expansion. As outlined in section 1.1, this capacity is associated with a predominantly transverse orientation of cellulose microfibrils on the inner cell wall face, deposited along cortical microtubule tracks (Paredez *et al.*, 2006; Crowell *et al.*, 2011). Mature cells, by contrast, accumulate longitudinal cellulose layers and undergo wall stiffening and lignification. Both processes compromise the directional extensibility required for asymmetric elongation. In the maize stem pulvinus, the loss of gravitropic responsiveness coincided with a microtubule rearrangement from transverse to longitudinal arrays and with lignification of supporting tissues (Collings *et al.*, 1998). The present histological data are consistent with a model in which gravitropic competence in *Mentha* × *piperita* internodes is constrained downstream of gravity perception, by the developmental state of the cell wall.

The polarization microscopy approach implemented in this work was intended to test this interpretation directly by comparing cellulose microfibril orientation between responsive (internode 1) and non-responsive (internode 4) internodes. The birefringence colors observed in cortical parenchyma and phloem cells of both internodes (Figure A1, Appendix) confirm that the methodological principle is applicable to *Mentha* × *piperita* tissue. However, the absence of a cotton fiber reference standard across all sections precluded calibration of birefringence colors to absolute microfibril orientation. The cellulose microfibril orientation hypothesis therefore remains untested by the present data and represents an important methodological gap for future work. Inclusion of a cotton fiber reference in every section, complemented by quantitative retardance mapping, would allow polarization microscopy to serve as a rapid in situ readout of gravitropic competence along the shoot developmental axis.

4.2 Gravitropic Reaction: Kinetics and Adaptation

Mentha × *piperita* shoots mounted a clear gravitropic curvature response, but its kinetics showed four features that are not obviously connected. A transient downward deflection occurred within the first 30 min after strong reorientation. Upward curvature then developed with a magnitude that depended on the stimulus. Repeated stimulation modulated the response in opposite directions under light and darkness. Finally, curvature persisted for at least one hour after the tilt direction was reversed. Can a single signaling architecture account for all four? The following sections address these features in turn and use them to develop a working model for the gravitropic response in *Mentha* × *piperita*.

The transient downward deflection observed within the first 30 min after extreme stress tilting (Figure 15A) corresponds to a phenomenon documented since the early kinetic studies of cereal coleoptiles. Hild and Hertel (1972) showed that maize coleoptiles exposed to a strong gravity stimulus initially bend towards gravity before the conventional upward bending develops after approximately 15–20 min. They attributed this to overstimulation of the auxin secretion machinery on the physically lower flank. At high local statolith pressure, auxin efflux is inhibited rather than enhanced, leading to a net upward redistribution of auxin and consequently to downward bending. Using the amylomaize mutant with smaller amyloplasts, they showed that this initial response appears only at 10×g, providing direct evidence that the negative bending scales with stimulus strength. Hertel (1983) subsequently formalized this behavior in a gating-cycle model of the auxin exit carrier with a biphasic dose-response. Myers *et al.*, (1994) argued that such sign reversals are not an artefact of particular model systems but a widespread feature of shoot gravitropism that any mechanistic model must accommodate. Consistent with these reports, the present data show a clear stimulus dependence of the initial deflection. The deflection reaches approximately −2.5° at 90° in darkness (Figure 15A), is essentially absent at 45° (Figure 15B), and is only mildly expressed under light at 54° (Figure 17). This pattern is consistent with the overstimulation interpretation, in which the magnitude of the initial negative phase scales with the effective local gravity signal experienced by the perceiving cells.

The subsequent development of upward curvature is gated by a reaction time downstream of perception. Chauvet *et al.*, (2019) introduced a minimum reaction time $\tau_{reaction}$ of approximately 13 min for the onset of the gravitropic growth response in wheat coleoptiles. Comparable estimates of around 30 min have been reported for rice coleoptiles (Iino *et al.*, 1996) and maize roots (Nelson and Evans, 1986). These values were obtained in young, highly active embryonic organs whose function is rapid reorientation after germination. In the more mature *Mentha* × *piperita* shoot, a longer reaction time may be expected, given the general decline of gravitropic sensitivity with tissue maturity (section 1.1). The observation that significant upward curvature is first detected between 30 and 60 min in both the 90° and 45° experiments (Figures 15) is consistent with this expectation. Since the reaction time is independent of gravity intensity, it likely reflects downstream molecular processes such as auxin transport establishment rather than the perception step itself.

The divergent modulation of response magnitude observed under repeated stimulation in light and darkness requires a framework that can accommodate both directions of change within a single signaling architecture. A useful starting point is the conceptual distinction between

sensory adaptation and habituation (Wang *et al.*, 2020). Sensory adaptation shifts the dose-response curve along the stimulus axis. Habituation modulates response amplitude at constant perception. Both processes can coexist and act on different components of the signaling chain. The progressive reduction in maximum curvature observed in darkness (Figure 16), accompanied by a faster onset, is consistent with such a combined modulation of perception sensitivity and downstream response amplitude.

An open question concerns the cellular substrate of this modulation. Several mechanistic candidates can be invoked from the current literature, but the available evidence does not permit an unambiguous assignment. One possibility derives from the susceptor model developed for cold signaling by Wang *et al*., (2020). In this model, microtubules do not transduce the physical signal themselves but determine the sensitivity with which a physical stimulus is converted into a chemical readout. In a grapevine cell system, prior stress modified microtubule organization and rendered subsequent perception more efficient, a phenomenon termed priming. The extension of this model to gravitropism is motivated by the work of Nick *et al*., (1991), who identified a distinct, drug-sensitive microtubule population selectively required for gravitropic but not phototropic signal transduction. This places the microtubule substrate upstream of the convergence point of the two signaling chains. The role of microtubules in gravitropism was characterized as speculative by the authors themselves and has not been conclusively resolved since. The transfer of the susceptor model from cold to gravity is therefore a plausible working hypothesis rather than a directly demonstrated mechanism.

An alternative or complementary mechanism arises from the more recent findings on the LAZY protein family summarized by Roychoudhry and Kepinski (2024). In this model, LAZY proteins migrate on the sedimenting amyloplasts to the new lower side of the cell. There, they recruit the auxin transporters PIN3 and PIN7 to the plasma membrane via RLD adapter proteins, establishing the lateral auxin gradient. The attachment of LAZY proteins to the amyloplasts is regulated by MPK3/MKK5-mediated phosphorylation. This model does not involve microtubules and instead postulates direct position-sensitive perception, consistent with the increasing evidence for position-based rather than force-based gravitational perception (Chauvet *et al.*, 2016; Nishimura *et al.*, 2023). One may speculate that altered activity of the MPK3/MKK5 cascade or altered pools of phosphorylated LAZY proteins could contribute to such sensitization, although this has not been experimentally tested. An experimental discrimination between a microtubule-based susceptor and a LAZY-mediated mechanism is not possible on the basis of the kinetic data presented here. The shortened latency of curvature onset

across consecutive tilting days, from 240 min on day 1 to 10 min on day 10 at 75° under light (Figure 18B), is consistent with the sensitization pattern predicted by both candidate mechanisms.

This raises the question why repeated stimulation reduces response amplitude in darkness but increases it under light. A plausible explanation emerges from the interplay between two competing tropistic systems. Nick *et al*., (1990b) showed in maize coleoptiles on a clinostat that the suppressing effect of phototropic stimulation on gravitropic responses is global rather than localized. The converse suppression by gravitropic stimulation, in contrast, is confined to the plane of stimulation. This asymmetry implies that a phototropic signal coming from one constant direction can suppress gravitropic responses across the entire organ. In the present light experiments, the light source was tilted together with the plants. Light therefore continued to enter from the morphological upper side of the shoot and acted as a continuous phototropic stimulus that confirmed the original growth direction. This explains why the initial curvature responses under light (Figure 17) were markedly weaker than under comparable conditions in darkness (Figures 15). The gravitropic stimulus was initially suppressed by the dominant phototropism.

Under repeated tilting across multiple days, this balance may shift. Because the light source was co-tilted, the phototropic stimulus retained the same quality and direction across all days. It therefore offered no basis for adaptive modulation. The gravitropic stimulus, in contrast, occurred each day as a fresh stimulation and could progressively sensitize its underlying substrate, whether microtubule-based or LAZY-mediated. This is consistent with the priming concept of Wang *et al*., (2020). As the sensitivity of the gravitropic system increased, the balance between the two tropisms shifted. The initially dominant phototropism remained constant. The initially suppressed gravitropic drive grew progressively stronger until it overcame the phototropic suppression. This interpretation accounts for the apparently paradoxical observation that on day 10 the plant actively curved out of the phototropically optimal orientation (Figure 18). The gravitropic drive had overtaken the phototropic one.

This interpretation is complemented by the phytochrome-based findings of Gaiser and Lomax (1993). They showed that phytochrome modulates the gravitropic response machinery at the level of auxin transport. In light, phytochrome is photoreversibly active and maintains the downstream transport machinery in a responsive state. The sensitization of the perception system gained through priming can therefore translate into enhanced auxin redistribution. In darkness, this phytochrome-dependent maintenance of transport readiness is absent. The

adaptive sensitivity change described by Hild and Hertel (1972), with a half-life of 10–20 min, and the covalent carrier modification mechanism proposed by Hertel (1983) provide a plausible molecular basis for the habituating downregulation observed here. These phenomena were originally characterized in coleoptiles rather than in dark-grown mature shoot tissue.

Within this framework, the persistence of curvature after reversal of the tilt direction (Figures 15 and 17) reflects a separate but compatible process. Nick and Schäfer (1988) demonstrated for maize coleoptiles that tropistic stimulation establishes a stable directional memory developing in three phases: a labile phase up to 65 min, a transient phase between 65 and 95 min, and a stable phase from 95 min onwards. Once stable, this memory determines the final curvature direction even when an opposing stimulus of equivalent strength is applied subsequently. The second stimulus then produces only transient bending. This memory is induced by both phototropic and gravitropic stimulation. The memory-integration time scale τ_memory introduced by Chauvet *et al.*, (2019) provides a quantitative parallel. It predicts that a sufficiently long first stimulation establishes a directional bias that dominates over a subsequent opposing stimulus for several hours. The observation that the shoot tip maintained its curvature for at least 60 min after reversal and only declined significantly between 120 and 240 min is in qualitative agreement with this prediction.

Taken together, the data are compatible with the following model (Figure 47). The initial downward deflection reflects transient overstimulation of the auxin transport machinery in cells experiencing the strongest local gravity signal. The subsequent kinetics of the main upward curvature are gated by a reaction time downstream of perception. The gravitropic perception and transduction system is progressively sensitized under repeated stimulation, with both a microtubule-based susceptor (Nick *et al.*, 1991; Wang *et al.*, 2020) and a modulated LAZY-MPK3 cascade (Roychoudhry and Kepinski, 2024) representing plausible mechanistic substrates. The divergent amplitude modulation under light and in darkness arises from the interplay between globally acting phototropic suppression (Nick *et al.*, 1990b) and phytochrome-dependent modulation of auxin transport (Gaiser and Lomax, 1993). The persistence of curvature after reversal reflects a stable directional memory (Nick and Schäfer, 1988) established during the first stimulation phase. An experimental resolution of the competing molecular models of gravitropic perception and sensitivity modulation lies beyond the scope of this work.

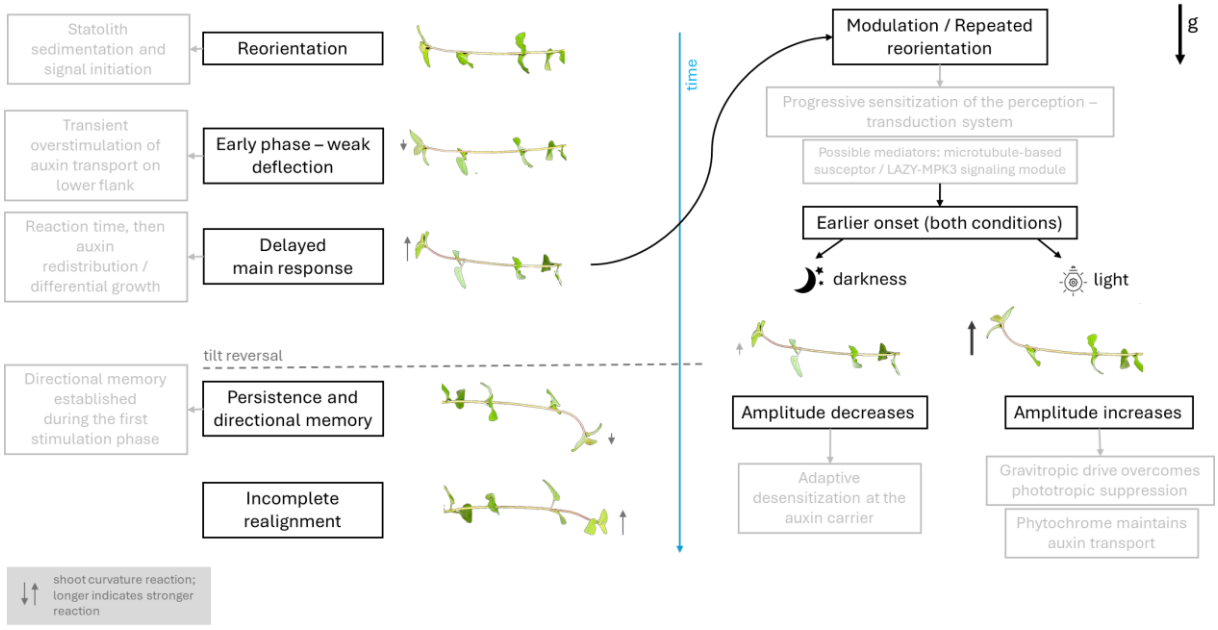

Figure 47 Working model of gravitropic curvature kinetics and its modulation in *Mentha* × *piperita*. *The model integrates the four kinetic features observed in this study with plausible mechanisms drawn from the literature. Solid boxes denote features observed in the present work. Grey dashed boxes denote proposed or literature-based mechanisms. Representative shoots illustrate each phase. The small arrows next to the shoots indicate the curvature reaction, with longer arrows denoting a stronger reaction. The left column shows the single response over time, read from top to bottom. After reorientation, statolith sedimentation initiates the gravitropic signal. An early transient downward deflection reflects a transient overstimulation of auxin transport on the lower flank (Hild and Hertel, 1972; Hertel, 1983). After a reaction time downstream of perception (Chauvet* et al.*, 2019), auxin redistribution and differential growth drive the delayed main upward response. Below the tilt-reversal line, the curvature persists transiently in the established direction and does not fully return to the initial position, consistent with a stable directional memory established during the first stimulation phase (Nick and Schäfer, 1988). The right column shows the modulation under repeated reorientation. Repeated stimulation progressively sensitizes the perception–transduction system and produces an earlier onset in both conditions, with a microtubule-based susceptor (Nick* et al.*, 1991; Wang* et al.*, 2020) and a LAZY–MPK3 signaling module (Roychoudhry and Kepinski, 2024) as possible mediators. The curvature amplitude diverges between conditions. In darkness it decreases, attributed to adaptive desensitization at the auxin carrier (Hild and Hertel, 1972; Hertel, 1983). In light it increases, as the sensitized gravitropic drive overcomes the constant phototropic suppression (Nick* et al.*, 1990b) while phytochrome maintains the readiness of the auxin transport machinery (Gaiser and Lomax, 1993). The arrow labelled g indicates the direction of gravity.*

4.3 Hormonal Signaling Pathways During the Gravitropic Response

Three marker genes were analyzed after gravitropic stimulation to distinguish between jasmonate signaling, auxin-related regulation and cell-wall remodeling: JAZ1 was used as a marker for jasmonic acid signaling, ARF1 for auxin signaling and Expansin for growth-associated cell-wall loosening (Section 3.1.3). Together, these markers addressed whether gravitropic stimulation induces jasmonate signaling, whether this response is associated with an upstream auxin signal, and whether cell-wall remodeling occurs in the same tissues and time window.

All three markers responded to gravitropic stimulation, but their expression patterns were tissue- and phase-specific. Four observations frame the interpretation. First, JAZ1 was clearly upregulated in internodes 1–2 and internode 3, indicating that gravitropic stimulation induced

jasmonate signaling in the responding stem tissue. Second, ARF1 expression was consistently high in the same internodes in both control and stimulated plants. Third, ARF1 and JAZ1 were upregulated in apical leaves with a temporal delay and strict treatment specificity. Finally, Expansin followed a tissue-specific pattern that temporally coincided with the JAZ1 response. These patterns suggest that the hormonal response to gravitropic stimulation cannot be interpreted as a simple linear auxin-to-jasmonate cascade. Instead, light conditions, the distribution of statocyte-containing tissues and potential long-distance signaling routes need to be considered.

4.3.1 Light-Induced Auxin Availability as a Background Effect in the Shoot

The consistently high ARF1 expression in the internodes of both experimental groups can most parsimoniously be explained as a consequence of the light conditions. Plants were tilted approximately one hour after the end of an eight-hour dark phase. Sampling therefore began during a period in which the phytochrome-dependent auxin machinery was already activated. Several studies have demonstrated that light increases auxin availability in the shoot through enhanced biosynthesis, polar auxin transport or mobilization from the cotyledons (Lam and Leopold, 1966; Tillberg, 1974; Ćulafić and Nešković, 1974; Liu *et al.*, 2011).

These findings are not entirely convergent. The quantitative light response depends on species, organ, developmental stage and experimental conditions, and partly opposite effects have been reported (Tillberg, 1974; Mano *et al.*, 2006; Kim *et al.*, 2026). A general statement on the magnitude of the light-induced auxin increase in *Mentha* × *piperita* can therefore not be directly derived. It is plausible that at sampling time t = 0, a systemic, non-gravitropism-specific auxin mobilization was already in progress. This mobilization would have led to a measurable ARF1 activation in both control and treatment plants and thereby masked the treatment-specific effect in the shoot.

According to the Cholodny–Went theory, auxin is laterally redistributed after gravistimulation, resulting in higher concentrations on the physically lower side and lower concentrations on the upper side of a horizontally placed shoot (Digby and Firn, 1976). In this work, RNA was extracted from whole internode rather than from the upper and lower sides separately. The lateral auxin gradient is therefore largely averaged out in the gene expression measurement. The treatment-specific response in internodes 1–2 and internode 3 only becomes visible when the asymmetry is large enough not to be compensated by this averaging. A separate analysis of the upper and lower stem sides would be the next logical step to resolve this experimentally.

4.3.2 Treatment-Specific Response in the Apical Leaves

In contrast to the internodes, the apical leaves show a clear, treatment-specific upregulation of ARF1 and JAZ1, peaking during the reverse phase (60 minutes after reversal of the tilt). This temporal lag compared to the shoot response, together with the strict treatment specificity of JAZ1 induction, points to a gravitropism-specific mechanism. This mechanism becomes effective in the leaves more slowly than in the shoot.

An independent perception within the leaves is anatomically not excluded. Both *Calla palustris* and *Arabidopsis* possess functional statocytes with sedimenting amyloplasts in their petioles, and gravitropism-defective mutants (pgm, sgr2-1) display a reduced leaf gravitropism (Psaras, 2004; Mano *et al.*, 2006). The fundamental mechanisms of gravity perception are therefore shared between leaves, shoots and roots.

Alternatively, the leaf response could be interpreted as a consequence of an auxin signal transported from the shoot. Long-distance directional auxin transport between plant parts has been shown to function as a signaling pathway (Küpers *et al.*, 2023). Such a transport in the direction of the young leaves would be possible. The underlying mechanism can, however, not be derived from the present data.

4.3.3 Does Auxin Mediate the Jasmonate Response?

Whether the treatment-specific upregulation of JAZ1 is mediated via auxin or arises independently cannot be decided directly from the present data. In the literature, the direction in which jasmonate modulates the auxin response is well established. MeJA stimulates auxin biosynthesis and signaling (Chen *et al.*, 2024). The opposite direction, a direct induction of JA biosynthesis by auxin, is much less well supported. In *Nicotiana attenuata*, IAA accumulation precedes JA accumulation after herbivore attack. However, auxin and JA act in parallel rather than in a simple hierarchical sequence, and JA signaling is not required for the IAA induction (Machado *et al.*, 2016). A direct activation of JA biosynthesis by auxin has not been demonstrated in this body of work.

The observed expression pattern additionally argues against a simple auxin-mediated JAZ1 response. JAZ1 is upregulated almost simultaneously in internodes 1–2 and internode 3, only attenuated in internode 3. If the JA response were triggered by a basipetally transported auxin signal, a clearly time-shifted rather than merely weaker response in internode 3 would be expected. Two alternatives appear more plausible. Either the gravitropic stimulus mediates auxin redistribution simultaneously in both internodes, with the response in internode 3 being

weaker due to its more advanced lignification and reduced cell plasticity. Or the JA response is triggered independently of auxin by other gravitropism-induced mechanisms, such as the mechanical displacement of statoliths and the downstream signaling pathways associated with it.

With respect to the leaves, the second interpretation supports the assumption that they perceive the gravitropic stimulus themselves, through a mechanism that only becomes measurable at the gene expression level with a temporal delay. The strict treatment specificity of the JAZ1 response argues against MeJA reaching the control plants as an inter-plant volatile signal. In that case, at least an attenuated response should also have been visible in the controls.

4.3.4 Expansin as a Marker of Cell Wall Loosening

Expansin shows overall markedly lower expression levels than JAZ1 and ARF1. Internodes 1–2 and internode 3 show a sustained gravitropism-induced upregulation across multiple time points. This upregulation largely coincides with the increased JAZ1 expression in the same tissues, suggesting that JA signaling may regulate cell-wall plasticity through Expansin-mediated wall loosening during the gravitropic response. The whole-internode analysis in this work cannot resolve whether this upregulation is symmetric or asymmetric across the stem. Within the Cholodny–Went framework, cell wall loosening would be expected primarily on the lower side of the tilted shoot (Digby and Firn, 1976). The observed treatment effect may therefore underestimate the true magnitude of the asymmetric response. A separate analysis of the upper and lower stem sides would be required to resolve this experimentally.

In the apical leaves, a locally significant Expansin increase appears in the treatment of apical leaf 2 at the same time point at which JAZ1 and ARF1 also reach their maxima (60 minutes after reversal). The temporal coincidence with the hormonal response suggests that Expansin is involved in a gravitropism-related growth adjustment in this tissue. It remains unclear why the same effect does not appear in apical leaf 1. A possible explanation is a developmental difference in cell wall plasticity or in the sensitivity to the hormonal signals between the two leaf pairs. A well-founded statement on this point cannot be made on the basis of the present data. Additional experiments with more finely resolved sampling according to leaf age and leaf position would be required to confirm this interpretation.

4.3.5 Integrative Interpretation

In summary, the findings can be most parsimoniously explained as follows. At the start of sampling, the plants are in a phase of light-induced auxin mobilization in the shoot. This

background activation leads to a measurable ARF1 upregulation in the internodes of both control and treatment plants. Onto this background, an additional gravity response is superimposed in the treatment, which in the internodes consists primarily of a lateral auxin redistribution. This asymmetry is largely masked by the whole-internode analysis. The treatment-specific upregulation of ARF1 and JAZ1 in the apical leaves can be interpreted either as a consequence of an auxin signal originating from the shoot or as an independent, temporally delayed leaf response. A direct causal mediation of the JA response by auxin is not supported by either the literature or the data. The simultaneous JAZ1 increase across several internodes rather argues for a direct, non-auxin-mediated mechanism. Expansin shows a sustained gravitropism-induced upregulation in internodes 1–2 and internode 3, with additional transient upregulation in apical leaf 2 coinciding temporally with JAZ1 and ARF1. Methyl jasmonate is excluded as an inter-plant signal carrier by the strict treatment specificity of the JAZ1 response. An inter-plant signal transfer is therefore not required to explain the patterns observed.

4.4 Effects of the Reference Protocol: Daily Tilting in Light

4.4.1 Growth: Shoot Morphology, Root Architecture and Biomass

Daily tilting in light affected shoot morphology, root architecture and biomass, and the three readouts share one interpretive frame. Repeated reorientation is not a purely gravitropic stimulus. It combines a change in perceived orientation with a mechanical component from the repeated movement and displacement of the plant. The thigmomorphogenetic literature, which describes dose-dependent growth responses to mechanical stimulation, therefore provides a useful comparative frame without implying that the two are identical. Within this frame, low doses are often tolerated or mildly promoting, while higher doses become inhibitory. The readouts below are read against this expectation.

Morphology

Under daily tilting in light, plant height showed a non-significant increase at mild and moderate stress, declining toward control levels at severe stress (Section 3.2.1). The non-significant height increase at mild and moderate stress is lost at severe stress. This is consistent with the classical thigmomorphogenetic response of reduced longitudinal growth under repeated mechanical stimulation (Coutand *et al.*, 2010; Braam and Chehab, 2017), with stress magnitude determining the extent to which longitudinal extension is suppressed.

Shoot number increased under daily tilting in light, with moderate and severe stress producing significantly higher counts than mild stress. No individual treatment differed significantly from the untilted control. Two non-exclusive explanations can be considered. Gravity-regulated release from apical dominance has been described, where bending of the upper shoot triggers outgrowth of buds adjacent to the curved region through a mechanism that is suppressed by clinorotation (Prasad and Cline, 1987; Kitazawa *et al.*, 2003; Shimizu-Sato *et al.*, 2009). In the present system, the progressive curvature of the apical internodes during the tilting phase produces an analogous geometry. Additionally, this curvature alters the illumination geometry. As the apical region bends away from the vertical while the light vector remains constant, lateral surfaces of the stem and lower leaf pairs receive increased light. A contribution from altered source–sink dynamics, whereby suppressed growth of the main shoot frees assimilates for axillary buds (Kebrom, 2017), may further support outgrowth.

Root architecture

Under daily tilting in light, root tip number decreased with increasing stress level, reaching significance at severe stress, while total root length was maintained at mild and moderate stress and declined only at severe. With average root diameter rising slightly across the range, this indicates a trade-off, in which fewer but longer and thicker roots replace the higher tip density of the control. The thickening is consistent with the canonical adaptation of roots to mechanical stimulation, where increased radial growth enhances stress resistance (Baiyin *et al.*, 2025). At severe stress this compensatory strategy reaches its limit, with both tip number and total length reduced, marking the upper end of a hormetic dose-response where adaptive capacity is exceeded (Calabrese, 2014).

An important methodological consideration qualifies the interpretation of these architectural changes. The aeroponic cultivation system used here suspends roots freely in air, eliminating the substrate-derived mechanical impedance that drives most documented thigmotropic and gravitropic root responses in soil-grown plants (Baiyin *et al.*, 2025). However, the setup is not entirely mechanically neutral. Nutrient solution is delivered through high-pressure spray nozzles operating at 3–4 bar, producing a continuous low-level mechanical stimulus on the root surface. Although this background stimulation is identical across all treatment groups and cannot account for treatment differences, comparative work from our laboratory has shown that aeroponic cultivation produces a substantially altered baseline root architecture compared to deep-water-culture hydroponics (Reisinger, 2024). This indicates that aeroponic cultivation

places roots in a mechanically and physiologically distinct state, which should be considered when comparing the present results to studies using other root environments.

More importantly, the geometry of the cultivation modules introduces a treatment-dependent confounding factor. With increasing root length over the two-week experimental period and increasing tilt angle, individual roots eventually come into contact with the module walls when the system is tilted. The probability of root-wall contact rises sharply with tilt magnitude. This contact provides both a local thigmotropic stimulus and a reorientation of individual root segments relative to the gravity vector, neither of which was controlled in the experimental design. The observed architectural changes therefore cannot be unambiguously attributed to a single stimulus pathway, and the contribution of direct local root stimulation to the response pattern likely scales with tilt angle.

Alongside this direct mechanical pathway, a systemic route via shoot-derived signaling remains a candidate mechanism, although the present data do not directly support it. As shown in Section 3.1.3 and discussed in Section 4.3, gravitropic stimulation induces JAZ1 expression in shoot internodes and apical leaves, indicating activation of the JA signaling pathway in aerial tissues. JA is also known to affect root gravitropism through modulation of PIN2 endocytosis and plasma membrane abundance in *Arabidopsis* roots (Sun *et al.*, 2011), providing a literature precedent for JA-mediated effects on root architecture. Whether the shoot-induced JA signal in the present system reaches the root and contributes to the observed architectural changes is not established by the available data. Root JA levels were not measured, and the question of long-distance JA transport from shoot to root has not been addressed experimentally in this work. The systemic JA hypothesis is therefore presented as one possibility consistent with the literature, while a parsimonious interpretation favors the local mechanical pathway as the primary driver.

Biomass

The only statistically significant biomass difference relative to the untilted control was the increase in leaf biomass at mild stress under daily light (Section 3.2.1). All other differences remained at the level of consistent but non-significant tendencies.

The observation that mild gravitropic stimulation tends to promote biomass accumulation is consistent with earlier reports that altered gravitational conditions can stimulate growth. Clinorotation increased hypocotyl and root dry weight by 40% in *Veronica arvensis* (Driss-Ecole *et al.*, 1994), and prolonged hyper gravity exposure increased total dry mass in

Arabidopsis thaliana (Ohara *et al.*, 2024). Both effects have been attributed at least in part to mechanical loading rather than gravity magnitude per se (Tuominen *et al.*, 2009). These studies manipulated the magnitude of the gravity vector, while the present study applied repeated changes in the direction of the gravity vector at constant magnitude. Herranz and Medina (2013) emphasize that gravitropism and gravity resistance are distinct mechanisms responding to different components of the gravity vector. The convergence of biomass-stimulating effects across these mechanistically distinct paradigms suggests that mechanical loading, broadly construed, can promote biomass accumulation independent of gravity-magnitude manipulation.

The present pattern is consistent with the hormetic dose-response (dose = gravitropic intensity) documented across plant systems, in which low-dose stimulation gives way to high-dose inhibition (Calabrese, 2014). The typical magnitude of hormetic stimulation (30 to 60 percent above control) matches the modest, often non-significant nature of the effects observed here. Under daily light the hormetic optimum lies at mild stress (27°).

Beyond the overall biomass response, several organ-level patterns become informative when read against the morphological data (Section 3.2.1). Under daily light at mild stress, leaf biomass was significantly elevated while leaf number remained essentially unchanged. The leaf surface area analysis was restricted to the apical leaf pairs, which (given a plastochron of approximately 2.3 days per leaf pair in *Mentha* × *piperita*, Turner *et al.*, 2000) predominantly represent leaves newly formed during the two-week experimental period. No significant area increase was observed at mild stress within this sampled set. Only at moderate stress did the older leaf pairs expand. The elevated total leaf mass at mild stress must therefore originate either from increased specific mass in the newly formed leaves, or from continued mass accumulation in the older leaves present before the experiment began. The latter were not included in the leaf area analysis. The available data cannot distinguish between these contributions. Both an increase in specific leaf weight under mechanical stimulation and a preferential effect on young tissue are documented thigmomorphogenetic responses (Biddington, 1986), providing a conceptual link to the morphological and trichome responses in younger leaf pairs discussed in subsequent sections.

4.4.2 Glandular Trichomes

Glandular trichomes are the primary site of essential oil biosynthesis and storage in *Mentha* × *piperita* (Section 1.4) and were therefore assessed as a potential indicator of gravitropic effects on secondary metabolite production capacity. Three parameters were quantified per leaf pair: trichome density (number per unit leaf area), leaf surface area, and total trichome count per leaf.

The interpretation of these data requires all three parameters to be read together. Trichome density is a quotient and can be altered either by a change in trichome number or by a change in leaf area. A constant total trichome count combined with a reduced leaf surface area, for example, yields an elevated density without any additional trichomes having been produced. As Turner et al., (2000) demonstrated, new peltate glands continue to be initiated as long as leaf expansion proceeds, following the basipetal maturation pattern of the leaf.

A further consideration applies to the interpretation of trichome density across leaf pairs of different developmental stage. Across all experiments and treatments in this work, younger and smaller leaf pairs consistently showed higher trichome density than older and larger leaf pairs. The total trichome count per leaf reached a plateau relatively early in leaf development rather than scaling continuously with leaf age. This pattern indicates that the bulk of glandular trichome initiation occurs early in leaf development, with subsequent leaf expansion diluting the existing trichome population over an enlarging surface. Trichome density is therefore not only a readout of trichome initiation activity but also of the developmental stage and the leaf-expansion trajectory of the sampled leaf. Treatments that modify leaf expansion can alter density independently of any true change in trichome initiation. The total trichome count per leaf is therefore the more biologically interpretable parameter, as it integrates over the developmental trajectory and is less confounded by leaf area variation. Maintaining the total trichome count on a reduced leaf surface therefore does not represent a passive arithmetic outcome. It requires sustained trichome initiation on a smaller substrate, which is itself a biologically active response.

Under daily tilting in light, two distinct response patterns emerged across the stress range (Section 3.2.2). At mild and moderate stress, mean trichome density across all leaf pairs was only slightly and non-significantly elevated. The most informative response was the significant expansion of leaf surface area at moderate stress in lp2 and lp3, accompanied by significant increases in total trichome count at moderate stress in the same leaf pairs. This pattern is consistent with a moderate-stress response in which leaf expansion is promoted and trichome initiation tracks the expanding leaf surface, producing more trichomes overall without raising the density. At severe stress, the pattern shifted. Mean density rose significantly, with the strongest increases in lp1 and lp2 where leaf area was now slightly reduced rather than expanded. Total trichome count reached statistical significance in lp2 and lp3. The combination of unchanged or reduced leaf area with elevated density and increased total count at severe stress indicates that trichome production was actively maintained or enhanced on a smaller leaf

substrate. This is a qualitatively different response from the leaf-expansion-driven pattern observed at moderate stress.

Taken together, the trichome data under daily tilting in light show two phenomenologically distinguishable responses. The first is a leaf-expansion-coupled response, in which moderate stress promotes leaf expansion and trichome initiation tracks the expanding leaf surface. This produces more trichomes overall without raising the density. The second is an actively enhanced trichome initiation response, in which the rate of trichome formation per unit leaf area is increased. This produces elevated density. Under daily light, the first response was observed at moderate stress and the second at severe stress. Both definitions rely primarily on the total trichome count rather than on density alone, as discussed above. Density is confounded by the developmental gradient and by treatment-induced changes in leaf expansion, while total count integrates trichome initiation over the developmental trajectory and is therefore the more reliable indicator. Whether these two responses reflect a single intensity-dependent mediator acting differently across stress levels or involve separate mechanistic pathways cannot be decided from the present data. This question is examined further in Section 4.6 through the pharmacological dissection of the JA signaling pathway, and the resulting integrated model is shown in Figure 48.

4.4.3 Essential Oil Yield and Composition

Oil yield

Essential oil yield was assessed as oil volume per gram dry leaf mass to determine whether the trichome responses described above are reflected in overall oil production capacity. An important methodological consideration applies. Trichome parameters were quantified only on the three to four apical leaf pairs, while oil was extracted from the leaves of the entire plant. The two datasets therefore sample different parts of the plant, and discrepancies between trichome and oil responses may in part reflect this sampling asymmetry rather than purely biological differences.

Under daily tilting in light, essential oil yield was significantly increased at all stress levels compared to the control (Section 3.2.3). Mild stress produced the highest yield and differed significantly from moderate stress. Severe stress was at an intermediate level and was not significantly different from either mild or moderate stress. The oil response therefore peaks at mild stress and declines at moderate stress. This pattern stands in contrast to the total trichome count, which increases monotonically with stress level and reaches statistical significance only

at moderate and severe stress. The two responses are inversely related across the intensity range. The highest oil yield occurs where trichome induction is weakest, and the lowest oil yield where trichome induction is strongest. This inversion indicates that trichome number alone does not determine oil yield in this system.

This dissociation between trichome number and oil yield is consistent with the well-established framework that peppermint oil production reflects the combined contribution of trichome number and per-trichome biosynthetic capacity (Gershenzon *et al.*, 2000; Rios-Estepa *et al.*, 2010). Trichome development proceeds in two temporally distinct phases. An initiation phase generates the secretory disc, and a subsequent secretory phase forms and fills the subcuticular storage cavity with essential oil (Turner *et al.*, 2000). The two phases are mechanistically separable, and the rate of monoterpene biosynthesis within mature trichome cells has been identified as the principal regulatory level controlling monoterpene accumulation. A possible explanation, which the present data cannot test directly, is that low stress stimulates per-trichome biosynthetic capacity more strongly than trichome initiation. Under this interpretation the trichomes at mild stress would be comparatively well filled, while at moderate and severe stress additional trichomes are formed but are, on average, less effectively filled, lowering oil yield per dry mass despite the higher count. Per-trichome oil content was not quantified, so this remains an inference rather than a measured result.

Relative composition

Beyond total oil yield, the composition of the essential oil determines its quality and commercial value. The three quality-determining components menthol, menthone, and menthofuran are biosynthetically derived from the same branch-point intermediate pulegone. Pulegone reductase (PR) directs flux toward menthone and menthol via the principal reductive branch, while menthofuran synthase (MFS) directs flux toward menthofuran as a competing branch (Mahmoud and Croteau, 2003). Their relative proportions therefore reflect the balance between these two branch-point enzymes, and shifts in the relative composition can be interpreted as differential modulation of PR and MFS activity. For clarity, only these three components are considered here. Their reported percentages reflect their relative distribution among each other rather than their absolute contribution to total oil composition.

Under daily tilting in light, mild stress produced only a small compositional shift. Menthofuran was slightly reduced or unchanged, menthol decreased slightly, and menthone correspondingly increased. Moderate and severe stress produced a markedly different and quantitatively similar

pattern. Menthofuran rose substantially, menthol fell, and menthone remained largely stable. This shift to menthofuran at higher stress is consistent with the broader literature, in which a range of abiotic stressors such as heat, drought, salinity, and suboptimal light promote pulegone and menthofuran accumulation at the expense of menthol (Rios-Estepa *et al.*, 2008; Fuchs *et al.*, 2022; Khameneh *et al.*, 2025). The response is mediated through transcriptional regulation of the branch-point enzymes PR and MFS (Mahmoud and Croteau, 2003).

A mechanistic interpretation of these patterns can be built on the established JA-dependent regulation of the branch-point enzymes. MeJA application in *Mentha* × *piperita* induces transcription of both PR and MFS, with PR responding earlier than MFS (Afkar *et al.*, 2013; Afkar and Karimzadeh, 2025). The relative activation of PR versus MFS shifts the metabolic flux between menthone/menthol and menthofuran accordingly (Soleymani *et al.*, 2017). Promoter motif analyses have shown that in *Mentha* × *piperita*, both the PR and the MFS promoter carry MeJA-responsive elements (Hering, 2023). This provides a cis-regulatory basis for the MeJA induction of both enzymes. The temporal precedence of PR over MFS therefore likely reflects promoter-specific binding kinetics or post-transcriptional regulation rather than the presence or absence of the cis-regulatory motif itself.

One possible interpretation links these patterns to the JA-dependent regulation of the branch-point enzymes, although the present data do not allow this to be tested directly. If gravitropic stimulation raised endogenous JA in a dose-dependent way, the mild-stress shift toward menthone without menthofuran accumulation would be compatible with a low JA dose acting mainly on the earlier-responding PR pathway, and the moderate-and-severe-stress rise in menthofuran with a higher JA dose additionally engaging MFS (Afkar *et al.*, 2013; Afkar and Karimzadeh, 2025). This remains a hypothesis. Endogenous JA was not quantified, and the pharmacological tests in Section 4.6 are required to assess whether JA is actually involved.

Taken together, two responses appear under daily tilting in light. At moderate and severe stress the composition shifts toward menthofuran. The most parsimonious explanation is a JA-mediated activation of MFS over PR. Mild stress produces a distinct, qualitatively different response that resembles low-dose JA induction without MFS activation. The pharmacological dissection of the JA pathway in Section 4.6 provides further evidence on whether this proposed mechanism is causally responsible.

Absolute amounts

To complement the relative composition and the oil volume measurements above (Section 3.2.3), the absolute quantities of the five major monoterpene components were determined by GC-MS as mg per gram dry leaf mass. Whereas hydro distillation captures the total volume of all volatile compounds, the GC-MS measurement is specific to the five quantified monoterpenes.

Under daily tilting in light, the absolute amount of the five major components was reduced relative to the control across all stress levels, with moderate stress reaching statistical significance, while oil volume under the same protocol was simultaneously elevated (Section 3.2.3). One plausible interpretation is a compositional shift toward minor monoterpenes, with gravitropic stimulation increasing overall volatile production while redirecting allocation toward components not captured by the targeted quantification. Such stress-induced shifts in monoterpene allocation are well documented (Rios-Estepa *et al.*, 2008; Fuchs *et al.*, 2022; Khameneh *et al.*, 2025) and reflect transcriptional regulation of multiple biosynthetic enzymes rather than only the branch-point pair PR and MFS (Mahmoud and Croteau, 2003; Afkar *et al.*, 2013).

Taken together, the absolute amounts are consistent with three at least partly independent regulatory layers. The first is total biosynthetic capacity, reflected in oil volume. The second is branch-point partitioning between menthone/menthol and menthofuran. The third is allocation between the five major components and the remaining monoterpene spectrum. Under daily tilting in light, moderate stress shows the strongest reallocation across all three layers. The pharmacological dissection of the JA pathway in Section 4.6 provides further evidence on which of these layers is JA-mediated.

4.5 Protocol Specificity: Light Dependence and Time Regime

Section 4.4 characterized the gravitropic intensity response under daily tilting in light. Two manipulations test how far that response depends on the conditions of stimulation rather than on reorientation as such. Removing the light period isolates the contribution of light, and removing the upright recovery phase isolates the contribution of the daily rhythm. The mechanisms introduced in Sections 4.2 and 4.4 are not repeated here. This section reports only the contrasts and what they add.

4.5.1 Light Dependence: Daily Tilting in Light versus Darkness

When tilting occurred during the dark phase, the growth responses of the daily tilting in light protocol largely disappeared or reversed. Plant height showed a non-significant decrease at all angles rather than the maintenance seen under light, consistent with the loss of the phototropic counterweight that attenuates the gravitropic response under light (Section 4.2; Yoshihara and Spalding, 2017). The shoot-number increase did not occur in darkness, the outcome predicted by the illumination-geometry mechanism proposed in Section 4.4.1, since tilting in the dark phase exposes no newly lateral surfaces to light. Essential oil yield was suppressed across all stress levels rather than increased, plausibly because no photosynthetic carbon is assimilated during dark-phase tilting, limiting the secretory phase even where trichome initiation proceeds. The productively useful responses of the reference protocol, height maintenance, shoot number and oil yield, therefore all required the light period.

The trichome response did not vanish in darkness but shifted along the leaf axis, with density rising mainly in the older leaf pair lp3 rather than in the younger pairs. Because density normally falls with leaf age (Section 4.4.2), a density increase in an older leaf pair runs against the developmental gradient and is a robust indicator of active initiation. It is conceivable that the absence of photosynthetic activity during the tilting phase limits the capacity of the youngest, still-expanding leaf pairs to mount the trichome response seen under light, with the older leaf pairs taking on this role instead. This remains speculative and would require dedicated experiments to test. The essential oil composition behaved differently from the yield. The shift toward menthofuran at moderate and severe stress appeared under both light and darkness, identifying it as a light-independent stress response rather than a feature of the tilting in light specifically.

Root architecture was not measured under darkness, so the architectural basis of the reduced root biomass observed in this protocol remains untested.

4.5.2 Time Regime: Daily versus Continuous Tilting

Continuous tilting removes the upright recovery phase and leaves the gravi-proprioceptive control system in a permanently perturbed state. The morphological consequence was the canonical thigmomorphogenetic phenotype, with plant height decreasing significantly and progressively with intensity while shoot width tended to increase (Coutand *et al.*, 2010; Braam and Chehab, 2017). Shoot width was recorded only under this protocol, so a direct comparison with daily tilting is not possible.

Consistent with this radial phenotype, the significant height reduction under continuous tilting did not translate into reduced total biomass, which even tended to increase slightly at moderate stress. Since shoot biomass integrates main and lateral shoots while shoot width was measured only on the main shoot, the relative contributions of main-shoot thickening and lateral shoot production cannot be separated, but both are plausible within the thigmomorphogenetic framework (Biddington, 1986; Coutand *et al.*, 2010).

Relative to daily light, the intensity at which the responses appeared also shifted. Under continuous tilting the beneficial optimum for biomass and root architecture lay at moderate rather than mild stress, while the trichome density increase already appeared at mild and moderate stress in the younger leaf pairs and declined again at severe stress. The response types are the same as under the reference protocol (Section 4.4). What differs between protocols is the intensity level (tilt angle) at which each phase is reached.

4.5.3 Consequences for Secondary Metabolism and Oil Quality

Two consequences for the oil follow from the protocol comparison. The yield increase was specific to daily tilting in light, since darkness suppressed yield and continuous tilting raised it only slightly. The compositional shift toward menthofuran was light-independent and appeared wherever the gravitropic intensity was moderate or severe. For oil quality this separates a desirable effect, the light-specific yield gain at mild stress, from an undesirable one, the intensity-driven menthofuran increase that raises a hepatotoxic minor component (Section 1.4).

The continuous series additionally carried an anomalous baseline. All samples, including the untilted control, showed a markedly higher menthofuran and lower menthol than the controls of the other two protocols, with stable menthone. In the absolute amounts the same series showed substantially elevated quantities of the five major components and a near-complete absence of menthol. The composition of the continuous control thus already resembled the moderate-and-severe-stress response of the daily protocols, with only a small additional menthofuran increase induced by severe stimulation.

Two non-exclusive explanations can be considered. The first relates to the cutting time of the propagation material. The three experimental series were otherwise identical in mother plant clone, aeroponic protocol, nutrient solution, environmental conditions and extraction, and the cutting time was the only systematic difference between them. Seasonal variation in mother plant physiology, or developmental differences in the cuttings at the time of propagation, could plausibly produce a baseline compositional shift that persists into the experimental phase, since

harvest time and developmental stage are established modulators of monoterpene composition in *Mentha* × *piperita*. The second concerns the accumulation of volatile methyl jasmonate in the cultivation environment. All plants of a series shared the same small room, air-conditioned by a unit that recirculated rather than exchanged the air. Under daily tilting the stimulation lasted only 4–8 h per day, whereas under continuous tilting all tilted plants produced gravitropically induced JA over the entire two-week period, so the untilted controls of this series could have been exposed to a low-level MeJA atmosphere sufficient to shift their composition toward the stress-typical pattern. The relatively flat intensity dependence across the continuous series would be consistent with such a homogeneous background exposure.

Of the two, the cutting-time explanation is the more parsimonious, since it rests on the one known systematic difference between series, whereas the volatile-MeJA explanation requires an unmeasured atmospheric exposure. Neither can be excluded without direct measurement of room-atmosphere MeJA or spatial separation of controls from tilted plants. The question also operates on a longer timescale than the acute volatile transfer ruled out for the gene expression experiments (Section 4.3), where treatment-specific JAZ1 induction in tilted but not control plants argued against volatile transfer over an eight-hour cycle.

The leaf-pair-resolved SPME analysis, performed for continuous tilting only and qualitatively, adds supporting detail rather than a primary finding. Composition shifted from menthone-dominated younger leaves toward menthol-enriched older leaves, consistent with the later developmental activity peak of menthone reductase (McConkey *et al.*, 2000; Croteau *et al.*, 2005). Superimposed on this gradient, pinene and eucalyptol responded divergently to intensity, both deriving from the GPP branch upstream of the principal menthol pathway, suggesting that gravitropic stress modulates flux differentially across pathway branches rather than uniformly (Fuchs *et al.*, 2022; Khameneh *et al.*, 2025). Menthol was notably elevated in lp4 at severe stress, an observation taken up in Section 4.6. Menthofuran was largely undetectable by SPME despite its clear hydro-distillation signal (Section 3.3.3), most plausibly because SPME sampled only lp1–lp4 while hydro distillation also captured older tissue and internodes where menthofuran may accumulate. This is best treated as a limitation of the qualitative analysis rather than a substantive result.

4.5.4 Synthesis

Across the three axes, the reference protocol and its variants separate cleanly. The productively useful responses of daily tilting in light, maintained height, increased shoot number and elevated oil yield, all depended on the light period and disappeared or reversed in darkness. The

compositional shift toward menthofuran at moderate and severe stress, by contrast, was light-independent and is best read as a generic stress response rather than a feature of the daily tilting in light protocol. Removing the upright recovery phase under continuous tilting did not change the type of response but shifted the intensity at which each phase appeared, alongside the canonical reduced-height, increased-width phenotype. The continuous series additionally carried an anomalous compositional baseline whose origin, cutting time or volatile MeJA, remains unresolved. Two implications carry into the following section. First, the yield benefit and the menthofuran penalty are separable, since one is light-dependent and the other intensity-dependent. Second, the recurrence of the menthofuran shift across protocols points to a shared downstream mediator, which the pharmacological experiments in Section 4.6 address directly.

4.6 The Role of Jasmonic Acid as a Mediator of Gravitropic Effects

4.6.1 Sufficiency of JA Pathway Activation: MeJA Treatment

To assess whether exogenous activation of the JA signaling pathway is sufficient to replicate the gravitropism-induced responses on trichomes and essential oil described in section 3.2, plants were treated with methyl jasmonate (100 µM) in a separate experimental setup. Because MeJA is volatile, the aeroponic tilting modules could not be used. Plants were instead cultivated in closed glass containers and sprayed at three-day intervals (Burkard, 2023; section 2.6.1).

Glandular Trichomes

MeJA treatment significantly increased total glandular trichome count per leaf. The strongest effect was in the youngest leaf pairs lp1 and lp2, where the increase reached statistical significance. Mean trichome density across all leaf pairs was unchanged. Leaf surface area was significantly enlarged in lp2 and lp3. This combination of increased total count, stable density, and increased leaf area is the signature of a leaf-expansion-coupled trichome response, in which new trichomes are initiated as the leaf surface expands but trichome formation does not exceed the rate of leaf expansion. The same response pattern was observed under daily tilting in light at moderate stress (section 3.2.2). Moderate gravitropic stimulation produced significant leaf expansion in lp2 and lp3, together with significant increases in total trichome count and unchanged mean density. The fact that exogenous MeJA application alone produces this signature provides evidence that the moderate-stress component of the gravitropic trichome response is JA-mediated.

This interpretation is consistent with the established role of JA in regulating peltate glandular trichome density and essential oil production in *Mentha* × *piperita*, demonstrated by Cappellari *et al*., (2019) at higher MeJA concentrations (1–4 mM). It is also consistent with the canonical COI1–JAZ signaling pathway involving MYB- and bHLH-type transcription factors, which has been associated with trichome development in several plant systems (Pauwels and Goossens, 2011; Taheri, 2019; Chalvin *et al.*, 2020).

What MeJA treatment does not replicate is the actively enhanced trichome initiation response observed under daily tilting in light at severe stress and under continuous tilting at mild to moderate stress (section 3.2.2). In this response, trichome density is significantly elevated and total trichome count is maintained or increased despite a reduced leaf surface area. MeJA treatment at 100 µM produces only the leaf-expansion-coupled response. This dose-specific replication is interpreted further in section 4.6.3.

Essential Oil

The compositional response of the essential oil to MeJA treatment was assessed for the same three principal components menthol, menthone, and menthofuran that were analyzed under gravitropic stimulation in section 3.2.3. The oil extraction method differed between experiments. Gravitropically stimulated plants were analyzed by hydro distillation. MeJA-treated plants and their solvent controls were extracted in hexane following the protocol described in section 2.12. Direct comparison of absolute amounts between the two experiments is therefore not appropriate, but relative compositional shifts can be compared meaningfully.

Under MeJA treatment, menthone proportions increased. Menthol and menthofuran proportions both decreased relative to the solvent control. This composition closely resembled that observed under mild gravitropic stress during daily tilting in light (section 3.2.3). The mild-stress condition showed a similar slight shift from menthol toward menthone without substantial menthofuran accumulation. The MeJA-induced composition therefore reproduces the mild-stress phenotype of the gravitropic compositional response, but not the moderate and severe-stress phenotype characterized by elevated menthofuran and reduced menthol.

The mechanistic basis for this partial replication is consistent with the cis-regulatory and transcriptional framework outlined in section 4.4.3. The earlier and faster PR response relative to MFS following MeJA application (Afkar *et al.*, 2013; Afkar and Karimzadeh, 2025) can explain why the 100 µM exposure used here preferentially activates the PR-mediated branch toward menthone. Whether potentially higher endogenous JA doses under moderate and severe

gravitropic stress additionally engage MFS is taken up in Section 4.6.2, since this was not directly measured here.

The MeJA experiment shows that JA pathway activation is sufficient to produce parts of the gravitropic phenotype, but not whether endogenous JA is necessary. The pharmacological inhibition of JA biosynthesis with phenidone, examined next, addresses this complementary question.

4.6.2 Necessity of Endogenous JA Biosynthesis: Phenidone Treatment

To test whether endogenous JA biosynthesis is required for the gravitropism-induced trichome and oil responses described in section 3.2, plants were treated with phenidone (2 mM), a lipoxygenase inhibitor that blocks the first committed step of JA biosynthesis. Phenidone treatment was combined with gravitropic stimulation at 45° (moderate stress, daily tilting, light conditions). All four groups in this experiment received spray treatments (ctrl, ctrl + Ph, 45°, 45° + Ph). Any spray-induced mechanical stress was therefore homogeneously distributed across groups. Comparisons in the following sections are made within this experiment only and not with the unsprayed tilting experiments described in section 3.2.

Glandular Trichomes

Glandular trichome density was significantly elevated in the 45° group compared to the solvent control, replicating the gravitropic trichome response described in section 3.2.2 under similar conditions. The 45° + Ph group showed a slight non-significant reduction relative to 45° alone in the mean density and across the individual leaf pairs. The two groups were statistically indistinguishable. Phenidone therefore did not suppress the gravitropism-induced increase in trichome density. Total trichome count per leaf showed an even clearer pattern. The 45° + Ph group reached values comparable to or exceeding 45° alone across all leaf pairs. Multiple per-leaf-pair comparisons in lp2, lp3 and lp4 showed 45° + Ph significantly elevated above the solvent control. The gravitropism-induced increase in total trichome count is therefore not attenuated by phenidone treatment. Endogenous JA biosynthesis is not required for this response.

This result is informative when combined with the MeJA experiment from section 4.6.1. The MeJA experiment shows that exogenous JA pathway activation is sufficient to produce the leaf-expansion-coupled trichome response. The present finding shows that JA is not necessary for the gravitropic trichome response. The most parsimonious interpretation is that JA represents one of several parallel pathways capable of inducing trichome formation in response to

gravitropic stimulation, and that blocking JA biosynthesis allows alternative pathways to compensate. The molecular identity of these alternative pathways cannot be derived from the present data.

A second observation that warrants attention is the phenidone-only effect. The ctrl + Ph group showed a significant increase in trichome density compared to the unsprayed-equivalent solvent control. At first sight, this is unexpected. If JA were a positive regulator of trichome formation, phenidone-mediated inhibition of JA biosynthesis should reduce rather than increase trichome density.

Interpreted in light of the developmental gradient discussed in section 4.4.2, however, a more parsimonious explanation becomes available. Total trichome count per leaf in the ctrl + Ph group was only slightly and non-significantly elevated, while leaf surface area in lp1 was significantly reduced. The combination of a near-control total count with a reduced leaf surface area mathematically produces an elevated density, even in the absence of any substantial change in trichome initiation. The density increase in the phenidone-only group is therefore most parsimoniously interpreted as a consequence of phenidone-induced reduction of leaf expansion. This is itself consistent with the dose-dependent JA model proposed in section 4.6.3, in which low-dose JA promotes leaf expansion as part of the leaf-expansion-coupled response. Pharmacological inhibition of JA biosynthesis would therefore be expected to reduce leaf expansion under non-stressed conditions, with the density elevation as a passive arithmetic consequence rather than an active trichome induction.

Two secondary explanations cannot be excluded but are less parsimonious. First, phenidone may affect lipoxygenase-dependent oxylipin pathways beyond JA biosynthesis, with downstream effects that promote trichome formation independently of JA signaling. Second, the dose-dependent JA model leaves open the possibility that at very low JA levels, such as those resulting from baseline JA biosynthesis inhibition under non-stressed conditions, trichome formation is de-repressed rather than reduced. Both interpretations remain speculative and would require dedicated experimental testing.

Leaf surface area showed a complex pattern across the experiment. Phenidone treatment reduced leaf surface area in lp1, with both ctrl + Ph and 45° + Ph significantly smaller than ctrl. This reduction is consistent with the dose-dependent JA model and was discussed in the preceding paragraph in the context of the phenidone-only density effect. In lp3, the 45° + Ph group showed a significant increase compared to the solvent control. This response is harder to

reconcile with the JA framework and may reflect off-target effects of phenidone on lipoxygenase-dependent oxylipin pathways beyond JA biosynthesis. Within the broader phenidone literature, leaf size effects are commonly observed and reflect multiple downstream consequences of altered oxylipin signaling.

Essential Oil

The compositional response was assessed by leaf-pair-resolved SPME analysis of the three principal components menthol, menthone, and menthofuran. Due to limited plant material in this experiment, no hydro distillation was performed. Overall compositional values were calculated from the combined SPME data across all leaf pairs, as in the MeJA experiment (section 4.6.1). The most striking compositional effect of phenidone treatment was a consistent reduction in menthofuran proportion, observed both in the comparison of ctrl + Ph vs. ctrl and in the comparison of 45° + Ph vs. 45°. Phenidone therefore reduces menthofuran proportions both in the absence and presence of gravitropic stimulation, suggesting that the MFS-mediated branch toward menthofuran requires intact JA biosynthesis. Menthone proportions increased correspondingly under phenidone treatment. Menthol proportions decreased slightly, while a more nuanced leaf-pair-resolved pattern for menthol is examined in a dedicated paragraph below. The combination of reduced menthofuran and elevated menthone is the diagnostic signature of preferential PR activation without strong MFS engagement. This is the same compositional signature observed under MeJA treatment in section 3.4.1 and under mild gravitropic stress in section 3.2.3.

Taken together with the MeJA results, the compositional data are consistent with JA signaling acting on the MFS-mediated branch-point shift toward menthofuran, both as a sufficient input at the PR end and as a required input for the menthofuran component. Exogenous MeJA at 100 µM produces preferential PR activation without strong MFS induction (section 4.6.1). Pharmacological inhibition of JA biosynthesis selectively reduces the menthofuran proportion regardless of whether gravitropic stimulation is applied. This dual evidence is consistent with the dose-dependent JA hypothesis developed in Section 4.6.3, in which low JA doses would favor PR-mediated flux toward menthone and higher doses would additionally engage MFS to produce the menthofuran-elevated profile. Phenidone-mediated suppression of JA biosynthesis prevents the high-JA regime from being reached and therefore selectively suppresses the menthofuran-elevated component of the gravitropic compositional response.

Leaf-Pair resolved Essential oil

The leaf-pair-resolved SPME analysis confirmed this overall pattern at the level of individual leaf pairs. Menthone dominated across all leaf pairs and treatments. Menthol accumulated progressively toward lp4, as expected from the developmental program described in section 4.5.3. Menthofuran was reliably detectable in lp2 and lp3 across all four groups in this experiment. This contrasts with the largely undetectable menthofuran signal in the continuous tilting SPME analysis (section 3.3.3). Menthofuran showed visibly reduced intensity in the phenidone-treated groups compared to their solvent counterparts. The reduction was visible both in the comparison of ctrl + Ph vs. ctrl and in the comparison of 45° + Ph vs. 45°. This is consistent with the overall compositional pattern documented above and reinforces the conclusion that JA-dependent MFS activation is required for menthofuran accumulation across the leaf developmental axis.

The three minor monoterpenes pinene, eucalyptol/cineol and limonene each showed gravitropism-induced compositional changes that were consistently reversed by the addition of phenidone, returning the composition toward both control levels. This indicates that the gravitropism-induced shifts in these three components are JA-mediated. The mechanism is likely an indirect one, since pinene, eucalyptol and limonene are produced from the geranyl pyrophosphate (GPP) branch upstream of the principal menthol pathway and are not direct substrates of PR or MFS. Possible explanations include JA-mediated regulation of upstream GPP-branching enzymes or JA-mediated changes in the overall flux distribution between the central pathway and competing upstream branches. The qualitative nature of the present SPME data does not allow further mechanistic resolution. The JA-mediation of these minor-monoterpene shifts therefore extends the role of JA in the gravitropic compositional response beyond the well-characterized PR/MFS branch-point and indicates broader JA-regulation of the monoterpene network as a whole.

A more nuanced pattern emerged from the leaf-pair-resolved menthol distribution. The combined 45° + Ph treatment showed an opposing response in young versus older leaf pairs. In lp1 and lp2, menthol levels were reduced, as would be expected if the gravitropism-induced menthol increase in young leaves were JA-mediated and blocked by phenidone. In lp3 and lp4, by contrast, menthol was elevated above all other groups in this experiment.

This divergence indicates that JA is not the only mediator of menthol biosynthesis in older leaves under gravitropic stimulation. A plausible interpretation is that gravitropic stimulation

activates a JA-independent pathway in lp3 and lp4 that promotes pulegone reduction toward menthol. Under unrestricted JA signaling at 45°, this pathway is masked because the JA-driven MFS branch competes for the pulegone substrate and diverts flux toward menthofuran. When JA biosynthesis is blocked by phenidone in tilted plants, the MFS branch is suppressed and the pulegone substrate becomes more available for the JA-independent PR-driven pathway in the older leaves. This results in the menthol elevation in lp3 and lp4 observed under 45° + Ph.

A consistent observation supports this interpretation in the gravitropic stimulation data alone. Under severe gravitropic stress in the continuous tilting protocol, menthol was notably elevated in lp2 through lp4 (section 3.3.3). This elevation occurred without phenidone treatment and presumably reflects a similar JA-independent pathway becoming engaged at high gravitropic doses. The convergence of these observations suggests that the JA-mediated PR/MFS branch-point regulation, while necessary for the menthofuran-elevated stress phenotype, is not the only regulator of the menthol pathway. A second, JA-independent gravitropic input on monoterpene biosynthesis appears to operate preferentially in older leaves and at higher stress doses. The molecular identity of this second pathway cannot be derived from the present data and remains an open question for future investigation.

4.6.3 Synthesis: Necessary versus Sufficient JA-mediation

The MeJA and phenidone experiments together provide a stratified picture of JA involvement in the gravitropism-induced responses. For each response category, the experiments address two complementary questions. First, whether exogenous JA pathway activation is sufficient to reproduce the response. Second, whether endogenous JA biosynthesis is required for it.

The compositional branch-point shift between menthone, menthol, and menthofuran is the clearest case for JA mediation. MeJA at 100 µM produces preferential pulegone reductase (PR) activation toward menthone without strong menthofuran synthase (MFS) engagement, consistent with JA pathway activation being sufficient at low dose. Phenidone reduces menthofuran proportions in both untilted and tilted plants, consistent with JA biosynthesis being required for the MFS branch. The compositional response therefore appears JA-associated in both directions. These patterns can be drawn together into a dose-dependent JA hypothesis: low JA doses would produce the mild-stress compositional signature, while higher doses would additionally engage MFS to produce the menthofuran-elevated profile of moderate and severe stress, with phenidone preventing the high-JA regime from being reached. This is proposed as a hypothesis consistent with the directional data across Sections 3.2.3 and 4.6.

Beyond the central PR/MFS branch-point, the phenidone-mediated reversal of gravitropism-induced shifts in pinene, eucalyptol/cineol and limonene (section 4.6.2) indicates that JA-regulation extends to the upstream GPP-branching enzymes as well. The role of JA in the gravitropic compositional response is therefore broader than the canonical menthone/menthol/menthofuran branch-point alone and influences the monoterpene network at multiple regulatory levels.

A more nuanced picture emerges from the leaf-pair-resolved menthol distribution. In the older leaf pairs lp3 and lp4, combined gravitropic stimulation and JA biosynthesis inhibition produced menthol levels above all other treatment groups, indicating a JA-independent gravitropic input on menthol biosynthesis that is normally masked by the JA-driven MFS branch and becomes visible only when the MFS branch is pharmacologically suppressed (section 4.6.2). The JA-mediated PR/MFS regulation seems therefore necessary for the menthofuran-elevated stress phenotype, but not the only regulator of the menthol pathway. A second, JA-independent gravitropic signal appears to operate preferentially in older leaves and at higher stress doses. The molecular identity of this second pathway is an open question for future investigation.

The trichome response presents a more nuanced picture. MeJA reproduces the leaf-expansion-coupled trichome signature observed under daily tilting in light at moderate stress, establishing JA pathway activation as sufficient. Phenidone does not suppress the gravitropism-induced increase in total trichome count, indicating that JA biosynthesis is not strictly required for the trichome response. The most parsimonious interpretation is that JA is one of several pathways capable of mediating gravitropic trichome induction. Alternative pathways appear to compensate when JA biosynthesis is blocked. This redundancy is consistent with the broader literature on trichome regulation, in which multiple hormonal and developmental inputs converge on the same MYB- and bHLH-type transcription factor networks (Pauwels and Goossens, 2011; Taheri, 2019; Chalvin *et al.*, 2020). The interpretation rests primarily on total trichome count rather than on density, for the reasons discussed in section 4.4.2. The phenidone-only density increase in the ctrl + Ph group does not contradict this picture, since it is most parsimoniously explained as a passive consequence of phenidone-induced reduction of leaf expansion rather than as a direct effect on trichome formation (section 4.6.2).

The actively enhanced trichome initiation response, defined by an increase in trichome density rather than by total count, was not reproduced by 100 µM MeJA treatment. This response appears under daily tilting at severe stress, where density rises across the leaf pairs, and under

continuous tilting, where the density increase is strongest at mild and moderate stress (Sections 3.2.2 and 3.3.2). MeJA at 100 µM raised total trichome count through the leaf-expansion-coupled response but did not produce this density increase. Whether the density response requires higher MeJA concentrations or non-JA mechanisms cannot be decided from the present data.

Taken together, the JA pathway emerges as a likely multi-level regulator of the gravitropism-induced compositional shifts in essential oil. The data are consistent with JA acting as both a sufficient and a required input for the MFS-mediated menthofuran branch. JA also regulates the upstream GPP-branching enzymes that govern pinene, eucalyptol and limonene allocation. A JA-independent gravitropic input on menthol biosynthesis is additionally apparent in older leaf pairs and at higher stress doses. For the trichome response, JA is sufficient but not strictly required, with alternative pathways compensating when JA biosynthesis is blocked. The remaining components of the gravitropic phenotype, particularly the actively enhanced trichome initiation response and the per-trichome biosynthetic capacity modulation that underlies the oil yield response in section 4.4.3, are not directly addressed by these experiments. The molecular identity of the JA-independent gravitropic input on menthol biosynthesis and the question of whether the actively enhanced trichome initiation response can be reproduced at higher MeJA concentrations remain open questions for future investigation.

Figure 48 integrates these observations into a working model in which jasmonate is the principal but not the sole mediator of the gravitropic response, with biomass arising mechanically in parallel and oil yield increasing through a trichome-independent contribution.

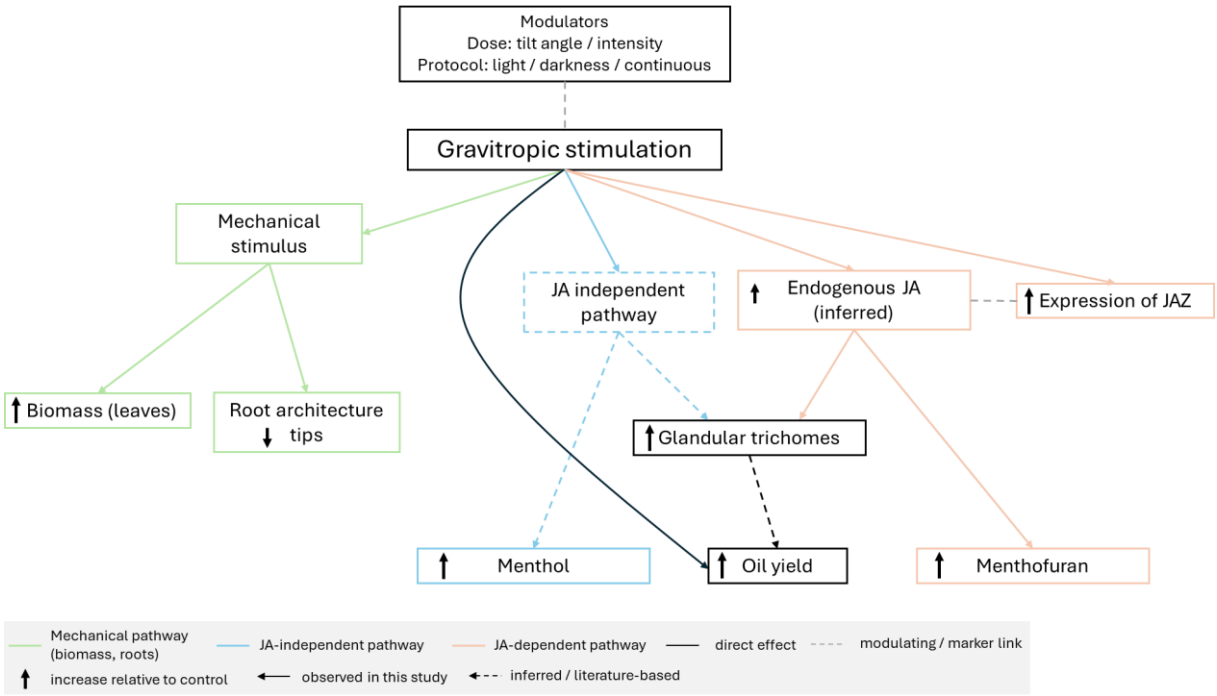

Figure 48 Integrated working model of gravitropic effects on growth, glandular trichomes and essential oil in *Mentha* × *piperita*, evaluated against the experimental data. *Gravitropic stimulation acts through three parallel routes. A mechanical route (green) raises leaf biomass and remodels root architecture. A jasmonate-dependent route (orange) is inferred from the induction of JAZ as a marker of jasmonate signaling and links to glandular trichome formation and to the menthofuran shift. A jasmonate-independent route (blue), inferred from the phenidone experiments, contributes to trichome formation and to the menthol increase in older leaf pairs. The increase in oil yield is shown as a direct, observed effect of stimulation (black) that is not explained by trichome number, indicating a contribution decoupled from trichome density. Tilt dose and protocol act as experimental modulators of the stimulus. Solid arrows denote relationships observed in this work, dashed arrows relationships that are inferred or literature-based, and the grey dashed link marks a non-causal modulating or marker relationship. This model represents the pathway architecture as supported and qualified by the present data.*

5 Conclusion and Outlook

5.1 Conclusion

The present work investigated the potential of gravitropic stimulation as a non-invasive elicitation strategy for medicinal plant production under controlled environment agriculture. Three research questions were addressed.

5.1.1 Gravitropic perception and response in *Mentha* × *piperita*

The gravitropic response of *Mentha* × *piperita* is concentrated in the two youngest internodes. Statoliths are present along the full length of the shoot, including in internodes that show no curvature response. Gravity perception is therefore retained in older tissues but not translated into bending. Polarization microscopy of cellulose microfibril orientation and the developmental state of the cell wall provide a mechanistic basis for this localization. Gravitropic competence is constrained downstream of perception by the developmental capacity of the responding cells for asymmetric elongation.

The kinetic analysis revealed a biphasic reorientation response. An initial fast phase reorients the shoot apex within hours of gravitropic stimulation. A subsequent slower phase establishes a stable curvature. Repeated gravitropic stimulation produced a clear adaptation response. The magnitude of the curvature response progressively decreased with successive stimulation cycles, indicating a habituation mechanism that limits the cumulative bending output of the shoot. A microtubule-based susceptor mechanism, in which microtubule organization modulates the sensitivity of gravity perception, is proposed as a plausible working hypothesis but remains to be tested directly.

Signal transduction analysis showed treatment-specific induction of JAZ1 and Expansin in apical leaves and internodes. The co-incident expression patterns support a hormonal-mechanical coupling that integrates gravity perception with downstream growth and stress signaling.

5.1.2 Biomass and secondary metabolite production under gravitropic stimulation

Targeted gravitropic stimulation modulated both biomass accumulation and the secondary metabolite profile of *Mentha* × *piperita*. The effects depended systematically on the interaction of dose (tilt angle) and protocol (light condition and continuity). Daily tilting in light served as the reference protocol for the production-oriented assessment, while daily tilting in darkness and continuous tilting were used as specificity and control treatments across plant morphology, root architecture, biomass, glandular trichomes, essential oil yield, and oil composition.

Under the reference protocol, the productively relevant responses followed a dose axis with an optimum at the low end. Mild stress produced the only statistically significant biomass effect, an increase in leaf biomass relative to upright controls, consistent with a hormetic response in which gravitropic stimulation at the appropriate dose may act as a positive elicitor of productivity rather than as a purely stress-inducing intervention. The effect was modest and largely non-significant beyond leaf biomass. Plant height was maintained at mild to moderate stress and shoot number tended to increase, while root architecture showed dose-dependent remodeling whose causal basis could not be separated from the cultivation geometry. These growth responses required the light period and were lost or reversed under dark-phase tilting.

The trichome response under the reference protocol comprised two phenomenologically distinguishable patterns. The first is a leaf-expansion-coupled response, in which moderate stress promotes leaf expansion and trichome initiation tracks the expanding surface, yielding

more trichomes overall without a net density change. The second is an actively enhanced initiation response, defined by an increase in trichome density on a maintained or reduced leaf surface, which appeared at severe stress. Whether these reflect one dose-dependent mediator or separate pathways could not be decided from the present data.

The essential oil response separated total yield from composition. Oil yield was highest at mild stress and did not track trichome number, which is most parsimoniously interpreted as a stronger per-trichome biosynthetic capacity at low dose, although per-trichome oil content was not measured directly. This yield gain was specific to daily tilting in light. The compositional response was largely light-independent, with moderate and severe stress shifting the profile toward menthofuran and away from menthol, while mild stress produced a distinct, qualitatively different response resembling low-dose JA induction. For oil quality this separates a desirable, light-specific yield gain at mild stress from an undesirable, dose-driven increase in menthofuran. Together, these findings indicate that gravitropic stimulation can modulate phytochemical profiles and biomass output in CEA-cultivated peppermint, supporting its further investigation as an elicitation strategy.

5.1.3 Jasmonic acid as a mediator of gravitropism-induced secondary metabolism

Jasmonic acid emerges here as a likely multi-level regulator of the gravitropism-induced compositional shifts. A dose-dependent JA model is proposed to account for the protocol- and dose-specific shifts observed across the gravitropic stimulation experiments. Under this model, low effective JA doses would preferentially activate pulegone reductase and produce the mild-stress compositional signature, while higher effective doses would additionally engage menthofuran synthase and produce the menthofuran-elevated profile of moderate and severe stress. Endogenous JA was not quantified, so this model is advanced as a hypothesis rather than a tested result.

The pharmacological experiments point to JA acting at more than one level. The data are consistent with JA being both a sufficient and a required input for the menthofuran synthase branch toward menthofuran, within the limits of the untested compositional comparison. JA additionally appears to influence the upstream geranyl pyrophosphate-branch enzymes governing pinene, eucalyptol and limonene allocation, extending its role beyond the canonical menthone/menthol/menthofuran branch-point. For the trichome response, MeJA was sufficient to reproduce the leaf-expansion-coupled pattern, but phenidone did not block the gravitropic

trichome response, indicating that endogenous JA biosynthesis is not strictly required and that alternative pathways, most plausibly converging on the canonical MYB- and bHLH-type transcription factor networks of trichome regulation, can compensate when JA biosynthesis is blocked.

A JA-independent gravitropic input on menthol biosynthesis was additionally observed in the older leaf pairs at higher stress doses. This input is normally masked by the competing JA-driven menthofuran synthase branch and became visible only when that branch was pharmacologically suppressed. JA therefore appears to be the principal but not the sole mediator of the gravitropic compositional response. The data are most consistent with a hierarchically organized signaling system in which JA dominates but does not exclusively determine the outcome.

5.2 Outlook

The present work raises three sets of open questions that should be addressed in future research.

5.2.1 Mechanistic Questions

The molecular identity of the JA-independent gravitropic input on menthol biosynthesis in older leaf pairs remains unresolved. Quantitative JA measurements across tissues and developmental stages, combined with transcriptomic profiling under combined gravitropic and phenidone treatment, would help distinguish the contributing signaling routes. The actively enhanced, density-defined trichome initiation response observed at higher gravitropic doses was not reproduced by 100 µM MeJA and may require higher exogenous JA concentrations, comparable to the 1–4 mM range used by Cappellari *et al.*, 2019, or involve additional non-JA inputs. The per-trichome biosynthetic capacity that underlies the oil yield response is similarly not directly addressed by the present experiments and would benefit from single-trichome metabolomic or transcriptomic analysis. The proposed microtubule-based susceptor mechanism for gravitropic adaptation should be tested directly using microtubule-targeting drugs in combination with repeated gravitropic stimulation. The role of long-distance JA transport between shoot and root tissues, suggested by the JAZ1 induction in apical leaves combined with the gravitropic effects on root architecture, also remains to be tested directly.

5.2.2 Methodological Refinements

Several observations in this work would benefit from methodological refinement. The continuous tilting baseline shift in the compositional data could not be definitively resolved and

may reflect either cutting-time-dependent variation or volatile MeJA accumulation in the cultivation room. Direct measurements of room-atmosphere MeJA and spatial separation of controls from tilted plants would distinguish between these possibilities. Higher MeJA concentrations and genetic manipulation of pulegone reductase, menthofuran synthase and menthone-menthol reductase would allow direct causal tests of the multi-level JA model proposed here. The trichome density data would benefit from leaf-developmental-stage normalization to disentangle initiation activity from passive density variation arising from leaf expansion modulation. The absence of root architecture data for daily tilting in darkness, and of per-trichome oil quantification, were further limitations that future designs should close.

5.2.3 Implications for CEA-based Medicinal Plant Production

Gravitropic stimulation emerges from this work as a non-invasive, mechanically applied elicitor that may shift essential oil composition, enhance biomass accumulation, and modulate trichome formation in a protocol- and dose-dependent manner. This places it as a candidate alongside light, temperature and water stress as a controllable input variable in CEA-based medicinal plant production. The dose-and-protocol framework developed here provides a systematic basis for tailoring stimulation regimes to defined compositional and yield targets, with the reference protocol of mild daily tilting in light as the most promising starting point for the favorable yield response, and the dose-driven menthofuran increase as the main quality risk to be managed.

Peppermint was used in this work as a model species for rapid and accessible phenotypic and chemical analysis. Its commercial value is modest, as peppermint can be cultivated across a wide range of climates at low cost, which limits the economic case for CEA-based peppermint production. The conceptual demonstration that gravitropic stimulation can act as an elicitor on the secondary metabolite network of an aromatic plant suggests that the same approach might be extended to higher-value medicinal species where CEA cultivation is already economically justified by quality and traceability requirements. Future work should therefore translate the framework to commercially valuable medicinal plants, where modest compositional shifts can have substantial economic and pharmaceutical value. Such studies would test the generality of gravitropic elicitation as a CEA tool and would establish whether the JA-mediated multi-level regulation identified in *Mentha* × *piperita* generalizes to other monoterpene- or phenylpropanoid-producing species.

6 References

Abbas, M., Hernández-García, J., Pollmann, S., Samodelov, S.L., Kolb, M., Friml, J., *et al.* (2018) Auxin Methylation Is Required for Differential Growth in *Arabidopsis*. *Proceedings of the National Academy of Sciences* **115**: 6864–6869.

Afkar, S., and Karimzadeh, G. (2025) Changes in Physiological Traits, Gene Expression and Phytochemical Profile of *Mentha piperita* in Response to Elicitor. *Biochem Genet* **63**: 2025–2039.

Afkar, S., Karimzadeh, G., Jalali Javaran, M., Sharifi, M., and Behmanesh, M. (2013) Influence of Methyl Jasmonate on Menthol Production and Gene Expression in Peppermint (*Mentha x piperita* L.). *J Med Plants By-Prod* **1**: 75–82.

Ahkami, A., Johnson, S.R., Srividya, N., and Lange, B.M. (2015) Multiple Levels of Regulation Determine Monoterpenoid Essential Oil Compositional Variation in the Mint Family. *Mol Plant* **8**: 188–191.

Baiyin, B., Xiang, Y., Shao, Y., Son, J.E., Tagawa, K., Yamada, M., *et al.* (2025) Response of Plant Roots to Mechanical Environmental Stimuli. *Hortic Res* **13**: uhaf337.

Baldwin, K.L., Strohm, A.K., and Masson, P.H. (2013) Gravity Sensing and Signal Transduction in Vascular Plant Primary Roots. *American Journal of Botany* **100**: 126–142.

Baster, P., Robert, S., Kleine-Vehn, J., Vanneste, S., Kania, U., Grunewald, W., *et al.* (2013) SCFTIR1/AFB-Auxin Signalling Regulates PIN Vacuolar Trafficking and Auxin Fluxes During Root Gravitropism. *EMBO J* **32**: 260–274.

Behrens, H.M., Gradmann, D., and Sievers, A. (1985) Membrane-Potential Responses Following Gravistimulation in Roots of *Lepidium sativum* L. *Planta* **163**: 463–472.

Bhattarai, K., Ogden, A.B., Pandey, S., Sandoya, G.V., Shi, A., Nankar, A.N., *et al.* (2025) Improvement of Crop Production in Controlled Environment Agriculture Through Breeding. *Front Plant Sci* **15**.

Biddington, N.L. (1986) The Effects of Mechanically-Induced Stress in Plants — A Review. *Plant Growth Regul* **4**: 103–123.

Blancaflor, E.B. (2013) Regulation of Plant Gravity Sensing and Signaling by the Actin Cytoskeleton. *American Journal of Botany* **100**: 143–152.

Blancaflor, E.B., and Masson, P.H. (2003) Plant Gravitropism. Unraveling the Ups and Downs of a Complex Process. *Plant Physiol* **133**: 1677–1690.

Boonsirichai, K., Guan, C., Chen, R., and Masson, P.H. (2002) ROOT GRAVITROPISM: An Experimental Tool to Investigate Basic Cellular and Molecular Processes Underlying Mechanosensing and Signal Transmission in Plants. *Annual Review of Plant Biology* **53**: 421–447.

Braam, J., and Chehab, E.W. (2017) Thigmomorphogenesis. *Current Biology* **27**: R863–R864.

Brauner, L., and Hager, A. (1958) Versuche zur Analyse der Geotropischen Perzeption. I. *Planta* **51**: 115–147.

Burk, D.H., and Ye, Z.-H. (2002) Alteration of Oriented Deposition of Cellulose Microfibrils by Mutation of a Katanin-Like Microtubule-Severing Protein. *Plant Cell* **14**: 2145–2160.

Burkard, P.M. (2023) Der Einfluss Von Methyl-Jasmonat Auf Den Sekundärstoffwechsel Der Pfefferminze (*Mentha x piperita*). .

Calabrese, E. (2014) Hormesis: A Fundamental Concept in Biology. *Microbial Cell* **1**: 145–149.

Cappellari, L.D.R., Santoro, M.V., Schmidt, A., Gershenzon, J., and Banchio, E. (2019) Induction of Essential Oil Production in *Mentha x piperita* by Plant Growth Promoting Bacteria Was Correlated with an Increase in Jasmonate and Salicylate Levels and a Higher Density of Glandular Trichomes. *Plant Physiol Biochem* **141**: 142–153.

Chalvin, C., Drevensek, S., Dron, M., Bendahmane, A., and Boualem, A. (2020) Genetic Control of Glandular Trichome Development. *Trends Plant Sci* **25**: 477–487.

Chandler, J.W. (2016) Auxin Response Factors. *Plant, Cell & Environment* **39**: 1014–1028.

Chauvet, H., Moulia, B., Legué, V., Forterre, Y., and Pouliquen, O. (2019) Revealing the Hierarchy of Processes and Time-Scales That Control the Tropic Response of Shoots to Gravi-Stimulations. *J Exp Bot* **70**: 1955–1967.

Chauvet, H., Pouliquen, O., Forterre, Y., Legué, V., and Moulia, B. (2016) Inclination Not Force Is Sensed by Plants During Shoot Gravitropism. *Sci Rep* **6**: 35431.

Chen, C.-L., Wu, D., Li, Q.-K., Liu, X., Niu, X.-G., Zhang, G.-X., *et al.* (2024) Methyl Jasmonate Enhances Rice Tolerance to Alkaline Stress Via the Auxin Pathway. *Plant Stress* **14**: 100612.

Chen, J., Yu, R., Li, N., Deng, Z., Zhang, X., Zhao, Y., *et al.* (2023) Amyloplast sedimentation repolarizes LAZYs to achieve gravity sensing in plants. *Cell* **186**: 4788-4802.e15.

Chin, S., and Blancaflor, E.B. (2022) Plant Gravitropism: From Mechanistic Insights into Plant Function on Earth to Plants Colonizing Other Worlds. In *Plant Gravitropism: Methods and Protocols*. Blancaflor, E.B. (ed.). Springer US, New York, NY. pp. 1–41 https://doi.org/10.1007/978-1-0716-1677-2_1. Accessed May 29, 2026.

Chini, A., Fonseca, S., Fernández, G., Adie, B., Chico, J.M., Lorenzo, O., *et al.* (2007) The JAZ Family of Repressors Is the Missing Link in Jasmonate Signalling. *Nature* **448**: 666–671.

Cholodny, N. (1927) Wuchshormone und Tropismen bei den Pflanzen. *Biologisches Zentralblatt* 604–626.

Collings, D.A., Winter, H., Wyatt, S.E., and Allen, N.S. (1998) Growth Dynamics and Cytoskeleton Organization During Stem Maturation and Gravity-Induced Stem Bending in *Zea Mays* L. *Planta* **207**: 246–258.

Coutand, C., Fournier, M., Alméras, T., Jaouen, G., and Moulia, B. (2010) Biomechanics of Habit and Plants Strategies of Growth in Height: Environmental Constraints, Regulator Processes and Traits. Clermont-Ferrand, France. p. 44 https://hal.science/hal-00797377.

Croteau, R.B., Davis, E.M., Ringer, K.L., and Wildung, M.R. (2005) (−)-Menthol Biosynthesis and Molecular Genetics. *Naturwissenschaften* **92**: 562–577.

Crowell, E.F., Timpano, H., Desprez, T., Franssen-Verheijen, T., Emons, A.-M., Höfte, H., and Vernhettes, S. (2011) Differential Regulation of Cellulose Orientation at the Inner and Outer Face of Epidermal Cells in the *Arabidopsis* Hypocotyl. *Plant Cell* **23**: 2592–2605.

Ćulafić, L., and Nešković, M. (1974) Indole Auxins in Spinach Plants Grown in Long and Short Days. *Biol Plant* **16**: 359–365.

Digby, J., and Firn, R.D. (1976) A Critical Assesment of the Cholodny-Went Theory of Shoot Geotropism. *Current Advances in Plant Science* **8**: 953–960.

Driss-Ecole, D., Cottignies, A., Jeune, B., Corbineau, F., and Perbal, G. (1994) Increased Mass Production of *Veronica Arvensis* Grown on a Slowly Rotating Clinostat. *Environmental and Experimental Botany* **34**: 303–310.

Dsouza, A., Dixon, M., Shukla, M., and Graham, T. (2025) Harnessing Controlled-Environment Systems for Enhanced Production of Medicinal Plants. *J Exp Bot* **76**: 76–93.

Dsouza, A., Newman, L., Graham, T., and Fraser, E.D.G. (2023) Exploring the Landscape of Controlled Environment Agriculture Research: A Systematic Scoping Review of Trends and Topics. *Agricultural Systems* **209**: 103673.

Engelberth, J. (2011) Selective Inhibition of Jasmonic Acid Accumulation by a Small A, B-Unsaturated Carbonyl and Phenidone Reveals Different Modes of Octadecanoid Signalling Activation in Response to Insect Elicitors and Green Leaf Volatiles in *Zea mays*. *BMC Res Notes* **4**: 377.

Engler, N., and Krarti, M. (2021) Review of Energy Efficiency in Controlled Environment Agriculture. *Renewable and Sustainable Energy Reviews* **141**: 110786.

European Medicines Agency (2016) Public Statement on the Use of Herbal Medicinal Products Containing Pulegone and Menthofuran. European Medicines Agency (EMA), Committee on Herbal Medicinal Products (HMPC), . https://www.ema.europa.eu/en/use-herbal-medicinal-products-containing-pulegone-menthofuran-scientific-guideline. Accessed May 14, 2026.

Fuchs, L.K., Holland, A.H., Ludlow, R.A., Coates, R.J., Armstrong, H., Pickett, J.A., *et al.* (2022) Genetic Manipulation of Biosynthetic Pathways in Mint. *Front Plant Sci* **13**.

Gaiser, J.C., and Lomax, T.L. (1993) The Altered Gravitropic Response of the Lazy-2 Mutant of Tomato Is Phytochrome Regulated. *Plant Physiol* **102**: 339–344.

Gaja, J., Bala, S., and Hugara, S. (2023) Cultivation of Medicinal Plants Using Hydroponic System. *Int J Res Rev* **10**: 17–21.

Gerlach, D. (1977) *Botanische Mikrotechnik: Eine Einführung*. 2., überarbeitete und erweiterte Auflage., G. Thieme Verlag, Stuttgart.

Gershenzon, J., McConkey, M.E., and Croteau, R.B. (2000) Regulation of Monoterpene Accumulation in Leaves of Peppermint. *Plant Physiol* **122**: 205–214.

Gill, A.R., Miller, T.K., Wijeweera, S., Herrero, E., Massa, G.D., Mortimer, J.C., *et al.* (2025) Turbocharging Fundamental Science Translation Through Controlled Environment Agriculture. *Trends in Plant Science* .

Giurgiu, R.M., Morar, G., Dumitraș, A., Vlăsceanu, G., Dune, A., and Schroeder, F.-G. (2017) A Study of the Cultivation of Medicinal Plants in Hydroponic and Aeroponic Technologies in a Protected Environment. *Acta Hortic* 671–678.

Gupta, S., Kumar, A., Gupta, A.K., Jnanesha, A.C., Talha, M., Srivastava, A., and Lal, R.K. (2023) Industrial Mint Crop Revolution, New Opportunities, and Novel Cultivation Ambitions: A Review. *Ecological Genetics and Genomics* **27**: 100174.

Gutjahr, C., and Nick, P. (2006) Acrylamide Inhibits Gravitropism and Affects Microtubules in Rice Coleoptiles. *Protoplasma* **227**: 211–222.

Gutjahr, C., Riemann, M., Müller, A., Düchting, P., Weiler, E.W., and Nick, P. (2005) Cholodny–Went Revisited: A Role for Jasmonate in Gravitropism of Rice Coleoptiles. *Planta* **222**: 575–585.

Hayden, A.L., Yokelsen, T.N., Giacomelli, G.A., and Hoffmann, J.J. (2004) Aeroponics: An Alternative Production System for High-Value Root Crops. *Acta Hortic* 207–213.

Hering, N. (2023) Chemical Evolution of Monoterpenes in *Mentha*. .

Herranz, R., and Medina, F.J. (2013) Cell Proliferation and Plant Development Under Novel Altered Gravity Environments. *Plant Biology* **16**: 23–30.

Hertel, R. (1983) The Mechanism of Auxin Transport as a Model for Auxin Action. *Zeitschrift für Pflanzenphysiologie* **112**: 53–67.

Hild, V., and Hertel, R. (1972) Initial Phases of Gravity-Induced Lateral Auxin Transport and Geotropic Curvature in Corn Coleoptiles. *Planta* **108**: 245–258.

Hudz, N., Kobylinska, L., Pokajewicz, K., Horčinová Sedláčková, V., Fedin, R., Voloshyn, M., *et al.* (2023) *Mentha piperita*: Essential Oil and Extracts, Their Biological Activities, and Perspectives on the Development of New Medicinal and Cosmetic Products. *Molecules* **28**: 7444.

Iino, M., Tarui, Y., and Uematsu, C. (1996) Gravitropism of Maize and Rice Coleoptiles: Dependence on the Stimulation Angle. *Plant, Cell & Environment* **19**: 1160–1168.

Kalemba, D., and Synowiec, A. (2020) Agrobiological Interactions of Essential Oils of Two Menthol Mints: *Mentha piperita* and *Mentha arvensis*. *Molecules* **25**: 59.

Kebrom, T.H. (2017) A Growing Stem Inhibits Bud Outgrowth – The Overlooked Theory of Apical Dominance. *Front Plant Sci* **8**.

Kerstens, S., and Verbelen, J. (2002) Cellulose Orientation in the Outer Epidermal Wall of Angiosperm Roots: Implications for Biosystematics. *Ann Bot* **90**: 669–676.

Khameneh, A.N., Eghlima, G., Ranjbar, M.-E., and Ghorbanpour, M. (2025) Exploring the Role of Abiotic Elicitors in the Biosynthesis of Secondary Metabolites in Peppermint (*Mentha piperita* L.). *Acta Scientiarum Polonorum Hortorum Cultus* **24**: 137–154.

Kim, K., Son, J., and Kim, W.-C. (2026) Short-Day Photoperiod Enhances Graft Success by Increasing Auxin Accumulation. *Plant Signaling & Behavior* **21**: 2648973.

Kitazawa, D., Fujii, N., Suge, H., and Takahashi, H. (2003) Effect of Gravity on Apical Dominance in *Pharbitis Nil. Uchu Seibutsu Kagaku* .

Kılıç, S., and Tarakci, O. (2018) Phytochemical Accumulation in Photomorphogenesis of Peppermint. *Adv Agric Sci* **7**: 116–131.

Knight, T.A. (1806) On the direction of the radicle and germen during the vegetation of seeds. *Phil Trans R Soc* 99–108.

Küpers, J.J., Snoek, B.L., Oskam, L., Pantazopoulou, C.K., Matton, S.E.A., Reinen, E., *et al.* (2023) Local Light Signaling at the Leaf Tip Drives Remote Differential Petiole Growth Through Auxin-Gibberellin Dynamics. *Current Biology* **33**: 75-85.e5.

Lam, S.-L., and Leopold, A.C. (1966) Role of Leaves in Phototropism. *Plant Physiol* **41**: 847–851.

Lange, B.M., Mahmoud, S.S., Wildung, M.R., Turner, G.W., Davis, E.M., Lange, I., *et al.* (2011) Improving Peppermint Essential Oil Yield and Composition by Metabolic Engineering. *Proceedings of the National Academy of Sciences* **108**: 16944–16949.

Leitz, G., Kang, B.-H., Schoenwaelder, M.E.A., and Staehelin, L.A. (2009) Statolith Sedimentation Kinetics and Force Transduction to the Cortical Endoplasmic Reticulum in Gravity-Sensing *Arabidopsis* Columella Cells. *Plant Cell* **21**: 843–860.

Li, S., Lei, L., Somerville, C.R., and Gu, Y. (2012) Cellulose Synthase Interactive Protein 1 (CSI1) Links Microtubules and Cellulose Synthase Complexes. *Proceedings of the National Academy of Sciences* **109**: 185–190.

Li, X., Liu, J., Li, Z., Chen, A., Zhao, R., Xu, S., and Sheng, X. (2024) Emerging *Arabidopsis* Roots Exhibit Hypersensitive Gravitropism Associated with Distinctive Auxin Synthesis and Polar Transport Within the Elongation Zone. *Plant Physiology and Biochemistry* **217**: 109257.

Limbach, C., Hauslage, J., Schäfer, C., and Braun, M. (2005) How to Activate a Plant Gravireceptor. Early Mechanisms of Gravity Sensing Studied in *Characean* Rhizoids during Parabolic Flights. *Plant Physiol* **139**: 1030–1040.

Liu, X., Cohen, J.D., and Gardner, G. (2011) Low-Fluence Red Light Increases the Transport and Biosynthesis of Auxin. *Plant Physiol* **157**: 891–904.

Livak, K.J., and Schmittgen, T.D. (2001) Analysis of relative gene expression data using real-time quantitative PCR and the 2(-Delta Delta C(T)) Method. *Methods* **25**: 402–408.

Löfke, C., Zwiewka, M., Heilmann, I., Van Montagu, M.C.E., Teichmann, T., and Friml, J. (2013) Asymmetric Gibberellin Signaling Regulates Vacuolar Trafficking of PIN Auxin Transporters During Root Gravitropism. *Proceedings of the National Academy of Sciences* **110**: 3627–3632.

Machado, R.A.R., Robert, C.A.M., Arce, C.C.M., Ferrieri, A.P., Xu, S., Jimenez-Aleman, G.H., *et al.* (2016) Auxin Is Rapidly Induced by Herbivore Attack and Regulates a Subset of Systemic, Jasmonate-Dependent Defenses. *Plant Physiol* **172**: 521–532.

Mahendran, G., and Rahman, L.-U. (2020) Ethnomedicinal, Phytochemical and Pharmacological Updates on Peppermint (*Mentha × piperita L.*)—A Review. *Phytotherapy Research* **34**: 2088–2139.

Mahmoud, S.S., and Croteau, R.B. (2003) Menthofuran Regulates Essential Oil Biosynthesis in Peppermint by Controlling a Downstream Monoterpene Reductase. *Proc Natl Acad Sci U S A* **100**: 14481–14486.

Mano, E., Horiguchi, G., and Tsukaya, H. (2006) Gravitropism in Leaves of *Arabidopsis thaliana* (L.) Heynh. *Plant and Cell Physiology* **47**: 217–223.

Marchant, A., Kargul, J., May, S.T., Muller, P., Delbarre, A., Perrot-Rechenmann, C., and Bennett, M.J. (1999) AUX1 Regulates Root Gravitropism in Arabidopsis by Facilitating Auxin Uptake Within Root Apical Tissues. *EMBO J* **18**: 2066–2073.

McConkey, M.E., Gershenzon, J., and Croteau, R.B. (2000) Developmental Regulation of Monoterpene Biosynthesis in the Glandular Trichomes of Peppermint. *Plant Physiol* **122**: 215–224.

Medina, F.J., Manzano, A., Kamal, K.Y., Ciska, M., and Herranz, R. (2023) Plants in Space: Novel Physiological Challenges and Adaptation Mechanisms. In *Progress in Botany Vol. 83*. Lüttge, U., Cánovas, F.M., Risueño, M.-C., Leuschner, C., and Pretzsch, H. (eds). Springer International Publishing, Cham. pp. 29–64 https://doi.org/10.1007/124_2021_53. Accessed May 29, 2026.

Mishra, A., Gupta, P., Lal, R.K., and Dhawan, S.S. (2021) Assessing and Integrating the Transcriptome Analysis with Plant Development, Trichomes, and Secondary Metabolites Yield Potential in *Mentha arvensis* L. *Plant Physiology and Biochemistry* **162**: 517–530.

Mishra, A., Lal, R.K., Chanotiya, C.S., and Dhawan, S.S. (2017) Genetic Elaborations of Glandular and Non-Glandular Trichomes in *Mentha arvensis* Genotypes: Assessing Genotypic and Phenotypic Correlations Along with Gene Expressions. *Protoplasma* **254**: 1045–1061.

Morita, M.T. (2010) Directional Gravity Sensing in Gravitropism. *Annual Review of Plant Biology* **61**: 705–720.

Moulia, B., Bastien, R., Chauvet-Thiry, H., and Leblanc-Fournier, N. (2019) Posture Control in Land Plants: Growth, Position Sensing, Proprioception, Balance, and Elasticity. *J Exp Bot* **70**: 3467–3494.

Myers, A.B., Firn, R.D., and Digby, J. (1994) Gravitropic Sign Reversal—a Fundamental Feature of the Gravitropic Perception or Response Mechanisms in Some Plant Organs. *J Exp Bot* **45**: 77–83.

Naik, P.M., and Al–Khayri, J.M. (2016) Abiotic and Biotic Elicitors–Role in Secondary Metabolites Production through In Vitro Culture of Medicinal Plants. In *Abiotic and Biotic*

Stress in Plants - Recent Advances and Future Perspectives. IntechOpen, https://www.intechopen.com/chapters/49289. Accessed May 13, 2026.

Nair, B. (2001) Final Report on the Safety Assessment of *Mentha piperita* (Peppermint) Oil, *Mentha piperita* (Peppermint) Leaf Extract, *Mentha piperita* (Peppermint) Leaf, and *Mentha piperita* (Peppermint) Leaf Water. *Int J Toxicol* **20 Suppl 3**: 61–73.

Nelson, A.J., and Evans, M.L. (1986) Analysis of Growth Patterns During Gravitropic Curvature in Roots of *Zea mays* by Use of a Computer-Based Video Digitizer. *J Plant Growth Regul* **5**: 73–83.

Nick, P. (2013) Microtubules, Signalling and Abiotic Stress. *The Plant Journal* **75**: 309–323.

Nick, P., Bergfeld, R., Schäfer, E., and Schopfer, P. (1990a) Unilateral Reorientation of Microtubules at the Outer Epidermal Wall During Photo- and Gravitropic Curvature of Maize Coleoptiles and Sunflower Hypocotyls. *Planta* **181**: 162–168.

Nick, P., Sailer, H., and Schäfer, E. (1990b) On the Relation Between Photo- and Gravitropically Induced Spatial Memory in Maize Coleoptiles. *Planta* **181**: 385–392.

Nick, P., and Schäfer, E. (1988) Spatial Memory During the Tropism of Maize (*Zea mays* L.) Coleoptiles. *Planta* **175**: 380–388.

Nick, P., Schafer, E., Hertel, R., and Furuya, M. (1991) On the Putative Role of Microtubules in Gravitropism of Maize Coleoptiles. *Plant Cell Physiol* **32**: 873–880.

Nishimura, T., Mori, S., Shikata, H., Nakamura, M., Hashiguchi, Y., Abe, Y., *et al.* (2023) Cell Polarity Linked to Gravity Sensing Is Generated by LZY Translocation from Statoliths to the Plasma Membrane. *Science* **381**: 1006–1010.

Ohara, K., Katayama, M., Kamachi, H., Kume, A., and Karahara, I. (2024) Prolonged Exposure to Hypergravity Increases Biomass and Alters Biomass Allocation in *Arabidopsis thaliana* (L.) Heynh. with No Apparent Impact on Element Content in the Shoot System. 2024.06.18.599652 https://www.biorxiv.org/content/10.1101/2024.06.18.599652v2. Accessed May 12, 2026.

Ottenschläger, I., Wolff, P., Wolverton, C., Bhalerao, R.P., Sandberg, G., Ishikawa, H., *et al.* (2003) Gravity-Regulated Differential Auxin Transport from Columella to Lateral Root Cap Cells. *Proceedings of the National Academy of Sciences* **100**: 2987–2991.

Paredez, A.R., Somerville, C.R., and Ehrhardt, D.W. (2006) Visualization of Cellulose Synthase Demonstrates Functional Association with Microtubules. *Science* **312**: 1491–1495.

Parrey, Z.A., Shah, S.H., Mohammad, F., Siddiqui, M.H., Alamri, S., and Kalaji, H.M. (2023) Exogenous Epibrassinolide Application Improves Essential Oil Biosynthesis and Trichome Development in Peppermint Via Modulating Growth and Physicochemical Processes. *Sci Rep* **13**: 12924.

Pauwels, L., and Goossens, A. (2011) The JAZ Proteins: A Crucial Interface in the Jasmonate Signaling Cascade. *Plant Cell* **23**: 3089–3100.

Philosoph-Hadas, S. (1999) Signal Transduction Pathway of Hormonal Action in Control and Regulation of the Gravitropic Response of Cut Flowering Stems During Storage and Transport. .

Pickard, B., and Ding, J. (1993) The Mechanosensory Calcium-Selective Ion Channel: Key Component of a Plasmalemmal Control Centre? *Australian Journal of Plant Physiology* **20**: 439–459.

Prasad, T.K., and Cline, M.G. (1987) The Role of Gravity in Apical Dominance : Effects of Clinostating on Shoot Inversion-Induced Ethylene Production, Shoot Elongation, and Lateral Bud Growth. *Plant Physiol* **83**: 505–509.

Psaras, G.K. (2004) Direct Microscopic Demonstration of the Statolith Sedimentation in Endodermal Cells of Leaf Petioles after Gravistimulation; Evidence for the Crucial Role of Actin Filaments. *Phyton (Horn)* **44**: 191–201.

Reimann, A., Vogel, S., Rademacher, T., Drossard, J., and Buyel, J. (2018) Innovative CEA-basierte Pflanzenproduktion - Von der Gewächshaus-basierten Anwendung bis zum Vertical Farming. *Julius-Kühn-Archiv* **460**: 23–24.

Reisinger, L. (2024) Effects of Different Cultivation Systems on the Root Architecture and Growth of Different Plants. .

Rios-Estepa, R., Lange, I., Lee, J.M., and Lange, B.M. (2010) Mathematical Modeling-Guided Evaluation of Biochemical, Developmental, Environmental, and Genotypic Determinants of Essential Oil Composition and Yield in Peppermint Leaves. *Plant Physiol* **152**: 2105–2119.

Rios-Estepa, R., Turner, G.W., Lee, J.M., Croteau, R.B., and Lange, B.M. (2008) A Systems Biology Approach Identifies the Biochemical Mechanisms Regulating Monoterpenoid Essential Oil Composition in Peppermint. *Proceedings of the National Academy of Sciences* **105**: 2818–2823.

Rita, P., and Animesh, D.K. (2011) An Updated Overview on Peppermint (*Mentha piperita L* .). *Int Res J Pharm* **2**: 1–10.

Rorabaugh, P.A., and Salisbury, F.B. (1989) Gravitropism in Higher Plant Shoots : VI. Changing Sensitivity to Auxin in Gravistimulated Soybean Hypocotyls. *Plant Physiol* **91**: 1329–1338.

Roychoudhry, S., and Kepinski, S. (2024) Things Fall into Place: How Plants Sense and Respond to Gravity. *Nature* **631**: 745–747.

Ruan, J., Zhou, Y., Zhou, M., Yan, J., Khurshid, M., Weng, W., *et al.* (2019) Jasmonic Acid Signaling Pathway in Plants. *Int J Mol Sci* **20**: 2479.

Salisbury, F.B., Gillespie, L., and Rorabaugh, P. (1988) Gravitropism in Higher Plant Shoots : V. Changing Sensitivity to Auxin. *Plant Physiol* **88**: 1186–1194.

Shil, S., and Dewanjee, S. (2022) Impact of Drought Stress Signals on Growth and Secondary Metabolites (SMs) in Medicinal Plants. *J Phytopharmacol* **11**: 371–376.

Shimizu-Sato, S., Tanaka, M., and Mori, H. (2009) Auxin–Cytokinin Interactions in the Control of Shoot Branching. *Plant Mol Biol* **69**: 429–435.

Sievers, A., Behrens, H.M., Buckhout, T.J., and Gradmann, D. (1984) Can a Ca2+ Pump in the Endoplasmic Reticulum of the *Lepidium* Root Be the Trigger for Rapid Changes in Membrane Potential After Gravistimulation? *Zeitschrift für Pflanzenphysiologie* **114**: 195–200.

Soleymani, F., Taheri, H., and Shafeinia, A.R. (2017) Relative Expression of Genes of Menthol Biosynthesis Pathway in Peppermint (*Mentha piperita* L.) After Chitosan, Gibberellic Acid and Methyl Jasmonate Treatments. *Russ J Plant Physiol* **64**: 59–66.

Song, K., Shao, G., Yu, Z., and Sun, C. (2026) Classification, Pharmacological Properties, and Applications of Bioactive Constituents in *Mentha* Species. *J Agric Food Chem* **74**: 4183–4198.

Souza, M.A.A. de, Santos, L.A. dos, Brito, D.M.C. de, Rocha, J.F., Castro, R.N., Fernandes, M.S., and Souza, S.R. de (2016) Influence of Light Intensity on Glandular Trichome Density, Gene Expression and Essential Oil of Menthol Mint (*Mentha arvensis* L.). *Journal of Essential Oil Research* **28**: 138–145.

Stutte, G.W. (2016) Controlled Environment Production of Medicinal and Aromatic Plants. In *Medicinal and Aromatic Crops: Production, Phytochemistry, and Utilization*. American Chemical Society, pp. 49–63.

Su, S.-H., Gibbs, N.M., Jancewicz, A.L., and Masson, P.H. (2017) Molecular Mechanisms of Root Gravitropism. *Current Biology* **27**: R964–R972.

Sun, J., Chen, Q., Qi, L., Jiang, H., Li, S., Xu, Y., *et al.* (2011) Jasmonate Modulates Endocytosis and Plasma Membrane Accumulation of the *Arabidopsis* PIN2 Protein. *New Phytologist* **191**: 360–375.

Taheri, H. (2019) Transcriptional Modulation of Structural and Regulatory Genes Involved in Isoprene Biosynthesis and Their Relevance to Oil Yield and Menthol Content in Peppermint (*Mentha piperita* L.) upon MeJA and GA3 Treatments. *Russ J Plant Physiol* **66**: 503–508.

Takeda, K., and Shibaoka, H. (1981) Changes in Microfibril Arrangement on the Inner Surface of the Epidermal Cell Walls in the Epicotyl of *Vigna angularis ohwi et ohashi* During Cell Growth. *Planta* **151**: 385–392.

Thines, B., Katsir, L., Melotto, M., Niu, Y., Mandaokar, A., Liu, G., *et al.* (2007) JAZ Repressor Proteins Are Targets of the SCFCOI1 Complex During Jasmonate Signalling. *Nature* **448**: 661–665.

Tillberg, E. (1974) Levels of Indol-3yl-Acetic Acid and Acid Inhibitors in Green and Etiolated Bean Seedlings (*Phaseolus vulgaris*). *Physiologia Plantarum* **31**: 106–111.

Touliatos, D., Dodd, I.C., and McAinsh, M. (2016) Vertical Farming Increases Lettuce Yield Per Unit Area Compared to Conventional Horizontal Hydroponics. *Food and Energy Security* **5**: 184–191.

Tuominen, L.K., Levine, L.H., and Musgrave, M.E. (2009) Plant Secondary Metabolism in Altered Gravity. *Methods Mol Biol* **547**: 373–386.

Turner, G.W., Gershenzon, J., and Croteau, R.B. (2000) Distribution of Peltate Glandular Trichomes on Developing Leaves of Peppermint. *Plant Physiol* **124**: 655–664.

Ulmasov, T., Hagen, G., and Guilfoyle, T.J. (1997) ARF1, a Transcription Factor That Binds to Auxin Response Elements. *Science* **276**: 1865–1868.

Vandenbrink, J.P., and Kiss, J.Z. (2019) Plant Responses to Gravity. *Seminars in Cell & Developmental Biology* **92**: 122–125.

Verbelen, J.-P., and Stickens, D. (1995) In Vivo Determination of Fibril Orientation in Plant Cell Walls with Polarization CSLM. *Journal of Microscopy* **177**: 1–6.

Waite, J.M., and Dardick, C. (2021) The Roles of the IGT Gene Family in Plant Architecture: Past, Present, and Future. *Current Opinion in Plant Biology* **59**: 101983.

Wang, L., Sadeghnezhad, E., and Nick, P. (2020) Upstream of Gene Expression: What Is the Role of Microtubules in Cold Signalling? *Journal of Experimental Botany* **71**: 36–48.

Wasternack, C., and Song, S. (2017) Jasmonates: Biosynthesis, Metabolism, and Signaling by Proteins Activating and Repressing Transcription. *J Exp Bot* **68**: 1303–1321.

Wei, H., Kong, S., Jayaraman, V., Selvaraj, D., Soundararajan, P., and Manivannan, A. (2023) *Mentha arvensis* and *Mentha* × *piperita*-Vital Herbs with Myriads of Pharmaceutical Benefits. *Horticulturae* **9**: 224.

Went, F.W. (1926) On growth-accelerating substances in the coleoptile of <i>Avena sativa<i/>. *Proceedings of the Koninklijke Nederlandse Akademie van Wetenschappen* 10–19.

Xu, K., Jourquin, J., Xu, X., De Smet, I., Fernandez, A.I., and Beeckman, T. (2023) Dynamic GOLVEN-ROOT GROWTH FACTOR 1 INSENSITIVE Signaling in the Root Cap Mediates Root Gravitropism. *Plant Physiol* **192**: 256–273.

Yoshihara, T., and Spalding, E.P. (2017) LAZY Genes Mediate the Effects of Gravity on Auxin Gradients and Plant Architectured. *Plant Physiol* **175**: 959–969.

Zhang, F., Li, C., Qu, X., Liu, J., Yu, Z., Wang, J., *et al.* (2022) A Feedback Regulation Between ARF7-Mediated Auxin Signaling and Auxin Homeostasis Involving MES17 Affects Plant Gravitropism. *Journal of Integrative Plant Biology* **64**: 1339–1351.

Zheng, Z., Zou, J., Li, H., Xue, S., Wang, Y., and Le, J. (2015) Microrheological Insights into the Dynamics of Amyloplasts in Root Gravity-Sensing Cells. *Molecular Plant* **8**: 660–663.

Zobayed, S.M.A., Afreen, F., and Kozai, T. (2005) Necessity and Production of Medicinal Plants Under Controlled Environments. *Environment Control in Biology* **43**: 243–252.

7 Appendix

This appendix contains supplementary data referenced in the Results section. The figures are grouped according to the respective experimental focus, including anatomical observations, gene expression profiles, plant growth and root architecture, glandular trichome traits, and essential oil-related parameters. Statistical analyses and experimental conditions follow those described in Materials and Methods.

Supplementary anatomical observations

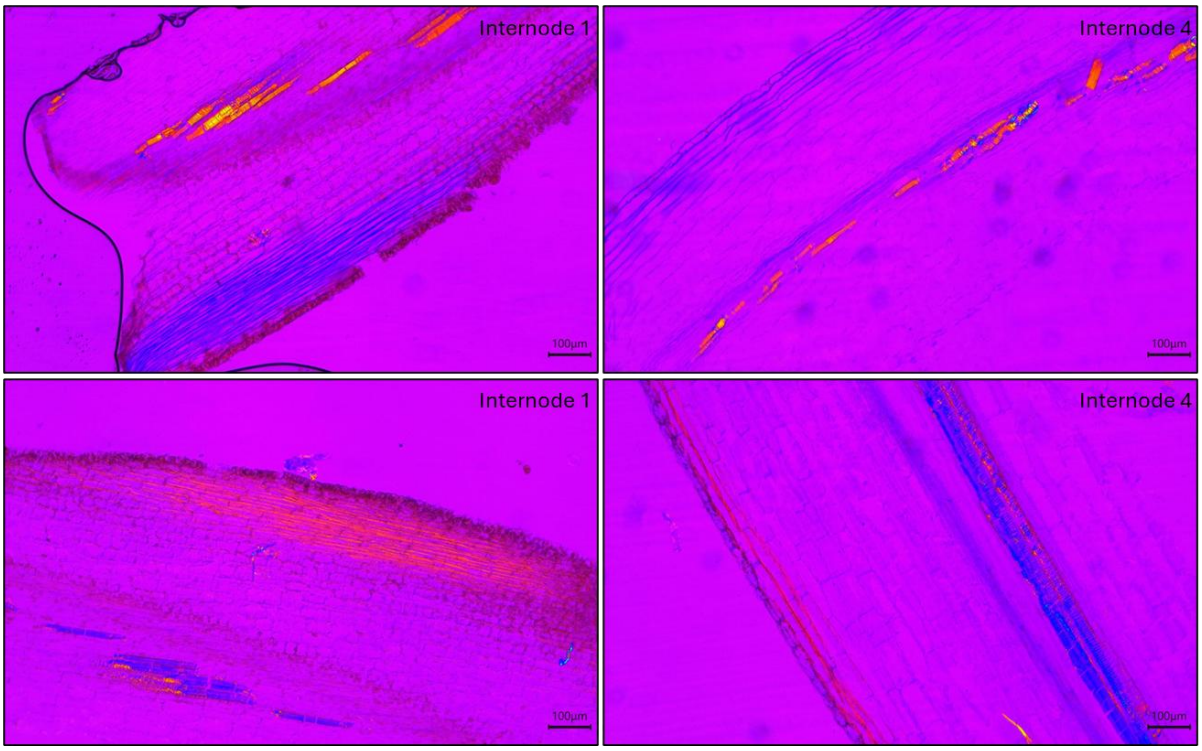

Figure A 1 **Longitudinal sections of internodes 1 and 4 of *Mentha* × *piperita* shoots examined under polarized light with a red gypsum compensator plate.** *Two sections per internode are shown at different orientations. Scale bar = 100 µm*

Supplementary gene expression profiles after gravitropic stimulation

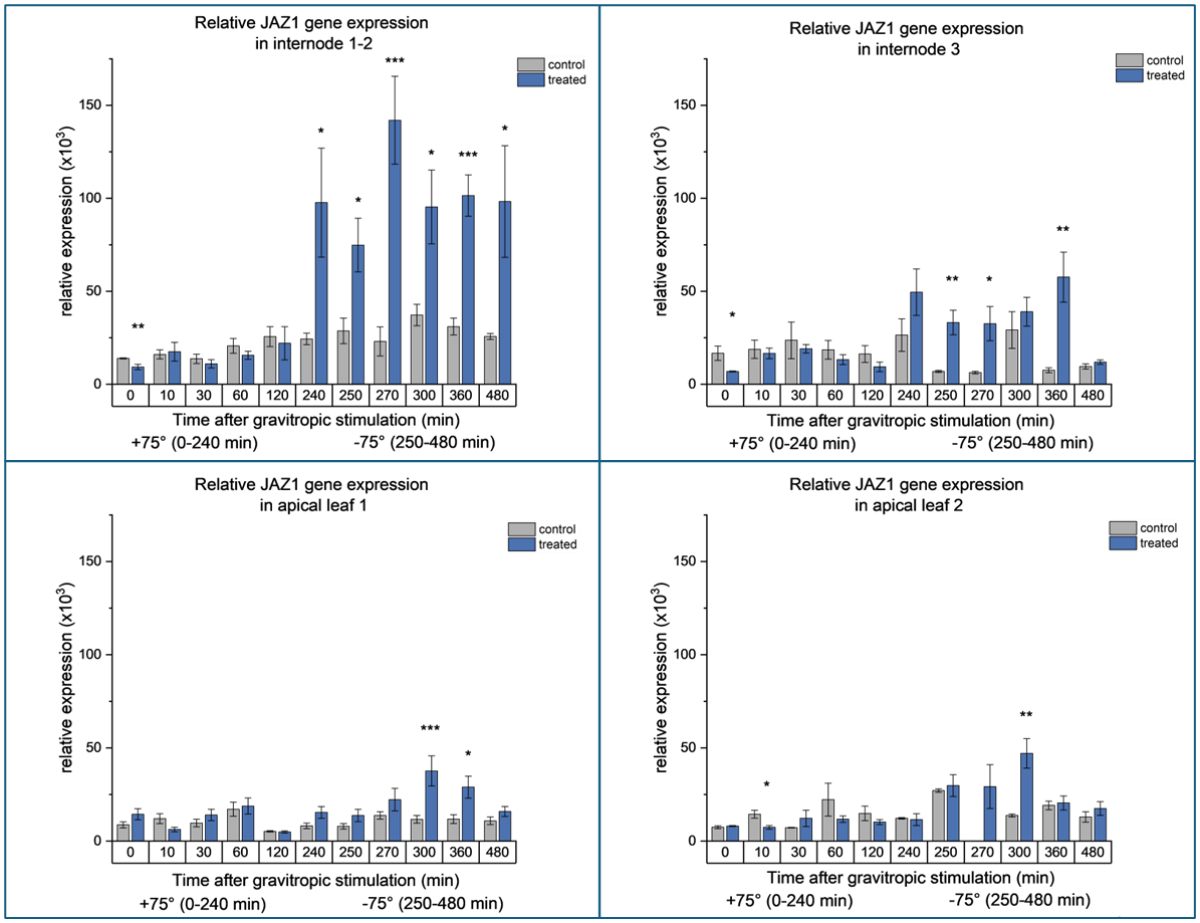

Figure A 2 Relative JAZ1 gene expression after gravitropic stimulation at 75° in four tissue types of *Mentha* × *piperita*. *Plants were tilted to +75° for 0–240 minutes, followed by reversal to −75° for 250–480 minutes. Gene expression was measured by RT-qPCR and normalized to reference genes; values shown are means ± SE (n = 3 biological replicates with 3 technical replicates each). Asterisks indicate significant differences between control (grey) and treated (blue) plants at the respective time point (* p < 0.05; ** p < 0.01; *** p < 0.001; one-way ANOVA followed by Tukey's HSD post-hoc test). Tissues analyzed: internode 1–2 (top left), internode 3 (top right), apical leaf 1 (bottom left), apical leaf 2 (bottom right). Note the different y-axis scale in internode 1–2 compared to the other tissues.*

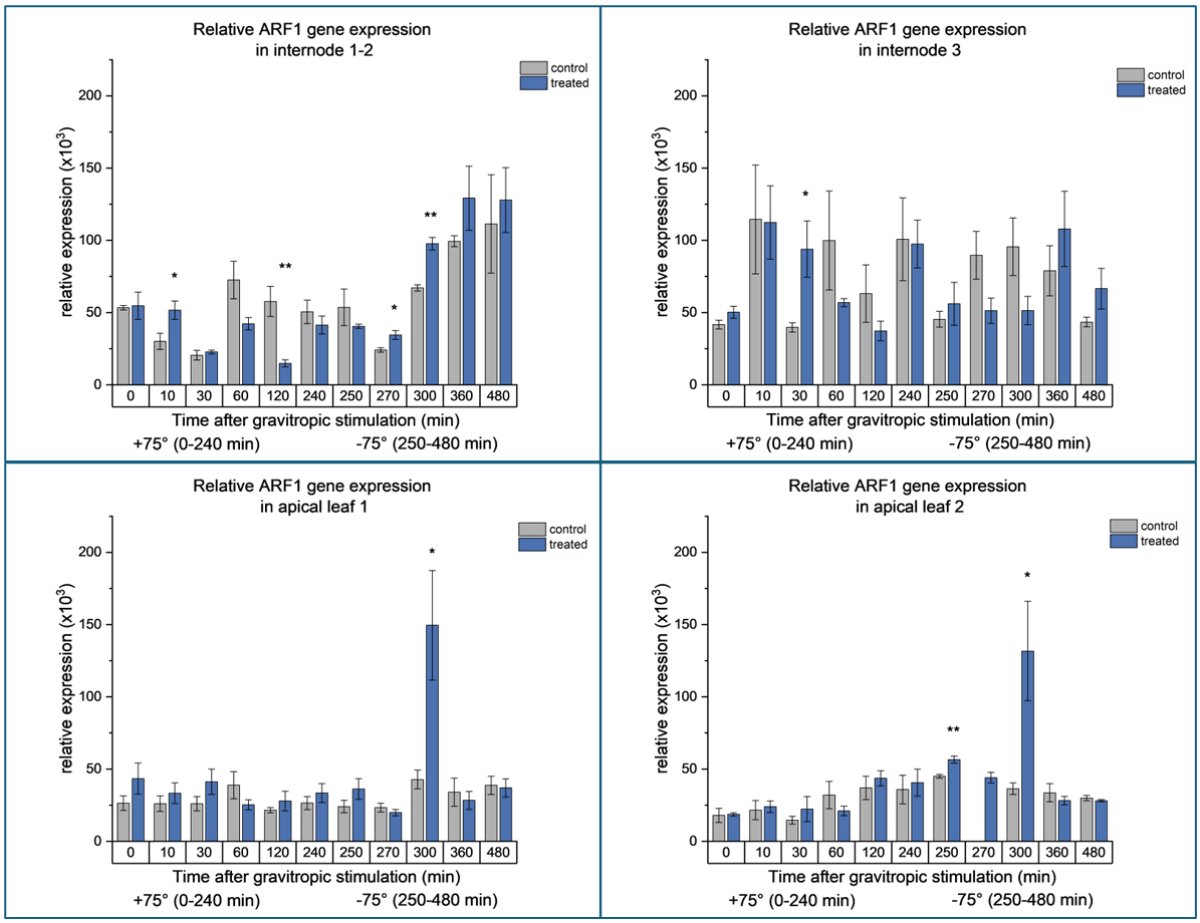

Figure A 3 Relative ARF1 gene expression after gravitropic stimulation at 75° in four tissue types of *Mentha* × *piperita*. *Plants were tilted to +75° for 0–240 minutes, followed by reversal to −75° for 250–480 minutes. Gene expression was measured by RT-qPCR and normalized to reference genes; values shown are means ± SE (n = 3 biological replicates with 3 technical replicates each). Asterisks indicate significant differences between control (grey) and treated (blue) plants at the respective time point (* p < 0.05; ** p < 0.01; one-way ANOVA followed by Tukey's HSD post-hoc test). Tissues analyzed: internode 1–2 (top left), internode 3 (top right), apical leaf 1 (bottom left), apical leaf 2 (bottom right). Note the elevated baseline expression of ARF1 in internode 3 compared to the other tissues, as well as the pronounced peak at 300 minutes after stimulation in apical leaves 1 and 2.*

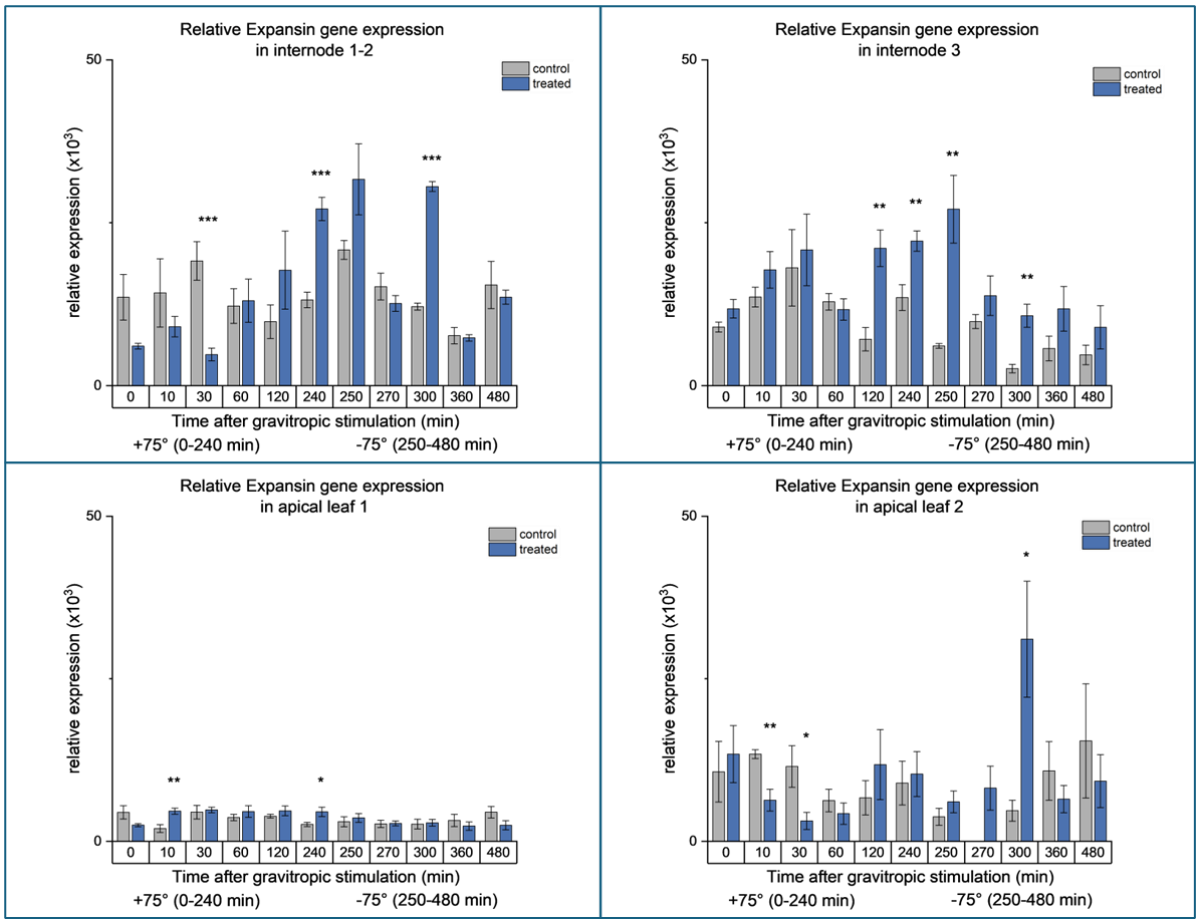

Figure A 4 Relative Expansin gene expression after gravitropic stimulation at 75° in four tissue types of *Mentha* × *piperita*. *Plants were tilted to +75° for 0–240 minutes, followed by reversal to −75° for 250–480 minutes. Gene expression was measured by RT-qPCR and normalized to reference genes; values shown are means ± SE (n = 3 biological replicates with 3 technical replicates each). Asterisks indicate significant differences between control (grey) and treated (blue) plants at the respective time point (* p < 0.05; ** p < 0.01; *** p < 0.001; one-way ANOVA followed by Tukey's HSD post-hoc test). Tissues analyzed: internode 1–2 (top left), internode 3 (top right), apical leaf 1 (bottom left), apical leaf 2 (bottom right).*

Supplementary data for daily tilting in light

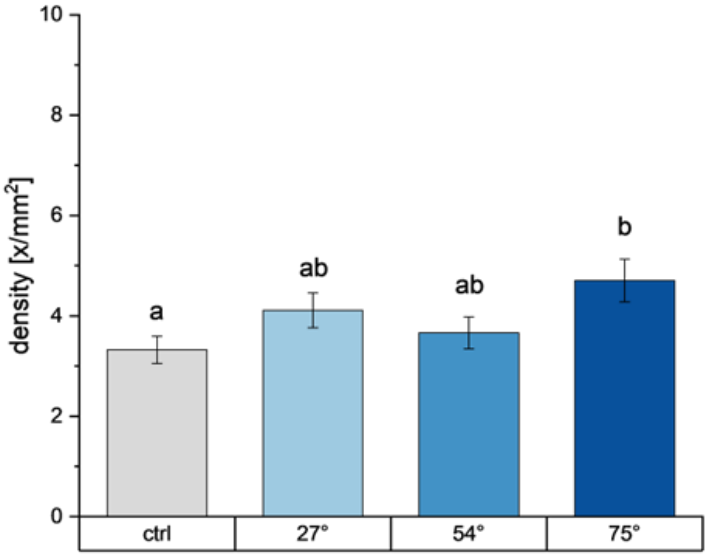

Figure A 5 Mean glandular trichome density under increasing gravitropic stress during daily tilting in light. *Density (x/mm²) is shown as the mean across all measured leaf pairs for mild (27°), moderate (54°) and severe stress (75°) compared to untilted controls (ctrl). Data represent means ± SE (n = 18). Different letters indicate statistically significant differences between groups as determined by one-way ANOVA followed by Tukey's HSD post-hoc test (p < 0.05).*

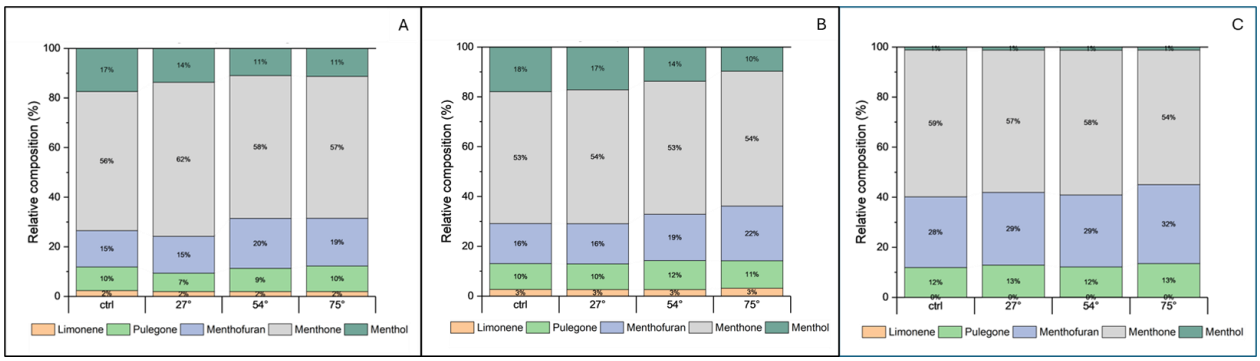

Figure A 6 Relative composition of the five major monoterpenes in peppermint essential oil increasing under gravitropic stress during daily tilting in light (A), daily tilting in darkness (B) and continuous tilting in light (C). *Relative proportions (%) of limonene, pulegone, menthofuran, menthone and menthol are shown for tilting angles of 27°, 54° and 75° compared to untilted controls (ctrl). Data represent means (n = 3). Note that percentages reflect the relative distribution among these five components only and do not represent absolute contributions to total oil composition.*

Supplementary growth and root architecture data

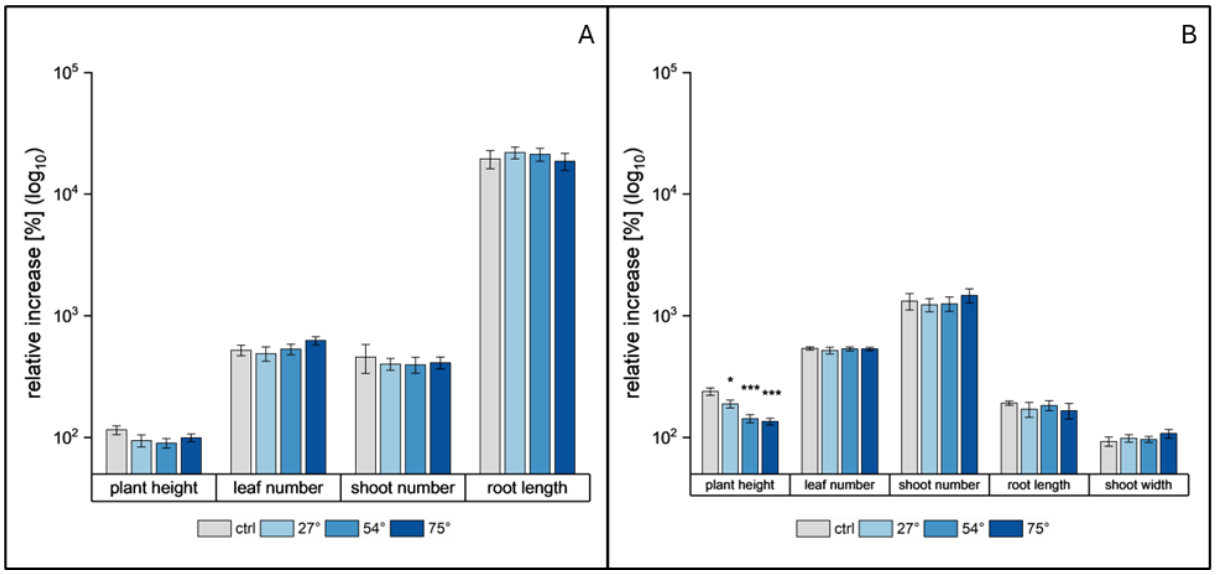

Figure A 7 Relative growth of plant organs under increasing gravitropic stimulation in darkness (A) and continuous tilting in light (B). *Relative increase (%) from experiment start to end is shown on a log_{10} scale for plant height, leaf number, shoot number, root length and shoot width (C only). Tilting angles of 27°, 54° and 75° are compared to untilted controls (ctrl). Data represent means ± SE (n = 11). Asterisks without brackets indicate statistically significant differences compared to the control. Asterisks with brackets indicate statistically significant differences between the indicated groups (*p < 0.05, *** p < 0.001).*

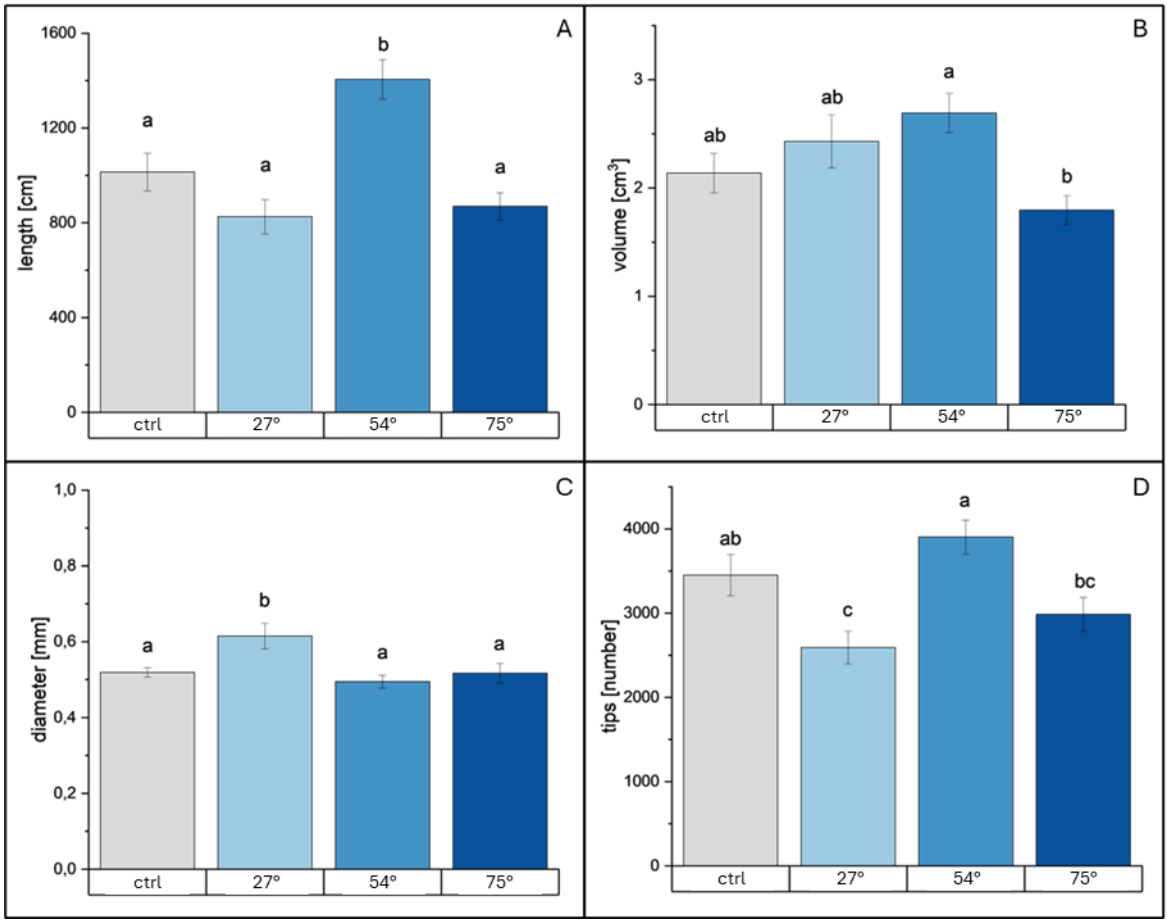

Figure A 8 Root architecture parameters of *Mentha* × *piperita* under continuous tilting in light at increasing gravitropic stress angles. *Total root length (A), root volume (B), average root diameter (C) and number of root tips (D) are shown for tilting angles of 27°, 54° and 75° compared to untilted controls (ctrl). Data represent means ± SE (n = 11). Different letters indicate statistically significant differences between groups as determined by one-way ANOVA followed by Tukey's HSD post-hoc test (p < 0.05).*

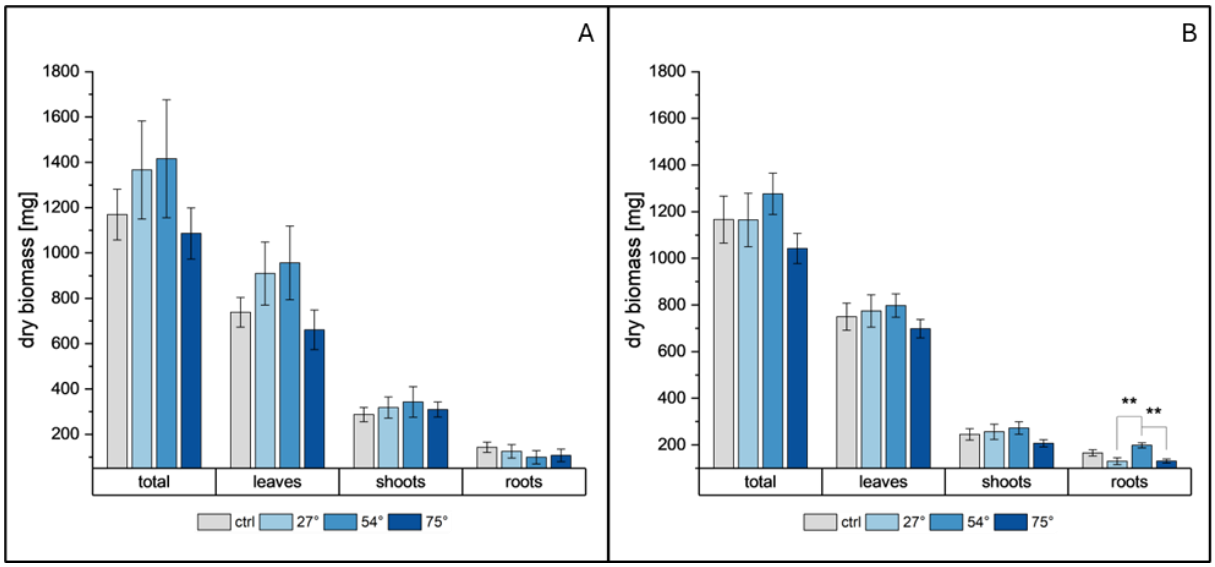

Figure A 9 Dry biomass of total plant, leaves, shoots and roots under increasing gravitropic stimulation in darkness (A) and continuous tilting in light (B). *Dry biomass (mg) is shown for tilting angles of 27°, 54° and 75° compared to untilted controls (ctrl). Data represent means ± SE (n = 11). Asterisks indicate statistically significant differences between the indicated groups (** p < 0.01).*

Supplementary glandular trichome traits

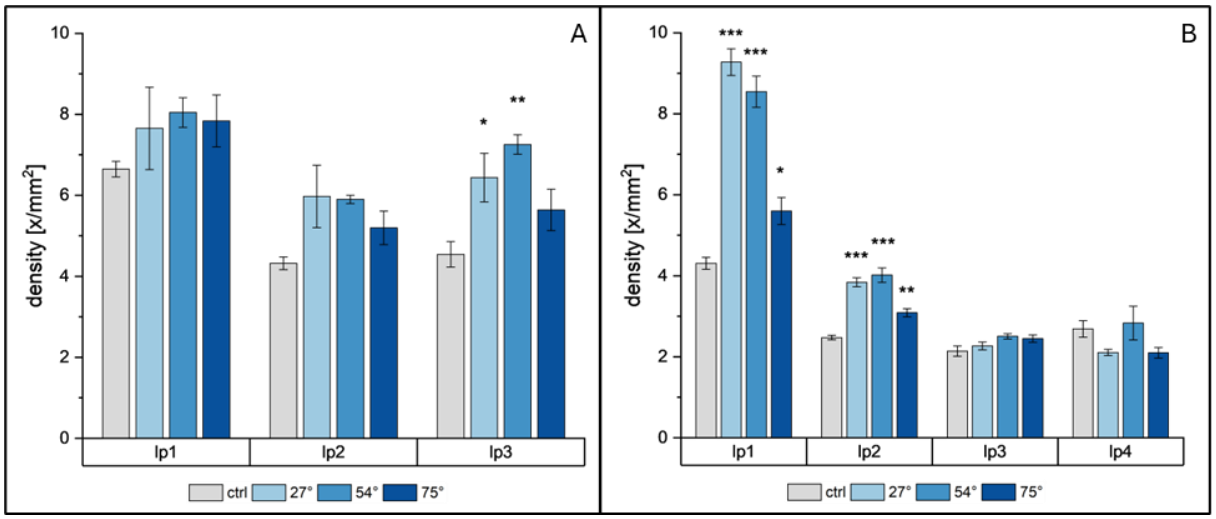

Figure A 10 Glandular trichome density per unit leaf area in individual leaf pairs under increasing gravitropic stress during daily tilting in darkness (A) and continuous tilting in light (B). *Density (x/mm²) is shown for leaf pairs (lp) 1–3 (A, B) and 1–4 (C), numbered from the apical (youngest) to the more basal (older) leaf pairs, for tilting angles of 27°, 54° and 75° compared to untilted controls (ctrl). Data represent means ± SE (n = 12 per leaf pair). Asterisks indicate statistically significant differences compared to the control (p < 0.05, ** p < 0.01, *** p < 0.001). In panel B, 75° differed significantly from all other groups in both lp1 and lp2.*

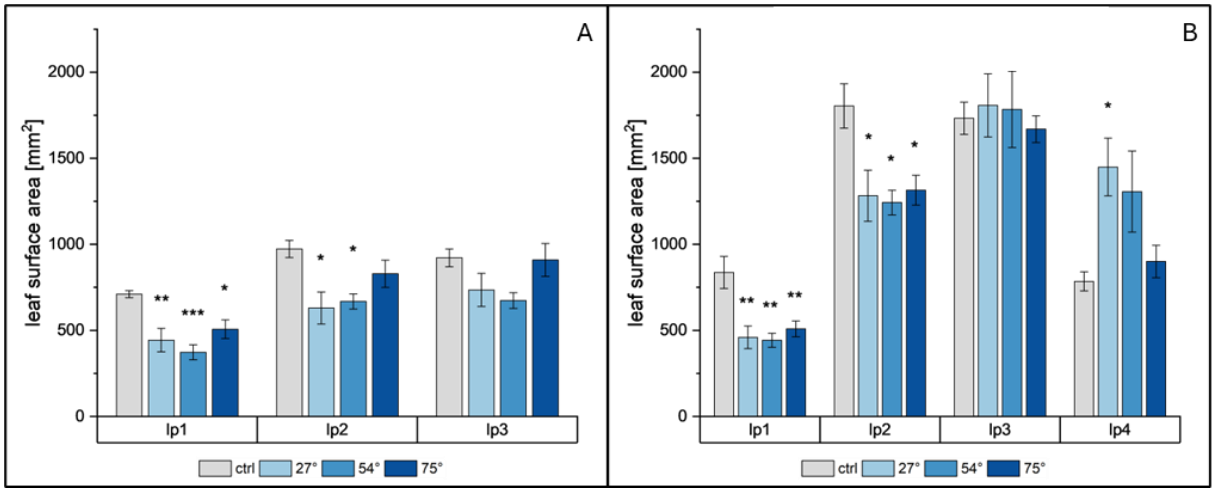

Figure A 11 Leaf surface area per leaf pair under increasing gravitropic stress during daily tilting in darkness (A) and continuous tilting in light (B). *Leaf surface area (mm²) is shown for leaf pairs (lp) 1–3 (A) and lp 1–4 (B), numbered from the apical (youngest) to the more basal (older) leaf pairs, for tilting angles of 27°, 54° and 75° compared to untilted controls (ctrl). Data represent means ± SE (n = 12 per leaf pair). Asterisks indicate statistically significant differences compared to the control (p < 0.05, ** p < 0.01, *** p < 0.001).*

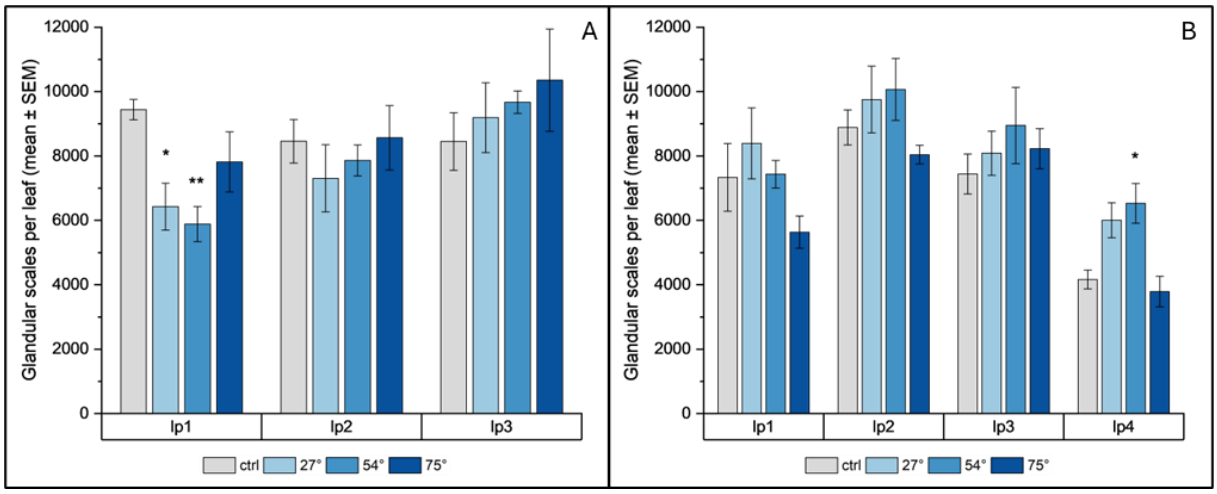

Figure A 12 Total glandular trichome count per leaf in individual leaf pairs under increasing gravitropic stress during daily tilting in darkness (A) and continuous tilting in light (B). *Glandular trichome count per leaf is shown for leaf pairs (lp) 1–3 (A) and lp 1–4 (B), numbered from the apical (youngest) to the more basal (older) leaf pairs, for tilting angles of 27°, 54° and 75° compared to untilted controls (ctrl). Data represent means ± SE (n = 12 per leaf pair). Asterisks indicate statistically significant differences compared to the control ($p < 0.05$, ** $p < 0.01$). In panel B, 27° and 75° as well as 54° and 75° differed significantly in lp4.*

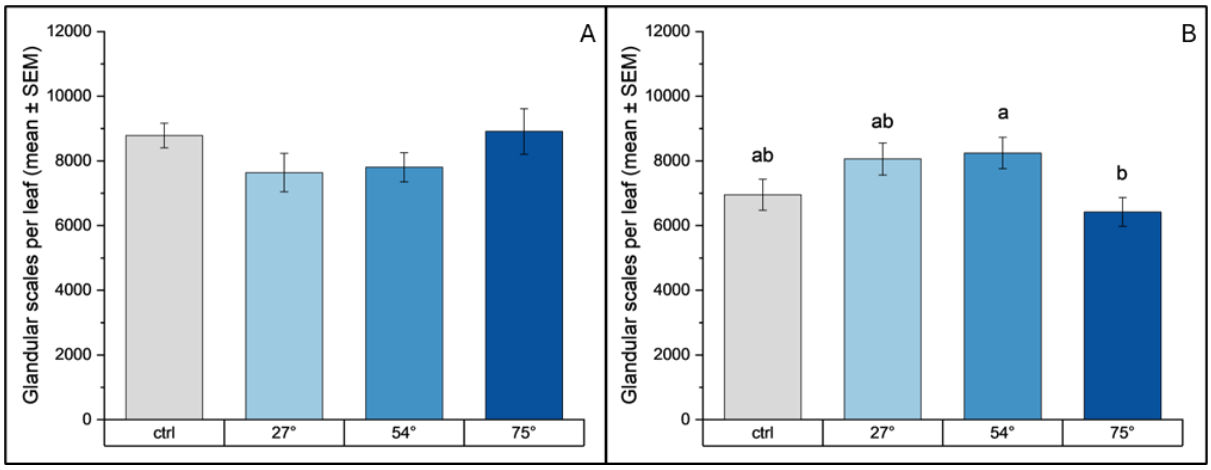

Figure A 13 Total glandular trichome count per leaf under increasing gravitropic stress during daily tilting in darkness (A) and continuous tilting in light (B). *Glandular trichome count per leaf is shown as the mean across all measured leaf pairs for tilting angles of 27°, 54° and 75° compared to untilted controls (ctrl). Data represent means ± SE (n = 18 for A; n = 24 for B). Different letters indicate statistically significant differences between groups as determined by one-way ANOVA followed by Tukey's HSD post-hoc test ($p < 0.05$).*

Supplementary essential oil data

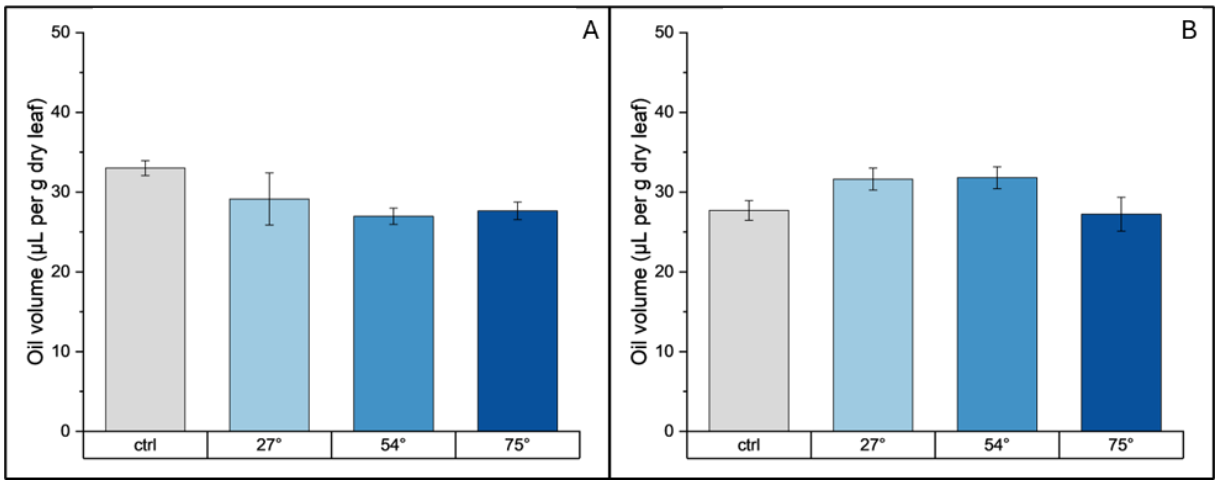

Figure A 14 Essential oil volume per gram dry leaf mass under increasing gravitropic stress during daily tilting in darkness (A) and continuous tilting in light (B). *Oil volume (µL per g dry leaf) is shown for tilting angles of 27°, 54° and 75° compared to untilted controls (ctrl). Data represent means ± SE (n = 3). No statistically significant differences were detected.*

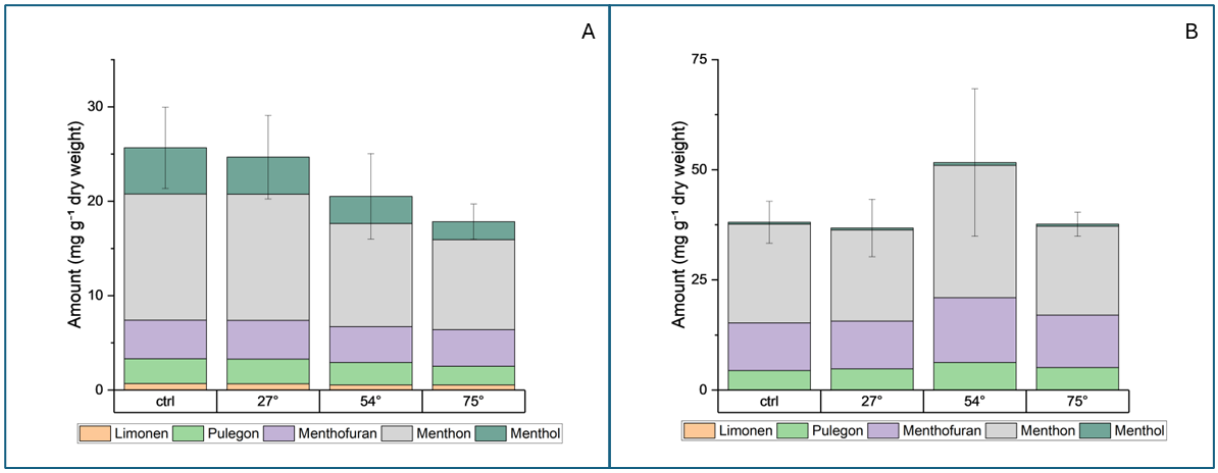

Figure A 15 Absolute quantity of principal essential oil components per gram dry leaf mass under increasing gravitropic stress during daily tilting in darkness (A) and continuous tilting in light (B). *Combined amount (mg g^{-1} dry weight) of limonene, pulegone, menthofuran, menthone and menthol is shown for tilting angles of 27°, 54° and 75° compared to untilted controls (ctrl). Data represent means ± SE (n = 3). No statistically significant differences were detected.*